Title Page

Deciphering paleogeography from orogenic architecture: constructing orogens in a future supercontinent as thought experiment

Douwe J.J. van Hinsbergen*, Thomas L.A. Schouten

Department of Earth Sciences, Utrecht University, Princetonlaan 8A, 3584 CB Utrecht, the Netherlands

*Correspondence to: Douwe J.J. van Hinsbergen, +31 30 2536712, d.j.j.vanhinsbergen@uu.nl

This paper was accepted for publication (on January 12, 2021) in the American Journal of Science

Abstract. Orogens that form at convergent plate boundaries typically consist of accreted rock units that form an incomplete archive of subducted oceanic and continental lithosphere, as well as of deformed crust of the former upper plate. Reading the construction of orogenic architecture forms the key to decipher the paleogeographic distribution of oceans and continents, as well as bathymetric and topographic features that existed thereon such as igneous plateaus, seamounts, microcontinents, or magmatic arcs. Current classification schemes of orogens divide between settings associated with termination of subduction (continent-continent collision, continent-ocean collision (obduction)) and with ongoing subduction (accretionary orogenesis), alongside intraplate orogens. Perceived diagnostic features for such classifications, particularly of collisional orogenesis, hinge on dynamic interpretations linking downgoing plate paleogeography to upper plate deformation, plate motion changes, or magmatism. Here, we show, however, that Mesozoic-Cenozoic orogens that undergo collision almost all defy these proposed diagnostic features and behave like accretionary orogens instead. To reconstruct paleogeography of subducted and upper plates, we therefore propose an alternative approach to navigating through orogenic architecture: subducted plate units comprise nappes (or mélanges) with Ocean Plate Stratigraphy (OPS) and Continental Plate Stratigraphy (CPS) stripped from their now-subducted or otherwise underthrust lower crustal and mantle lithospheric underpinnings. Upper plate deformation and paleogeography respond to the competition between absolute motion of the upper plate and the subducting slab. Our navigation approach through orogenic architecture aims to avoid *a priori* dynamic interpretations that link downgoing plate paleogeography to deformation or magmatic responses in the upper plate, to provide an independent basis for geodynamic analysis. From our analysis we identify 'rules of orogenesis' that link the rules of rigid plate tectonics with the reality of plate deformation. We use these rules for a thought experiment, in which we predict orogenic architecture that will result from subducting the present-day Indian ocean and colliding the Somali, Madagascar, and Indian margins using a published continental drift scenario for a future supercontinent as basis. We illustrate that our inferred rules (of thumb) generate orogenic architecture that is analogous to elements of modern orogens, unlocking the well-known modern geography as inspiration for developing testable hypotheses that aid interpreting paleogeography from orogens that formed since the birth of plate tectonics.

1. Introduction

The paleogeographic distribution of continents and oceans and their topography and bathymetry form key input for the analysis of past and present dynamics of system Earth, life, and resources (Dalziel, 1997, Groves and others, 1998, Stampfli and Borel, 2002, Scotese, 2004, Torsvik and Cocks, 2017, Poblete and others, 2021). Due to the destructive process of subduction, as much as 60% of the Earth's lithosphere that existed as recent as ~150 Ma ago has been recycled (Torsvik and others, 2010) and this number increases to 93% for times around 2.5 Ga ago (Hawkesworth and others, 2010). Hence, the largest part of the Earth's surface displayed on paleogeographic maps, including almost all of its former oceans, is interpreted. The basis for such interpretations are intensely deformed, in part metamorphosed, incomplete relics of subducted lithosphere hidden in orogenic belts. The challenge for paleogeographic reconstruction is thus to find diagnostic characteristics to date the series of arrivals of oceanic and continental crust in a trench from the unique architecture of an orogen.

The architecture and evolution of orogens have been studied for centuries, but particularly with the advent of plate tectonic theory, classifications of orogenic belts have been developed based on their interpreted formation history (for example, Şengör, 1990, Cawood and Buchan, 2007, Cawood and others, 2009). At first order, such classifications separate orogens that formed at long-lived oceanic subduction zones (for example, the Terra Australis orogen (Cawood, 2005, Cawood and others, 2011a), or the Central Asian Orogenic Belt (Xiao and others, 2010)) from orogens that are thought to result from continental collision (for example, the Caledonian orogen (Torsvik and others, 1996) or Himalaya-Tibetan orogen (Yin and Harrison, 2000)). But do such classifications also provide sufficient information to reconstruct paleogeography of lost lithosphere? Interpretations of orogenic history have long been used to infer pre-orogenic paleogeography (for example, Şengör and Yilmaz, 1981, Pindell and Dewey, 1982, Dercourt and others, 1986, Stampfli and others, 1991). But with the advent of the open plate reconstruction software GPlates (Müller and others, 2018), and the development of approaches to restore orogenic deformation using that software (van Hinsbergen, 2010, van Hinsbergen and others, 2011a, van Hinsbergen and Schmid, 2012, Boschman and others, 2014, Gurnis and others, 2018, Müller and others, 2019, Poblete and others, 2021), it is now timely to evaluate to what extent widely used orogen classifications provide a systematic and objective basis to quantitatively reconstruct paleogeography of lost lithosphere.

In this paper, we therefore first review current concepts of orogenesis and its link to paleogeography and motions of downgoing and overriding plates. We evaluate to what the predictions of these concepts fit with well-described, Mesozoic-Cenozoic orogens for which the syn-orogenic convergence history is constrained through plate circuits, and whose subducted lithosphere is still imaged by seismic tomography. From this analysis, and in addition to the 'rules of plate tectonics' that are based on the assumption of plate rigidity (Cox and Hart, 1986, Domeier and Torsvik, 2019), we then infer a set of general 'rules of orogenesis'. These rules (of thumb) aim to provide general guidelines to account for non-rigid plate behavior and link orogenic architecture as constrained from geological observations to the paleogeography and subduction history of a subducted plate, as well as the absolute motions of plates and slabs during subduction.

We then illustrate the use of these rules through a novel thought experiment. If our principles of reconstructing paleogeography out of modern orogenic architecture are valid, then we should arrive at realistic orogens when we construct orogens by subducting and colliding modern geography in a hypothetical future plate tectonic scenario. Our thought experiment uses modern geography of the Indian Ocean and its margins as a starting point and uses a recently constructed scenario of a future supercontinent (Davies and others, 2018) to subduct this ocean and collide the continental margins of Somalia and India. We will show the orogenic evolution and architecture as a function of two different initial subduction zone configurations. We will use the thus constructed orogens to evaluate whether the rules of orogenesis yield orogens with a structure similar to known orogens and discuss how similarities between thus predicted and existing orogens allows using modern geography as an analogue, inspiration, and test case for paleogeographic reconstructions.

2. Classification of orogens – a re-evaluation

2.1 Current concepts linking orogenesis to subduction and collision and how they apply to Mesozoic-Cenozoic orogens

2.1.1 Classifications of orogens

Orogenesis is the collective process of deformation, metamorphism, magmatism, mountain building, erosion, and sedimentation that typically occurs at convergent plate boundaries (Şengör, 1990). Of particular interest for paleogeography reconstruction, and a typical prelude to the end of orogenesis and subduction, is continent-continent collision. Such collisions are of interest to the wider geoscientific community as they mark the demise of prominent seaways, merge smaller continents into larger land masses, and raise topography potentially triggering major biological and environmental change (for example, Golonka and others, 1994, Cocks and Torsvik, 2002, Torsvik and Cocks, 2017, Poblete and others, 2021). Orogens have been widely recognized at suture zones (that is, fault zones that demarcate the location where a former ocean basin finally subducted) between continental blocks of different age, composition, and geological history. Orogenesis was therefore classically interpreted as the result of the continental collision stage of the Wilson cycle following the closure of an oceanic basin through subduction (Wilson, 1966). Since then, however, it has become clear that orogenesis also, or even predominantly, occurs during subduction in absence of collision (for example, Şengör, 1990) (Figure 1). A central theme in the debate on almost all orogens in collisional settings is thus when collision started and which features observed in the final orogen resulted from, or preceded collision.

Given the perceived impact of continental collision on a geological record, it is surprising that despite decades of study, estimated collision ages differ strongly even for young, well-constrained, and widely studied continent-continent collisions. Age estimates for the collision of the Indian continent with Asia vary from > 65 Ma to < 25 Ma (Ding and others, 2005, Leech and others, 2005, Aitchison and others, 2007, van Hinsbergen and others, 2012, Bouilhol and others, 2013, Hu and others, 2016, Kapp and DeCelles, 2019, Yuan and others, 2020). For the Arabia-Eurasia collision in Iran, ages vary from 40-5 Ma (McQuarrie and others, 2003, Agard and others, 2005, Vincent and others, 2007, Mouthereau, 2011, McQuarrie and van Hinsbergen, 2013, Zhang and others, 2017), and in eastern Turkey ages range from ~50-10 Ma (Keskin, 2003, Hüsing and others, 2009, Okay and others, 2010, Mouthereau, 2011, Cavazza and others, 2018, Darin and others, 2018, McPhee and van Hinsbergen, 2019). To place these ranges in plate kinematic perspective: between 65 and 25 Ma, there was 3200-4100 km (west to east) of India-Asia convergence, and between 50 and 5 Ma, there was 1000-1400 km (west to east) of Arabia-Eurasia convergence (van Hinsbergen and others, 2011b, Seton and others, 2012, McQuarrie and van Hinsbergen, 2013). It is thus impossible that the younger and older age estimates represent the same event.

The major spread in collision age estimates primarily results from different data types and concepts that are interpreted as diagnostic for initial collision. These concepts are for an important part derived from analogue and numerical modelling studies that have led to simple conceptual relationships between the arrival of topographic and bathymetric features on a downgoing plate in a trench, such as a major continent (but also 'blocks' or 'terranes' such as seamounts, oceanic plateaus, active or remnant volcanic arcs, accretionary orogens formed at outboard subduction zones (composite terranes) or microcontinental fragments (Tetreault and Buiter, 2012, 2014)) (Figures 1 and 2), and their effect on orogenesis. If such features do not simply subduct, they may leave three possible expressions in the rock record: (i) the highest rock units of the paleogeographic feature may decouple from the downgoing plate and accrete to the upper plate (Toussaint and others, 2004, van Hinsbergen and others, 2005a, Capitanio and others, 2010); (ii) the collision of the feature may cause deformation in the upper plate (Tapponnier and others, 1982, Cloos, 1993, Pusok and Kaus, 2015); or (iii) the feature may cause cessation, or relocation, of the subduction zone (for example, Hsü and others, 1995, Stern, 2004, Dewey, 2005).

Each of these expressions may leave records of deformation, sedimentation, metamorphism, and magmatism. The question in reconstructing paleogeography is which of these expressions are diagnostic for collision of small or large indenters. For instance, upper plate shortening and plateau uplift are thought typical for continent-continent collision (Cloos, 1993, Dewey and Burke, 1973), but are also common occur during oceanic subduction, such as in the Andes (Oncken and others, 2006, Şengör, 1990). Continental collision is thought to be typically followed by slab break-off (Davies and von Blanckenburg, 1995, Wortel and Spakman, 2000), but slab break-off may also result from, for example, arrival of a spreading ridge at a trench without continental collision (Atwater, 1989, Wu and Wu, 2019, Boschman and others, 2021b).

Following the early studies of orogenic evolution in context of plate tectonics (Dewey, 1969, 1976; Dewey and Bird, 1970) and the development of classification schemes for orogens (Şengör, 1987, 1990; Isozaki and others, 1990, Isozaki, 1996), Cawood and others (2009) proposed a simple, widely used, threefold classification of orogens. They provided a conceptual first-order correlation between paleogeography and orogenesis in which (i) 'Accretionary orogenesis' occurs during ongoing (oceanic) subduction, may form accretionary fold-thrust belts of ocean floor-derived rock units (including seamounts, plateaus, et cetera) and is associated with volcanic arcs that may be active for 100s of Ma. Examples of such accretionary orogens are the Japan orogen (Isozaki, 1996, Isozaki and others, 2010)(Isozaki, 1996, Isozaki and others, 2010), the Andes and North American Cordillera (Oncken and others, 2006, Wakabayashi, 2015), the Central Asian Orogenic Belt (Xiao and others, 2010), and the Terra Australis orogen of eastern Gondwana (Cawood and others, 2011a); with final ocean closure and the direct interaction of two continents at a trench, leading to short(er)-lived but large-scale shortening of both continental margins, arrest of subduction and slab break-off, deceleration and arrest of plate convergence, and termination of arc magmatism (Cloos, 1993), with the Alpine-Himalayan orogen a type example (Cawood and others, 2009); and (iii) intracratonic orogenesis results from shortening within continents due to far-field forcing. Examples are orogens in the South China Block from the Mesozoic (Li and Li, 2007) and mid-Paleozoic (Xu and others, 2016), both inferred to respond to far-field stresses associated with accretionary orogenesis, or the Atlas mountain belt of NW Africa (Brede and others, 1992) (Figure 3) and the Cenozoic Tien Shan and Mongolian orogens (Molnar and Tapponnier, 1975, Cunningham, 2005), both interpreted to respond to far-field stresses resulting from continent-continent collision (see also Dewey and Burke (1973). The accretionary orogenesis definition of Cawood and others (2009) includes all active margin processes that occur without continent-continent collision including, importantly, ophiolite obduction. Ophiolite obduction occurs when continents arrive in a trench below oceanic crust, and is thus essentially continental collision with an oceanic upper plate, the forearc of which may become preserved as ophiolites (Dewey, 1976, Agard and others, 2014). Şengör (1990) therefore identified 'obduction controlled' orogenesis as a separate class (see also Dewey, 2005), as it is typically associated with arrest and relocation of subduction, whereby the timing of obduction and the ensuing effects on subduction may vary along-strike of an orogen, depending on the shape of the obducted continental margin and the configuration of the subduction zone (Cawood and Suhr, 1992).

The concepts behind orogen classifications are widely used to inform paleogeographic reconstructions of the pre-orogenic upper and lower plates of subduction zones. Importantly these classifications interpret deformation in the upper plate and lower plate as dynamically linked and as a result, collision timing is often interpreted from the timing of upper plate shortening, plate motion changes, or arrest of arc magmatism (for example, Patriat and Achache, 1984, Vincent and others, 2007, Copley and others, 2010, Bouilhol and others, 2013). Such inferences then eventually feed into regional and global paleogeographic and plate tectonic reconstructions (Stampfli and others, 1991, Stampfli and Borel, 2002, Scotese, 2004, Windley and others, 2007, Li and others, 2008, Xiao and others, 2009, Merdith and others, 2017, 2020; Torsvik and Cocks, 2017, Müller and others, 2019). Systematic reconstruction of accretionary orogenic systems has already revealed that there are major variations between orogens of this type and many sub-types have been recognized, such as accretionary orogens that include continental fragments (for example, Stern, 1994, Badarch and others, 2002, Kröner and others, 2014), or accretionary orogens that underwent collisions with arcs, or with other accretionary orogens (Şengör, 1990, Şengör and others, 2008, Cawood and others, 2009, Xiao and others, 2015). Şengör (1990) identified at least 20 types and subtypes of orogens, and classifications are already simplifications. This shows that each orogen is unique and reconstructing the paleogeography of plates that were consumed during accretionary orogenesis thus requires a systematic, data-based approach that treats every orogen as windows into a unique plate tectonic and paleogeographic history. But given the importance of collision in paleogeographic, plate tectonic, and orogenic history, we first analyze whether the definition of collisional orogenesis allows unequivocal identification of the timing of major continent-continent collisions from the orogenic record.

2.1.2 Collisional orogenesis: what are diagnostic features of collision?

The definition of collisional orogenesis contains dynamic interpretations: it predicts that arrival of a continent (or another buoyant indenter) in a trench triggers upper plate shortening, causes slow-down and arrest of convergence, and ongoing gravitational pull on the subducted slab eventually causes its break-off, as well as arrest of arc magmatism (Cawood and others, 2009). Such features are indeed systematically found in numerical and analogue experiments of continents arriving in trenches (for example, Cloos, 1993, Chemenda and others, 1995, Boutelier and others, 2003, Luth and others, 2010, Duretz and others, 2011, 2014; van Hunen and Allen, 2011). It is important to note, however, that such experiments typically use a simplified setup using a two-plate system with convergence driven by a single slab that subducts below a mantle-stationary upper plate. Under those conditions, the buoyancy of a continent on the downgoing plate either leads to 'fender-bender'-style indentation into the upper plate (for example, Tapponnier and others, 1982, Pusok and Kaus, 2015), or to continental underthrusting and upper crust accretion while plate convergence decelerates to zero (for example, Toussaint and others, 2004, Van Gelder and others, 2017). Slab break-off is typically portrayed as a slow, diachronous process that may take 10 Ma or more, during which both plates and the intervening slab remain in a mantle-stationary position (for example, Duretz and others, 2011, 2014; van Hunen and Allen, 2011). If such conditions are met in reality, the definition of collisional orogenesis provides multiple ways of dating a collision, but these conditions are rarely, if ever, met in reality. We thus need to evaluate how the specific relationships between collision, deformation, plate convergence, and slab break-off apply to natural settings.

Geological records from the Mediterranean region suggest that many of the corellations predicted by the collisional orogenesis concept, between upper and lower plate deformation, plate convergence, and magmatism, are not, or certainly not always, applicable to collisional settings.

In the Mediterranean region, continental lithosphere has been arriving in trenches of the Mediterranean region for > 100 Ma, as recorded in the orogenic belts of for example the Dinarides, Hellenides, Anatolia, or the Alps (Stampfli and Hochard, 2009, Handy and others, 2010, Jolivet and Brun, 2010, Menant and others, 2016, Schmid and others, 2020, van Hinsbergen and others, 2020b) (Figures 4 and 5). This continental lithosphere rifted from northern Gondwana in the Triassic and Iberia and Eurasia in the Jurassic, and in the process became extended into elongated platforms and intervening deep basins (Frisch, 1979, Vissers and others, 2013). This continental realm was termed the Alps-Turkey plate (Stampfli and others, 1991) or Greater Adria (Gaina and others, 2013, van Hinsbergen and others, 2020b). Greater Adria was similar in size to Greenland (van Hinsbergen and others, 2020b) (Figure 3b) and had a comparable paleogeography as Zealandia in the southwest Pacific today (Mortimer and others, 2017) or as the continental fragments in Paleozoic time that now make up Central Tibet and SE Asia (Morley, 2018).

Arrival of Greater Adria lithosphere in trenches did not have the responses predicted by the concepts of collisional orogenesis in several important ways: (i) Continental arrival in trenches did not, or only after tens of millions of years of continental subduction, lead to termination of subduction. Instead, subduction of lower continental crust and mantle lithosphere continued almost everywhere, for example, inthe Aegean region (Figure 4), and Anatolia (Figure 5), but also in the Apennines, Alps, Dinarides, Betic-Rif, and Carpathians (Figure 3), and upper continental crust accreted as nappes forming continent-derived accretionary fold-thrust belts (Faccenna and others, 2004, van Hinsbergen and others, 2005a, Handy and others, 2010, Jolivet and Brun, 2010, Gągała and others, 2012, Romagny and others, 2020); (ii) arrival of continental crust in the subduction zone rarely led to upper plate shortening, but was instead widely accompanied by upper plate extension: the Tyrrhenian, Pannonian, Aegean, and Central Anatolian extensional back-arcs (Figure 3) mostly opened during continental subduction and nappe accretion (van Hinsbergen and others, 2005a, 2020b, Handy and others, 2010, Jolivet and Brun, 2010, Faccenna and others, 2014, Gürer and others, 2018). In fact, the region with the clearest upper plate shortening, central Anatolia in Oligocene to early Miocene time (Gülyüz and others, 2013, Lefebvre and others, 2013, Advokaat and others, 2014), was then situated above an oceanic subduction zone (Gürer and others, 2016); (iii) arrival of continental crust in trenches did not cease convergence, and even though decelerations of Africa-Arabia plate convergence have been tied to the arrival of the Arabian continent in subduction zones (Jolivet and Faccenna, 2000, Gürer and others, 2021), the arrivals of continental crust in the trenches of the Mediterranean region are not systematically associated with convergence rate changes; (iv) even though slab break-off events are multiple and widespread in the Mediterranean region (Davies and von Blanckenburg, 1995, Wortel and Spakman, 2000, Spakman and Wortel, 2004, van der Meer and others, 2018, Kästle and others, 2020), these only occasionally occur along, and more often within subducted continental margins (Figure 4); and (v) while some regions in the Mediterranean realm have well-developed magmatic arcs that formed above oceanic subduction zones (for example, northern Anatolia (Schleiffarth and others, 2018) and the northern Aegean to Pannonian region in the late Cretaceous (von Quadt and others, 2005, Zimmerman and others, 2007), orogens such as the Pyrenees and Alps have oceanic sutures (Figure 3) but no arcs, and an Eo-Oligocene arc in the Aegean region formed during continental subduction (Handy and others, 2010, Jolivet and Brun, 2010, van Hinsbergen and others, 2020b). Some volcanic chains with arc magmatic signature elsewhere on the planet have even been shown to occur in absence of active subduction, due to re-melting of previously subduction-enriched mantle (Richards, 2009, van Hinsbergen and others, 2020a).

Are these deviations from the general concept of collisional orogenesis the result of the extended nature of Greater Adria, calling for a distinct subtype of collisional orogenesis? We do not think so: recent data have shown that even the archetypal continental collision between India and Asia does not follow the predictions of the collisional orogenesis concept. The first continental crust of the Indian plate to arrive in a trench is dated at ~59 ± 1 Ma in the highest nappe of the Himalaya, the Tethyan Himalaya (Figure 6), through the first arrival of clastic sediment with Asian provenance in its stratigraphy (Hu and others, 2015). Several other ages for these flysch deposits along-strike reach ages of ~54 Ma (DeCelles and others, 2014, Orme and others, 2015). India-Asia convergence underwent a marked deceleration that is often ascribed to collision (Patriat and Achache, 1984, Copley and others, 2010), but this deceleration did not start until ~52 Ma (van Hinsbergen and others, 2011b). Because convergence rates were in excess of 15 cm/a, or 150 km/Ma, the delay between collision and deceleration reveals that there were hundreds, or even up to a thousand km of post-collisional subduction before deceleration started. Deceleration is thus not straightforwardly connected to collision with Asia (van Hinsbergen and others, 2019b) or with an oceanic upper plate that carried Asia-derived sediments (Kapp and DeCelles, 2019). Upper plate shortening in Tibet, and farther north towards Central Asia, has long been viewed as a direct response to collision (for example, Molnar and Tapponnier, 1975, Dewey, 2005). However, later documentation revealed that shortening in Tibet, and also in the Tien Shan and Mongolia, occurred already in the Cretaceous, during oceanic subduction and well before collision with continental rocks on the Indian Plate (Murphy and others, 1997, DeCelles and others, 2007, Kapp and others, 2007, Jolivet and others, 2010, van Hinsbergen and others, 2015a). Clearly, establishing which upper/intraplate shortening pulses are related to collision and which occurred during oceanic subduction cannot be constrained from intra-Asian shortening itself. Recent high-resolution stratigraphic records revealed distinct shortening pulses in Tibet that correlate with major India-Asia convergence rate changes around 70-65 Ma and 52-48 Ma, that is before and after collision, but not with the onset of continental collision itself (Li and others, 2020a, 2020b). Like in the Mediterranean region, multiple slab break-off events have been documented in the India-Asia collision zone from seismic tomography (for example, Van der Voo and others, 1999, Hafkenscheid and others, 2006, Replumaz and others, 2010b, van Hinsbergen and others, 2019b, Parsons and others, 2020). However, these break-off events occurred during ongoing subduction and slab volumes show that the first phase of slab break-off cannot have occurred before ~40-35 Ma (Replumaz and others, 2010a), that is, long after collision of the Tethyan Himalaya with Asia. Finally, interpretations of collision from arc magmatism in Tibet differ widely, but magmatism appears to have continued into the late Eocene (for example, Bouilhol and others, 2013, Zhu and others, 2015, Kapp and DeCelles, 2019). Hence, the relationships between collision, shortening, plate deceleration, and slab break-off predicted by the collisional orogenesis concept do not straightforwardly apply to the Paleocene collision recorded in the Himalaya.

While most authors insist that the Paleocene arrival of Asia-derived sediment in the Tethyan Himalaya recorded the collision between the Indian and Asian continents (for example, Ding and others, 2016, Hu and others, 2016, Ingalls and others, 2016, Searle, 2018), alternative hypotheses argue that this was a collision between an Asia-derived forearc with India that had drifted south in the Late Cretaceous opening a major back-arc basin that closed ~15 Ma after it collided with the Tibetan Himalaya (Kapp and DeCelles, 2019), or that the Tethyan Himalaya were part of a microcontinent that broke off India in the Cretaceous opening a several thousand km wide ocean basin in its wake (van Hinsbergen and others, 2012). The latter scenario advocates that continental collision between the main Indian continent and Asia occurred after a ~30 Ma period of oceanic subduction, in the latest Oligocene or early Miocene, around which time the Lesser Himalayan thin-skinned fold-thrust belt started to accrete (Figures 6 and 7). In this scenario, post-collisional shortening approximates contemporaneous convergence. If the latter scenario is correct, India-Asia collision could correspond to a shortening pulse recorded in the upper plate, for example in the Tien Shan (Sobel and others, 2006), to a mild deceleration of India-Asia convergence of a few cm / a (Molnar and Stock, 2009), and to the latest phase of slab break-off tomographically and geologically estimated to occur in Early to Middle Miocene time (Replumaz and others, 2010a, Webb and others, 2017, van Hinsbergen and others, 2019b). But even then, convergence did not stop - it is still > 4 cm / a today, of which 2 cm / a is accommodated by Indian underthrusting below Asia (Bilham and others, 1997), subduction was not associated with arc magmatism for the last ~15 Ma, and after the last phase of slab break-off, the Indian continent underthrust over a distance of 400-800 km below Tibet (Nabelek and others, 2009, Agius and Lebedev, 2013, van Hinsbergen and others, 2019b) (Figures 6 and 7): collision was clearly not associated with an arrest of convergence, the downgoing plate nor the trench were mantle stationary, and slab break-off did occur only 10 Ma after the arrest of convergence, but in an much different plate kinematic and geodynamic setting. The examples above identify that the interpreted causal relationships predicted by the concept of collisional orogenesis between collision and upper plate shortening, magmatism, plate motion change, and slab break-off are problematic.

2.1.3 Comparing collisional and accretionary orogens: how different are they?

The classification of accretionary versus collisional orogenesis already acknowledged that upper plate deformation may have entirely different causes. In collisional orogens, upper plate shortening and plateau formation is considered to result from friction at the nearest plate boundary due to the arrival of buoyant lithosphere (for example, Cloos, 1993). However, similar upper plate shortening and plateau formation during accretionary orogenesis (for example, in the Andes) is not tied to the arrival of indenters on a downgoing plate, but is a competition between (far-field driven) absolute upper plate motion and the absolute motion of the slab bend, that is of the knickpoint where a slab bends into the mantle (Şengör, 1990, Lallemand and others, 2005, 2008, Oncken and others, 2006, Schellart, 2008, Cawood and others, 2009, Schepers and others, 2017) (Figure 8). This means that changes in deformation in an upper plate are not only reflecting dynamic responses to the changes at the nearest plate boundary, but are the sum of effects on all plate boundaries as well as tractions at the base of the plate due to absolute plate motion and mantle flow (for example, Warners-Ruckstuhl and others, 2010). For instance, if the onset of absolute westward South American plate advance exceeded the roll-back rate of the subducting Nazca slab and caused the onset of upper plate shortening in the Andes in the early Eocene, as widely interpreted (Oncken and others, 2006, Schellart, 2008, Faccenna and others, 2017, Schellart, 2017, Schepers and others, 2017), then the same westward absolute South American plate motion explains the simultaneous opening of the Drake Passage between Patagonia and the Antarctic Peninsula by extension in the southern South American plate (Livermore and others, 2005) if it outpaced the advance of the northwest-dipping nascent South Sandwich slab (Lagabrielle and others, 2009, Vérard and others, 2012, Eagles and Jokat, 2014, Maldonado and others, 2014, van de Lagemaat and others, 2021) (Figure 9). Hence, the dynamic effects of collisions on upper plates need to be viewed in concert with all other stresses exerted on that plate and the geological records of stress changes in plates cannot be straightforwardly used to date collision.

The examples from the India-Asia collision and the Mediterranean region illustrate that also slab break-off or arrest in arc magmatism are not unequivocal diagnostic features to date collision of major continents, let alone smaller topographic and bathymetric features. They also illustrate that much of the orogenesis that formed these regions predated collision between major continents, and such a collision merely represents an end-stage of a long-lasting orogeny that for most of its history was syn-subduction (or accretionary, in the terminology of Cawood and others (2009). During this syn-subduction history, multiple 'collisions' of continental (or arc or plateau) blocks and terranes may have occurred during which only upper crustal nappes accreted and lower crustal and mantle lithospheric underpinnings subducted. Such lower crustal subduction is an efficient way to recycle large portions of continental crust into the deep mantle (for example, Spencer and others, 2017) – in addition to sediment subduction and subduction erosion that are more widely inferred mechanisms (for example, Stern, 2011, Cawood and Hawkesworth, 2019). This may add to the explanation why continental crustal volume has only slowly increased or even decreased since the onset of subduction despite similar production rates of new continental crust as prior to the onset of plate tectonics (Scholl and von Huene, 2009, Cawood and others, 2013, Hawkesworth and others, 2019).

So whereas particularly in the discussions on the amalgamation of pre-Pangean supercontinents it is common to interpret orogeny as the result of continent-continent collision (for example, Collins and Pisarevsky, 2005), pre-collisional accretionary orogenesis may produce many of the features of the collisional orogenesis definition, and may predate collision by tens or > 100 Ma. Discerning between collisional and pre-collisional orogenesis is thus challenging (for example, Brown, 2009), as illustrated by the difficulty in dating the collision between the North China cratons with the Central Asian Orogenic Belt along the Solonker suture that ended several hundred million years of oceanic subduction (Xiao and others, 2009). In fact, collisional orogenesis appears to behave the same as accretionary orogenesis: the downgoing plate may be offscraped to form an accretionary fold-thrust belt, and relative motion between slab, or continent, and upper plate determine the style of upper plate shortening: an underthrusting thick continental lithosphere such as India or Arabia generates an equivalent to a flat slab, whilst subducting thinned continental lithosphere such as in the Mediterranean region is able to subduct steeply and even roll back (Figure 8). To identify how plate convergence rate changes, upper plate shortening events, slab break-off phases, and changes in arc magmatism are related to collision, or to other geodynamic drivers, is an outstanding research goal. Using interpretations of these relationships to determine collision timing would introduce circular reasoning that is better carefully avoided. We therefore propose a set of field-based criteria for navigating through orogenic architecture free of dynamic interpretation, towards reconstruction of pre-orogenic paleogeography of the downgoing and overriding plate.

2.2 Navigating through orogenic architecture: subducted plate-derived units and upper/intraplate deformation

2.2.1 General characteristics of accretionary vs upper plate fold-thrust belts

We propose an orogenic reconstruction approach that uses geological observables to infer whether rock units in an orogen were derived from a subducted plate, and/or were part of a (deforming) upper plate, whereby we do not distinguish between upper plate or intracratonic deformation. This approach reconstructs subducted plate and upper plate deformation separately and interprets their paleogeography separately (Figures 1, 2, and 4). Magmatism or mineralization is best reconstructed separately throughout the orogen, in a purely kinematic approach without interpretations of dynamic drivers linking deformation, plate motion, magmatism or mineralization. This provides a dynamic interpretation-free kinematic basis for development or testing of dynamic concepts.

Accretionary fold-thrust belts form by transfer of rock from a downgoing to an overriding plate, whereby the original crustal and mantle lithospheric underpinnings of accreted rock units are lost to subduction or otherwise deep underthrusting (Figure 10). Upper or intra-plate portions of orogens may be extended or shortened, or both, but in absence of a subduction conveyor belt to transport large portions of lithosphere effectively into the mantle, such deformation necessarily affects the entire lithosphere. Shortening by a factor of two of an upper/intra plate leads to crustal thickening by a factor of two, whereas shortening in an accretionary fold-thrust belt could be 95% without leading to major crustal thickening if the accreting stratigraphy is thin. Thus, magnitudes of upper/intraplate shortening are typically much smaller than shortening accommodated in accretionary fold-thrust belts. For example, reconstructed shortening in upper plates of subduction zones reconstructed from the Cenozoic Andes is up to ~400 km (Eichelberger and McQuarrie, 2015, Schepers and others, 2017)) from the Cretaceous North American Cordillera is ~250 km (DeCelles, 2004)), and from Tibet and Tien Shan is ~1000 km, including the effects of lateral extrusion (van Hinsbergen and others, 2011a, 2019b)). For comparison, the rock units of the ~200 km wide Himalayan fold-thrust belt accommodated up to 900 km of shortening (Long and others, 2011), as much as the 1000 km wide upper plate area of the Tibetan plateau and Tien Shan. Minimum shortening of accreted units on the ~100 km wide small island of Timor is ~360 km (Tate and others, 2015, 2017), as much as in the > 600 km wide Andes. And shortening estimates only restoring known overlaps between the nappes of the ~400 km wide Aegean nappe stack, not even taking into account shortening accommodated within those nappes, yields ~1400 km of shortening (van Hinsbergen and others, 2005a), considerably more than for the much wider Tibetan plateau. And these shortening estimates only restore rock units that were left behind in the rock record and cannot take entirely subducted portions of (typically oceanic) lithosphere into account that may account for 1000's of km of additional convergence. Thus, whereas upper/intraplate shortening has a profound effect on paleogeography in developing high topography and plateaus (for example, Tibet, Andes, North American Cordillera, for example (Poblete and others, 2021)), it is of only secondary importance for concentrating and telescoping once far-apart paleogeographic units into narrow orogens. While accretionary fold-thrust belts may develop high and narrow ridges, they not necessarily do so (for example, on Cuba (Iturralde-Vinent and others, 2008)) and they may be of secondary importance for developing major topographic barriers. However, accretionary fold-thrust belts contain fragments of subducted lithosphere and hold the key to decipher lost plate paleogeography (for example, Isozaki and others, 1990, Isozaki, 1996). Below, we assess which geological observables are diagnostic features to recognize and reconstruct accreted versus upper/intraplate deformation and paleogeography.

2.2.2 Subducted plate-derived units: OPS and CPS

Accretion may occur in response to subduction of oceanic or continental lithosphere, and bathymetric and topographic features built thereon, such as magmatic plateaus, arcs, seamounts (Figure 2), or even pre-existing orogens that formed at other subduction zones (e.g., Figures 4, 5, and 7a). During accretion, rock units decouple from a downgoing lithospheric plate and accrete at the leading edge of the upper plate (frontal accretion) or below the upper plate (basal accretion) (van Gool and Cawood, 1994), while the lower crustal and mantle lithospheric underpinnings of the accreted rock units subduct or otherwise underthrust farther below the upper plate (Figure 10). Accretionary fold-thrust belts typically consist of a dominantly (meta)sedimentary crust comprising stacked upper crustal units that eventually rest upon the undeformed oceanic or continental foreland (which may still be actively subducting) (Figures 4, 5, and 7). Importantly, the nappes that constitute a crust of an accretionary fold-thrust belt were stripped from their pre-orogenic lower crustal and mantle lithospheric underpinnings: those underpinnings subducted and formed slabs (Figure 10). As a result, accretionary fold-thrust belts consist only of accreted crustal fragments, and typically contain no pre-orogenic lithospheric mantle: lithospheric mantle underlying accretionary fold-thrust belts regrew by post-accretionary cooling and by magmatic processes in orogens. Because the process of (re)growing of lithosphere is a slow process taking tens of millions of years or more (Caldwell and Turcotte, 1979, Lee and others, 2011), accreted portions of orogens tend to have a thick crust but thin lithospheric mantle (for example in the Aegean region (Endrun and others, 2011)) and this situation may prevail for at least tens of millions of years after the accretion. Indeed, much of the Tethyan accreted orogens, even from Mesozoic time, are underlain by low seismic velocity-mantle at shallow depth (for example, (Şengör and others, 2003, van Hinsbergen and others, 2010).

The composition, age, and pre-subduction geological history of subducted lithosphere may be inferred from the geochemistry and stratigraphy of the accreted relics that escaped subduction. A key concept to reconstruct the paleogeography of subducted ocean floor was developed from the orogenic architecture of Japan, by Isozaki and others (1990). Those authors identified accreted nappes of oceanic plate stratigraphy (OPS) (Figure 11). OPS consists from bottom to top of crystalline rocks of the ocean floor, mostly pillow lavas but occasionally also gabbros or peridotites that were exhumed to the sea floor (for example, Ueda and Miyashita, 2005), overlain by pelagic limestones or cherts and topped by coarsening upward trench fill deposits (hereafter referred to as 'flysch') that mark the arrival of the OPS sequence at the trench (Isozaki and others, 1990, 2010, Isozaki, 1996). We note, that flysch deposition requires land-derived clastic sediment transport to trenches, which particularly at intra-oceanic subduction zones is not always the case – approximately half of today's intra-oceanic trenches are sediment-starved (Geersen and others, 2018). In such cases, arrival of an OPS sequence in the trench may be better dated by volcaniclastic detritus or ashes overlying or intercalating with the (hemi-)pelagic sequence (Cawood, 1982, Cawood and others, 2009).

Geochemical analysis of the magmatic basement may reveal whether these formed at mid-ocean ridges, in which case the oldest chert approximates the age of the oceanic lithosphere that was underlying the OPS sequence (Isozaki and others, 1990, Isozaki, 1996). Alternatively, if the magmatic basement of an OPS sequence has a large igneous province (LIP), ocean island basalt, or island arc composition, it provides only a minimum age of the originally underlying lithosphere, but may reveal where hotspot tracks, LIPs, or arcs associated with other subduction zones developed within a now-subducted ocean basin (Isozaki and others, 1990, Ueda and Miyashita, 2005). OPS is widely recognized in orogens and has become instrumental in reconstructing lost oceanic lithosphere and paleogeographic features such as seamounts or plateaus thereon (Cawood, 1982, Wakita and Metcalfe, 2005, Maruyama and others, 2010, Kusky and others, 2013, Safonova and Santosh, 2014, Safonova and others, 2016, Ackerman and others, 2019, Wan and others, 2020, Boschman and others, 2021a, 2021b).

While well-preserved OPS sequences are found in many orogens, more commonly elements of OPS together with upper plate lithosphere become tectonically mixed, and often metamorphosed, in serpentinite or sediment-hosted mélanges (Cloos and Shreve, 1988, Maruyama and others, 1996, Festa and others, 2010). While the internal coherence of OPS sequences in mélanges is lost, they may still preserve an overall pseudostratigraphy with foreland younging metamorphism and stratigraphic ages (for example, in the Franciscan complex of California (Wakabayashi, 2015). The spread of stratigraphic ages of blocks in mélanges may thus still provide a first-order constraint on the age of the subducted lithosphere, and the age of accretion of mélange packages. For instance, the İzmir-Ankara mélange of Turkey (Figure 3a) contains radiolarian chert blocks with ages up to Triassic age (Tekin and others, 2002) constraining a minimum age for the subducted oceanic lithosphere of the Neotethys ocean in the eastern Mediterranean region (Figures 3b and 5).

Although stratigraphic sequences in continent-derived nappes are more diverse and complex, we here identify ‘continental plate stratigraphy’, or CPS, in analogy to OPS (Figure 11). Nappes in the Mediterranean region (for example, van Hinsbergen and others, 2005b, 2020b), but also in Cuba (Iturralde-Vinent and others, 2008), the Tethyan Himalaya (Gaetani and others, 1986, Garzanti, 1999), or Timor (Harris, 2011), may serve as examples of CPS sequences. In its simplest version, and based on the examples above, we infer that CPS consists from bottom to top of (i) pre-rift basement that itself may have formed, become metamorphosed, and intruded in a previous orogenic cycle; (ii) passive margin syn-rift clastic sediments often associated with rift-related magmatic rocks that fine upwards to hemipelagic sediments; (iii) open shallow- to deep-marine pelagic (limestones) or hemipelagic (clay-rich) sediments formed at passive margins; and (iv) coarsening upward flysch (Figure 11). The age of the flysch marks the arrival of the lithosphere carrying the CPS at the trench (for example, (van Hinsbergen and others, 2005a, Najman and others, 2010, Hu and others, 2015, Orme and others, 2015). The syn-rift sequence as well as the underlying basement are diagnostic markers for correlation with the original predrift conjugate continental margin (see for example the passive margin clastic sequences of the Indo-Burman ranges and NE Tethyan Himalaya to the west Australian passive margin by Cai and others (2016) and Yao and others (2017).

Accretion is a top-down process, and the deeper parts of an OPS or CPS sequence thus have a smaller chance of accretion. Accretion occurs when horizons in the downgoing plate become weaker than the plate interface and form a decollement horizon (see for example, Agard and others, 2016) (Figure 10). Such decollement horizons often coincide with for example evaporite layers, shale intervals (for example, the base of a trench-fill sequence), the basal unconformity between the sedimentary column and the underlying crystalline basement, or the brittle-ductile transition, and nappes are placed upon younger nappes along regionally contiguous thrusts (van Hinsbergen and others, 2005a, 2020b, Capitanio and others, 2010, Handy and others, 2010, Jolivet and Brun, 2010, Schmid and others, 2020). Also metamorphic soles, which are only 1-500 m thick lower-plate derived rock units that weld during incipient stages of subduction to the base of an upper plate preserved as ophiolites (Agard and others, 2016, Soret and others, 2017, Guilmette and others, 2018), classify as accretionary units.

When accreted rock units are relatively thin (they are typically a few hundred meters up to perhaps 10 km thick (for example van Hinsbergen and others, 2005a), identifying them follows straightforwardly from geological mapping. When the accreted units become thicker, recognizing them as accretionary becomes more challenging. In western Turkey, a thin-skinned, accretionary fold-thrust belt overlies a continental crust that is still ~30 km thick but that is located in the upper plate of an active, long-lived subduction zone that is associated with a single subducted slab that is still subducting today in the eastern Mediterranean region (Figure 3) or has recently detached (van Hinsbergen and others, 2010). This slab must contain the underpinnings of the western Turkish nappe stack, suggesting that it once contained also the 30 km thick crust of the deepest unit. Van Hinsbergen and others (2010) therefore suggested that the last accreted nappe comprised most of the crustal section, and subducting mantle lithosphere decoupled (delaminated) around the Moho. In western Turkey, this delamination may still be considered frontal accretion *sensu* (van Gool and Cawood, 1994) (Figure 10). In the Banda Sea and Scotia Sea regions 'whole crust' transfer from a downgoing to overriding plate during subduction of a single slab also occurred, but here delamination did not affect crust that arrived in the trench, but that instead was located adjacent to the trench along-strike of the subduction zone that was bounded by transform (or STEP (Govers and Wortel, 2005)) fault. Spakman and Hall (2010) proposed that the incorporation of continental crust of the Sula Spur – a continental promontory of Australia – into the SE Asian collage of the Eurasian plate was facilitated by a subducting slab expanding laterally by peeling off the mantle lithospheric underpinnings of the Sula Spur while rolling back (Figure 10). As a result, the Sula Spur crust became part of the upper plate, escaped deep burial and thrusting, and was instead fragmented by upper plate extension. Delamination through lateral slab growth (depicted as 'lateral delamination' in Figure 10) was recently proposed to explain how South America-derived continental fragments are currently located in between Scotia Sea back-arc basins in an upper plate position above subducting lithosphere of the South American Plate (van de Lagemaat and others, 2021). We thus classify the Sula Spur units and the Scotia Sea microcontinents (except for South Orkney and Jane Bank that were derived from the Antarctic Peninsula and were always part of the upper plate (Eagles and Livermore, 2002, van de Lagemaat and others, 2021) (Figure 9)) as accreted, even though the accretion process is mostly associated with crustal extension (Figure 10).

2.2.3 Diagnostic characteristics of accreted units

Diagnostic elements for accreted nappes, with CPS or OPS, is that they represent thrusted sequences decoupled from their original mantle and lithospheric underpinnings, contain flysch deposits at the top, and are separated by thrusts. The oldest flysch sediments in a nappe mark the moment that the OPS or CPS sequence came within reach of upper plate-derived sediments, and the youngest flysch below the upper nappe-bounding thrust marks the moment of nappe accretion and the onset of underthrusting of the next OPS or CPS sequence underneath (Isozaki and others, 1990, van Hinsbergen and others, 2005b). The youngest flysch (or continental foreland basin deposits ('molasse') such as the Siwaliks Group at the front of the Himalaya today (Parkash and others, 1980)) below the most frontal thrust of an inactive orogen marks the end of underthrusting (for example, Iturralde-Vinent and others, 2008, Hüsing and others, 2009). Accretion occurs as distinct events that may be synchronous for several hundred kilometers or more along-strike (for example, Schmid and others, 2004, 2008, 2020), as well as across-strike: in the Aegean region the age of the youngest flysch in portions of nappes that accreted in a foreland position correlates well with the estimated ages for peak pressure conditions in deeply buried, metamorphosed, and exhumed parts of that nappe (van Hinsbergen and others, 2005a). The accretion history in many nappe stacks is straightforwardly identified from flysch sections. Exceptions are where two decollement horizons form within the accreting sequence. Thrusts repeating units above the highest decollement then contain flysch sequences whereas those between two decollements repeat deeper CPS sections devoid of flysch (for example, the Kolbano sequence versus the Gondwana sequence of Timor (Tate and others, 2015, 2017), or the Balkanides versus the Rhodopes in southern Bulgaria and northern Greece (Schmid and others, 2020, van Hinsbergen and others, 2020b).

Another diagnostic phenomenon in accreted portions of orogens is high pressure, low-temperature (HP-LT) metamorphism, that is, at blueschist or eclogite facies conditions (Brown, 2007). While the presence of such metamorphism is a diagnostic marker for a geological unit accreted in a subduction zone, finding such units requires that rock units accreted at depth and that they were exhumed, in a subduction channel and/or through upper plate extensional unroofing (for example, Platt, 1993, Chemenda and others, 1995, Avigad and others, 1997, Gerya and others, 2002, Jolivet and others, 2003, Brun and Faccenna, 2008). HP-LT metamorphic rocks are widespread in the Tethyan region, but also in places in circum-Pacific orogens, but exhumation typically occurred episodically and in discrete, short-lived events (for example, Agard and others, 2009, Wakabayashi, 2015, Vitale Brovarone and others, 2018). Cenozoic HP-LT metamorphic rocks, or accretionary fold-thrust belts in general, are rare in the circum-Pacific orogens. Presence of HP-LT metamorphic rocks reveals accretion in a subduction zone, but absence of such rocks in an orogen is in itself not a conclusive argument that subduction did not occur.

The timing of peak pressure metamorphism provides a minimum age for the timing of accretion. When accretion occurs below extending upper plates, it is immediately followed by exhumation and decompression. Under such conditions peak pressure conditions coincide with the moment of accretion (for example, for the Aegean orogen (van Hinsbergen and others, 2005a)). For neutral upper plates, the duration of peak metamorphism may be long, and the ages may vary according to the method used. For instance, Lu/Hf dating of garnets in metamorphic soles in Oman and Anatolia revealed ages of prograde growth of garnets of

~104 Ma (Guilmette and others, 2018, Peters and others, 2018, Pourteau and others, 2019), whereas U/Pb zircon ages from the same rocks gave ages of 96 Ma (Oman) – 92 Ma (Anatolia) (Parlak, 2016, Rioux and others, 2016, Guilmette and others, 2018). The U/Pb ages coincide with U/Pb titanite and $^{40}Ar/^{39}Ar$ ages for hornblende as well as the onset of upper plate extension that follows from the formation of supra-subduction zone oceanic crust in the ophiolites above the sole (van Hinsbergen and others, 2015b). This suggests that the zircon ages recorded the end of peak metamorphism and the onset of exhumation but post-date accretion by as much as 12 Ma (Guilmette and others, 2018). For rock units that accrete below thickening upper plates, accretion may be followed by ongoing burial and continued prograde metamorphism. For such settings, which may include for example the Tso Morari eclogites that formed in deeply buried Tethyan Himalayan rocks that likely accreted in the Paleocene-early Eocene below the shortening and thickening Tibetan plateau (de Sigoyer and others, 2000, Leech and others, 2005), peak (pressure) metamorphism provides only a minimum age for accretion and the timing of flysch deposition in the same nappe is a better marker.

Conversely, as a rule of thumb, the presence of high temperature-low pressure (HT-LP) metamorphism is typical for upper plate settings, for example, within arcs or rapidly extending and exhuming back-arc regions (Brown, 2007, 2009). Where found in accretionary fold-thrust belts, HT-LP metamorphism often overprints preceding HP-LT metamorphism (Maruyama, 1997, Brown, 2009). There are some exceptions, in which accreted units reach high temperature during their burial: (i) metamorphic soles below ophiolites recorded prograde HT-HP to HT-LP metamorphism, which is thought to reflect elevated temperatures during subduction zone infancy prior to the cooling effects of long-lived subduction (Hacker and Gnos, 1997, Soret and others, 2017, Guilmette and others, 2018); (ii) elevated temperatures may result from (highly) oblique subduction, as it leads to low burial rates (Thompson and others, 1997, Plunder and others, 2018); (iii) a special case of (U)HT-LP metamorphism is documented from accreted crust of the Sula Spur in the Banda Sea region (Pownall and others, 2013, 2017), and also in western Turkey (Bozkurt and others, 2011, Schmidt and others, 2015). In these cases, HT-LP metamorphism is thought to be related to the inflow of asthenosphere below crust immediately after the delamination of its mantle lithosphere. This delamination marks the moment of accretion of the rock unit to the upper plate, and thus occurs immediately after accretion, but already in an upper plate setting (Spakman and Hall, 2010, van Hinsbergen and others, 2010) (Figure 10), where HT-LP metamorphism is more common.

2.2.4 Subduction without accretion: reconstructing entirely lost lithosphere

A key, but rarely explicitly formulated paradigm underlying paleogeographic reconstructions is the assumption that continental crust does not entirely subduct without leaving an accretionary geological record: if continental lithosphere subducts, it leaves a record of CPS behind in accretionary fold-thrust belts that, when restored for shortening, provide a reasonable approximation of the amount of subducted continental lithosphere. This basic assumption lies for instance at the basis of dating incipient continent-continent collision: the structurally highest CPS nappe, which is the first to arrive in the trench at which the orogen formed, is assumed to date collision, for example the Tethyan Himalaya (Najman and others, 2010, Hu and others, 2015, Orme and others, 2015) (Figure 6, Figure 7b). Independent arguments supporting this assumption may come from the CPS itself: the CPS of the Tethyan Himalaya contains Permo-Carboniferous syn-rift clastics and rift-related volcanics interpreted to have formed during continental break-up, suggesting that it indeed represents a distal continental margin stratigraphy (Garzanti and others, 1999).

If there, for instance, large age gaps between flysch sequences of successive nappes even though plate circuits demonstrate ongoing plate convergence, we generally assume that in the intervening period wholesale oceanic subduction occurred. The Phanerozoic orogens that formed during subduction of oceanic lithosphere at circum-Pacific margins demonstrate that accretion of OPS is rare and episodic. The vast majority of oceanic lithosphere of the Panthalassa, or Tethys, oceans subducted entirely, without accretion (Isozaki and others, 1990, Isozaki, 1996, Scholl and others, 2007). Such non-accretionary intervals may even be associated with subduction erosion during which previously accreted sequences may be removed from the geological record and buried in the subduction zone (von Huene and Scholl, 1991, Ranero and von Huene, 2000, Isozaki and others, 2010).

Conversely, there are no unequivocal cases where 100's to 1000's km of continental crust must have subducted without leaving CPS in the geological record. For instance, kinematic restoration of the CPS units that constitute most of the Mediterranean orogens, using their age of accretion based on flysch as well as minimum nappe dimensions revealed from modern orogenic architecture, leaves space for narrow ocean basins of which OPS is present and restores a continent whose shape and size straightforwardly corresponds to the conjugate north African-west Arabian passive margin (van Hinsbergen and others, 2020b) (Figure 3b). The Cimmerian blocks of Central Iran and Afghanistan appear to correspond well to the width of the conjugate Arabian margin from which they are thought to have rifted off in the

Permian (Stampfli and Borel, 2002) and there are no Mesozoic or Cenozoic passive margins of which the conjugate continental terrane must have entirely been lost to subduction.

One possible, but debated, exception may be the western margin of Australia. The Australian margin contains evidence for Triassic rifting and Jurassic oceanization, which is interpreted as a phase of continental breakup whereby a conceptual continent, known as Argoland, must have rifted off several tens of Ma prior to the breakup of India and Australia (Veevers and others, 1991, Gibbons and others, 2012).

SW Australia was conjugate to Greater India: restored area reconstructed from shortened CPS in the Himalaya accounts for 600-900 km of continental crust (Long and others, 2011) and provides a minimum width of Greater India that would make it reach a prominent fracture zone on the west Australian margin (the Wallaby Fracture Zone) when reconstructed in a Gondwana configuration, a reconstruction that is consistent with paleomagnetic data from the Tethyan Himalaya (Ali and Aitchison, 2005, van Hinsbergen and others, 2012, 2019b). But where the remains of Argoland reside that would have broken off western Australia, remains enigmatic. Fragments of Argoland conjugate to northwest Australia are likely represented by CPS sequences in the SE Asian orogenic collage (Hall, 2012), but recognized fragments are not large enough to cover the entire northwest Australian margin. The west Burma block and CPS in the adjacent Indo-Burman ranges thrust belt of Myanmar have been proposed as a candidate, for example based on correlations of detrital zircon spectra (Heine and others, 2004, Yao and others, 2017, Zhang and others, 2020), but detrital zircons have also been used as argument against this correlation (Sevastjanova and others, 2016). Ingalls and others (2016) instead constrained the distance from the Tethyan Himalaya at the timing of collision with Asia to the Indian continent (~2500-3500 km depending on the collision age and intra-Asian deformation reconstructions). They assumed that all of this area was continental, questioned the Jurassic age of rifting north of the Wallaby Fracture zone suggested by Gibbons and others (2012) and instead assumed that all of Australia's western conjugate margin was contained in Greater India and was consumed by subduction below Tibet after Paleocene collision. CPS records in the Himalaya show, based on ages of flysch and metamorphism, accretion in the Paleocene-Early Eocene (Tethyan, Greater Himalaya), and from the Miocene onwards (Lesser Himalaya) (Figure 7); there are no known records of flysch deposits that suggest accretion events in the intervening period in the Himalaya. This suggests that all lithosphere of Greater India that was subducted between the Early Eocene and Early Miocene, which covered that a reconstructed area equal to Arabia, has subducted without leaving an accretionary record (van Hinsbergen and others, 2019b). Van Hinsbergen and others (2012, 2019b) found it unlikely that this lithosphere was continental in nature, and proposed, supported by paleomagnetic data and volcanic evidence for rifting, that the Tethyan Himalaya rifted off India in the Cretaceous, opening an ocean basin that was subducted between Eocene and Miocene time without accretion. The debate on the paleogeography of Greater India is far from settled, but if the wholesale continental subduction interpretation of Ingalls and others (2016) is correct, this calls the basic paradigm of paleogeographic reconstructions into question, with far-reaching consequences for paleogeographic reconstructions and all biological, climatic, and geodynamic interpretations rooted therein. It would make dating continental collisions impossible: if thousands of km of continental lithosphere subducted without leaving a geological record after the accretion of the Tethyan Himalaya, such wholesale continental subduction might just as well have happened before that accretion. It would also require an alternative explanation for why continents become billions of years old instead of a few hundred million like oceanic crust. However, conclusive evidence from geology, tomography, or paleomagnetism for a 1000's of km wide continental Greater India as purported by Ingalls and others (2016), and required to justify the common assumption that the Paleocene collision of the Tethyan Himalaya with Asia represents the onset of continuous continent-continent collision, remains absent. Future detailed kinematic restoration of SE Asian OPS and CPS may be able to identify the paleogeographic extent of Argoland and resolve this paleogeographic debate, but for now the paradigm that continental subduction leads to accretion seems to be a reasonable assumption when interpreting paleogeography.

2.2.5 Juxtaposition of accretionary fold-thrust belts

Systematic identification of nappes and their timing of accretion may identify juxtaposition of accretionary fold-thrust belts that formed at different subduction zones. The key observation to this end is out-of-sequence thrusting and a break in the foreland younging ages of trench-fill sequences and/or HP-LT metamorphism. Juxtaposition of two pre-existing accretionary fold-thrust belts is common: it occurs at former trench-trench-trench triple junctions such as in Colombia (Pindell and Dewey, 1982) or Anatolia (Gürer and van Hinsbergen, 2019), may happen following back-arc basin closure (for example following Rochas Verdes basin closure in Patagonia (Eagles, 2016) or Arperos basin closure in Mexico (Martini and others, 2014)), or during collision of an accretionary orogen that formed below oceanic lithosphere preserved as ophiolites. For example, the Oman ophiolite and underlying accretionary fold-thrust belt derived from lithosphere that subducted below the Oman ophiolites will sooner or later arrive in the trench below Eurasia and become juxtaposed with the Makran fold-thrust belt. Such juxtapositions have been documented from the Balkan and eastern Mediterranean orogens: Early Cretaceous arrival of the passive margin of Greater Adria in the Balkan region in a trench below Jurassic oceanic lithosphere, exposed as ophiolites, led to accretion of OPS of the ocean floor off eastern Greater Adria, and subsequently to early Cretaceous accretion of continental nappes, after which slab break-off terminated subduction (Scherreiks and others, 2014, Tremblay and others, 2015, van der Meer and others, 2018, Schmid and others, 2020) (Figure 4). Following closure of the remaining ocean basin, the obduction-related orogen accreted in latest Cretaceous time as a composite nappe in the Aegean nappe stack and Upper Cretaceous flysch unconformably overlies a Jurassic and Early Cretaceous accretionary fold-thrust belt (van Hinsbergen and others, 2005a, Schmid and others, 2020). The southern part of the Anatolian orogen started forming below an oceanic upper plate that itself was consumed by subduction below Eurasia (Figure 5). The accretionary fold-thrust belt of Central and Southern Anatolia became during its ongoing formation juxtaposed against Eurasia. In conclusion, systematic stratigraphic, geochronological, and geochemical analysis of OPS and CPS sequences in orogens hold the key to deciphering the subduction history of lost oceanic or continental lithosphere, their paleogeography, the timing of arrival of paleogeographic features in a trench, as well as the juxtaposition of geological records that formed at different subduction zones.

2.2.6 Upper/Intraplate deformation

Because it is not possible to make an objective distinction between intraplate and upper plate deformation, we classify all deformation that affects upper plates of subduction zones, close to the margin or in the far field, oceanic or continental in composition, and contractional or extensional, as intra-plate deformation. As soon as a rock unit becomes accreted to an upper plate, it may become subject to intra-plate deformation. For instance, after their accretion, OPS and CPS nappes in the Aegean, Carpathian, and Apenninic orogens (Figure 3a) became extended, thinned, and exhumed as part of the upper plate while simultaneously accretion of new nappes at the trench continued (for example, van Hinsbergen and others, 2005a, 2020b, Jolivet and Brun, 2010, Royden and Faccenna, 2018). Accretion and intra-plate deformation may thus be diachronous across orogens (Gautier and others, 1999, Brunet and others, 2000, Jolivet and Brun, 2010, Tirel and others, 2013).

Upper plates above subduction zones may consist of oceanic or continental lithosphere (Figure 1). Studying upper plate oceanic lithosphere deformation is challenging because it is typically not exposed and will eventually subduct. Much of our knowledge of oceanic upper plate deformation comes from narrow strips of oceanic lithosphere preserved as ophiolites, which became incorporated in continental crust due to underthrusting of thick, buoyant crust (Dewey, 1976). Such buoyant crust may be a continental margin whose arrival led to arrest of subduction, such as in Oman (for example, Agard and others, 2010), but it may also be accreted OPS such as in Japan (Isozaki, 1996), California (Wakabayashi, 1992), or the Andaman Islands (Bandyopadhyay and others, 2020a, b), or accreted CPS, such as in Anatolia (van Hinsbergen and others, 2016) and ophiolite emplacement onto continental margins is typically preceded by OPS and CPS accretion (for instance, Béchennec and others, 1990).

Ophiolites consist of a more or less coherent (but often extended and fragmented (for example (Maffione and others, 2015b)) 'Penrose' pseudostratigraphy of mantle tectonites, lower crustal gabbros, sheeted dykes, pillow lavas, and pelagic sediments (Anonymous, 1972). It is important to note that in the literature, OPS and mélange derived from subducted oceanic lithosphere is sometimes also referred to as 'ophiolite' or 'meta-ophiolite' (for example, in Calabria (Rossetti and others, 2001, Liberi and others, 2006) (Figure 3). The ocean-derived units in Calabria, however, underwent HP-LT metamorphism, which is a diagnostic feature that they belonged to the downgoing plate (Rossetti and others, 2001, Liberi and others, 2006). Although accreted OPS units are certainly not always metamorphosed, they may be, whereas upper plate-derived ophiolites cannot become metamorphosed under HP conditions – at least not in the subduction zone of which they formed the upper plate.

Extensive geochemical research has demonstrated that the vast majority of ophiolites formed by spreading above a (nascent) subduction zone, so-called supra-subduction zone (SSZ) ophiolites (Pearce and others, 1984, Shervais, 2001, Wakabayashi and others, 2010), although occasionally coherent ophiolite bodies with a regular mid-ocean ridge geochemistry are found thrust upon continental margins (for example, the Masirah ophiolite of east Oman (Smewing and others, 1991, Peters and Mercolli, 1998). When oceanic crust or lithosphere has a SSZ geochemical signature it is a strong indicator that it formed in an upper plate setting close to a subduction zone (although such signatures are occasionally also found in regions where the no subduction can be independently demonstrated, such as in the Laxmi Basin off western India (Pandey and others, 2019) – perhaps such signatures can be inherited when mantle enriched during earlier subduction episodes re-melts (Richter and others, 2020, van Hinsbergen and others, 2020a)). Finally, an unequivocal indicator that an ophiolite formed as upper plate is the presence of a metamorphic sole at its base. As outlined above, metamorphic soles formed at a plate contact (Hacker, 1994, Hacker and others, 1996, Wakabayashi and Dilek, 2003, Agard and others, 2016, Guilmette and others, 2018) and ophiolites above soles unequivocally constitute the upper plate of a subduction zone – although not all upper plate-derived ophiolites have (exposed) metamorphic soles. Where these diagnostic features are present, former subduction zones below oceanic lithosphere are straightforwardly recognized in the geological record, and ophiolites are easily distinguished from underlying accretionary fold-thrust belts consisting of OPS and CPS.

Where continental upper plates are extended or not deformed, they are straightforwardly recognized from accretionary fold-thrust belts. More subjective is identifying upper plate shortening from accretion. Upper plate shortening is typically associated with thrusting, and thrust slices are necessarily decoupled from their original lower crustal and mantle lithospheric underpinnings. Even though intracontinental shortening, when viewed on the scale of an entire orogen like the Andes, is undergoing wholesale shortening and thickening of the lithosphere, this shortening is typically partitioned over multiple decollements (McQuarrie and others, 2005), and often only the rocks above the highest decollement are exposed. In the Andes, this highest decollement is east-verging (for example, McQuarrie and others, 2005), and could just as well be viewed as a westward continental subduction zone consuming the South American continental lithosphere. Such continental subduction of (mantle) lithospheric underpinnings decoupled from thrusted and thickened crust is for instance commonly portrayed for the Tibetan Plateau (Matte and others, 1996, Meyer and others, 1998, Tapponnier and others, 2001). Describing large-scale, asymmetric intracontinental deformation such as in Tibet and the Andes as continental subduction or intraplate shortening is to some extent semantic, but a key difference with subduction-accretion systems lies in (i) absence of OPS in intracontinental systems, and (ii) because the rate and amount of convergence in intraplate orogens is typically low (on the order of hundreds of km at a mm / a rates) and continental lithosphere do not form narrow, deep trenches but wider foreland basins (DeCelles and Giles, 1996), foreland propagating thrust slices dissect foreland basin stratigraphy. This makes that foreland basin sequences in adjacent nappes have overlapping ages (for example in the Andes (DeCelles and Horton, 2003, Horton, 2018). In subduction-accretion systems, where convergence rates are typically a few cm / a or more and trenches are narrow and deep even for subducting continental crust, the stratigraphies of foreland basin/flysch sequences between consecutive nappes are typically not overlapping in time: the arrest of flysch deposition in the higher nappe upon its accretion coincides with the onset in the flysch deposition and the onset of underthrusting of the lower nappe (for example, van Hinsbergen and others (2005b, 2020b).

A clear diagnostic feature for an upper plate position is the presence of subduction-influenced magmatism. The vast majority of orogens that form(ed) during subduction is associated with magmatic arcs, but as pointed out earlier in this paper, not all are, arcs are not always active, and particularly for intra-oceanic subduction zones, arcs not always preserved. For instance, ophiolites rarely obduct over distances of more than 150 km onto continental margins, that is less than the typical arc-trench distance (Gill, 1981). Hence, in most cases the volcanic arc associated with intra-oceanic subduction is not thrusted onto a continent but remains offshore and outside of the orogen. Such relict arcs then eventually subduct (and occasionally accrete as OPS sequences, for example in the Misis Mélange of southeastern Turkey (Floyd and others, 1991, 1992, Robertson and others, 2004) or in the Oku Niikappu OPS sequence in Hokkaido, Japan (Ueda and Miyashita, 2005), or the Kronotsky Arc of Kamchatka (Figures 12 and 13). Intra-oceanic arcs may be preserved in the geological record when obduction is followed by subduction polarity reversal. Such reversals often occur within the hot and weak arc (for example, (Dewey, 1976, 2005), and preserves the arc associated with the older subduction phase within an orogen. Examples are the Olyutorski arc of Kamchatka (Figures 12 and 13) (Konstantinovskaia, 2001, Shapiro and Solov'ev, 2009, Domeier and others, 2017, Vaes and others, 2019) and the Woyla arc of Sumatra (Barber, 2000, Plunder and others, 2020). Such accreted arcs may still be used to infer intra-oceanic subduction histories, particularly when combined with independent constraints such as seismic tomographic images of subducted slabs (van der Meer and others, 2012). The preservation potential of arcs that intruded continental upper plates, or accretionary fold-thrust belts, is high and arcs are widely recognized in orogens that date back billions of years (for example, Tatsumi and Eggins (1995). They provide excellent starting points for navigation through the deformation and accretion history of the orogen in which they formed.

In summary, wide foreland basins and overlapping foreland basin stratigraphies between adjacent thrust slices, arc magmatism, and regional HT metamorphism or, when oceanic, Penrose-type ophiolites particularly when associated with a SSZ signature above metamorphic soles, are diagnostic features of upper plates of subduction zones. However, none of these features or changes therein are directly diagnostic of the composition or paleogeography of the subducting plate. Instead, the independent analysis of the history of accretion and of upper plate deformation, magmatism, and metamorphism is key to understand the dynamic drivers of orogenesis, subduction, magmatism, and for example associated metallogenesis, and the role of changes in downgoing plate composition therein.

3. Future orogenesis as thought experiment

We now use our analysis of orogenic architecture and evolution above to formulate rules of thumb about the relationship between paleogeography, subduction, and absolute plate motion, summarized in Figures 2 and 4 and Table 1 and explained below. We will evaluate their use through a thought experiment in which we apply these 'rules' to construct future orogens from modern geography. The benefit of using present-day geography as starting point is that we avoid subjective interpretation of geological records, and also avoid circular reasoning: the analysis in the previous section is based on existing orogens and interpreted paleogeography. Obviously, whether our constructions correctly predict future orogens depends on a myriad of unknowns, and its predictive power is essentially meaningless: we would have to wait tens of Ma to test our hypotheses. But showing how well-known modern geography may evolve into an orogen as function of a set of 'rules' of orogenesis may provide a basis to show the plausibility of a paleogeographic interpretation based on a modern orogen. Moreover, it serves to illustrate how the combination of initial subduction zone geometry, downgoing and upper plate geography and stratigraphy (OPS, CPS), and absolute plate motion determine orogenic architecture.

Below, we deduce the 'rules of orogenesis', select a future plate tectonic scenario, and, for good measure, define a geological timescale for the future. With those, we then illustrate how orogens may evolve from subducting the modern Indian ocean and colliding its margins, with two selected, different subduction zone configurations as starting point.

3.1 Rules of orogenesis

The theory of plate tectonics describes horizontal motions of the lithosphere according to a set of geometric rules (for example Cox and Hart, 1986, Domeier and Torsvik, 2019). These prescribe that plates move along divergent (ridges), convergent (trenches) and transcurrent (transform) plate boundaries that end in triple junctions, and that area is conserved (that is, area consumed at trenches is globally balanced by area produced at ridges). New plate boundaries almost always form as a result of breakup of older plates or change of nature of existing plate boundaries (but see the origin of the Pacific plate at a triple junction for an exception (Boschman and van Hinsbergen, 2016)). New mid-ocean ridges following continental break-up form after rifting that typically starts at pre-existing weak zones and lasts for 10 Ma or more (for example the East African Rift is aligned along Precambrian crustal fabric (for example, Ring, 1994, Theunissen and others, 1996) and their formation is often associated with the arrival of mantle plumes and the eruption of LIPs (for example, Burke and Dewey, 1973, Buiter and Torsvik, 2014, van Hinsbergen and others, 2021). Formation of new mid-ocean ridges within oceanic lithosphere occurs much quicker, typically within 1 Ma (for example, Mittelstaedt and others, 2008) and hence appears to fit well with the assumption of plate rigidity. New subduction zones tend to initiate along existing plate boundaries (transform faults or STEP faults, mid-ocean ridges, or ridge-parallel detachment faults (Hall and others, 2003, Gurnis and others, 2004, Stern, 2004, Baes and others, 2011, Leng and Gurnis, 2011, Maffione and others, 2015a, Gülscher and others, 2019) or along passive continental margins or ancient fracture zones (Nikolaeva and others, 2010, Maffione and others, 2017, van Hinsbergen and others, 2019a, Auzemery and others, 2020).

As pointed out by Domeier and Torsvik (2019), additional rules for plate tectonic reconstructions may be inferred from our understanding of geodynamics – for example, subduction zones have a greater tendency to roll back than to advance (Schellart and others, 2008), or plate velocities typically do not exceed 20 cm/a, with a median velocity of 4 cm/a (Meert and others, 1993, Zahirovic and others, 2015). However, while these additional rules are firmly rooted in our current understanding of geodynamics, applying them as basis for kinematic reconstructions introduces circular reasoning when using plate reconstructions as boundary conditions for geodynamic analysis. Geodynamic arguments are thus best used with caution and moderation when making kinematic reconstructions.

An important caveat of the rules of plate tectonics, however, is that they describe the Earth as covered by horizontally moving rigid plates that move along discrete plate boundaries. While successful at first order and on long timescales, the process of orogenesis shows that this assumption is not always valid, particularly for convergent plate boundaries, but also on rifts. Our tentative set of 'rules of orogenesis' (Table 1) aim to provide a first-order prediction of how lithosphere deforms depending on its composition and its position on a subducting or overriding plate. For a subducting plate, these rules of orogenesis prescribe how geological units typical for a given geographic feature will behave once it arrives in a trench. For upper plates, we prescribe how deformation responds to relative and absolute motions of the subducting and overriding plate and the intervening slab (Figure 8). Our rules are kinematic: they prescribe deformation that will accommodate motion and make little inference on the dynamic drivers behind deformation. As a result, we make no rules for when and where relatively small-scale intraplate deformation will occur that results from the sum of stresses acting on the boundaries of a plate, its tractions with the mantle, and internal body forces.

Our rules of orogenesis primarily focus on deformation accommodated at convergent plate boundaries, but there is also intracontinental deformation associated with extension and breakup. Torsvik and others (2008) estimated that modern (hyper)extended continental margins generally accommodated ~150 km extension per margin during the 'rift' phase prior to onset of oceanic spreading (the 'drift' phase). We thus apply 300 km as a general number for 'pre-drift' extension, whereby we note that this number is depending on for example, initial crustal thickness, the width of the area that accommodates the extension, and the role of asymmetric (hyper) extension. The extensional provinces of the Aegean region and Basin & Range province, which both underwent crustal thickening prior to extension, accommodated ~400 km of extension without forming back-arc spreading ridges (McQuarrie and Wernicke, 2005, van Hinsbergen and Schmid, 2012), and perhaps up to 500 km of pre-drift extension would have been required for oceanization in these regions.

For subducting plates, we identify 'accretable' units that may accrete OPS or CPS sequences to an orogen (Figure 2) (see also (Tetreault and Buiter, 2012, 2014). For OPS units, we do not infer a necessity of accretion: there are well-known examples of accreted seamounts (Isozaki and others, 1990, Xenophontos and Osozawa, 2004, Sarıfakıoğlu and others, 2017, Yang and others, 2019, Wan and others, 2020), but the majority of subducting seamount chains in the Pacific basin are not associated with accretion. Similarly, OPS may accrete with subduction-related island arc (IAT) basement (for example the Oku-Niikappu arc of Hokkaido (Ueda and Miyashita, 2005) or the Kronotsky arc accreted to Kamchatka and exposed on the Komandorsky islands (Figures 12 and 13) (Bazhenov and others, 1992, Alexeiev and others, 2006)), or with MORB basement (Isozaki and others, 1990, Safonova and others, 2016), but we find no general rule to infer under which conditions such accretion occurs: in most cases, MORB basement and overlying sediments do not accrete at all but entirely subduct. Hence, we infer that periods of oceanic subduction may or may not lead to accretion of OPS units, as coherent units, or as chaotic mélange.

Particularly prominent features on oceanic plates are oceanic plateaus formed by LIPs. Such plateaus have a basaltic crust that may reach a thickness of 30 km or more and may cover large areas (Kerr, 2003): the Ontong-Java Plateau is as large as Madagascar. LIP arrival at trenches has led in places to arrest of subduction (for example, the Cretaceous arrival of the Hikurangi plateau in New Zealand (Davy and others, 2008)), or triggered subduction polarity reversal (for example, the arrival of the Ontong-Java plateau in the Vitiaz trench triggered the polarity switch to the New Hebrides trench (Hall, 2002)). Nevertheless, there are no major accretionary fold-thrust belts that represent accreted oceanic LIPs, suggesting that they eventually almost entirely subduct. For example, the Caribbean LIP is actively subducting along the Maracaibo trench in northwestern South America. Some relics of the Caribbean LIP were accreted to the NW South American margin in late Cretaceous time, and *in situ* crust of the Caribbean LIP is found on the Caribbean plate today (Mamberti and others, 2003, Neill and others, 2011). Plate reconstructions show that as much as 1500 km of LIP-covered lithosphere must have been consumed by subduction at the Maracaibo trench (Boschman and others, 2014). The vast majority of LIP crust and lithosphere thus subducted without accretion and resides in the shallow-dipping Maracaibo slab below northwestern South America (van der Hilst and Mann, 1994, van der Meer and others, 2018). Similarly, the Hikurangi plateau offshore New Zealand has undergone two phases of subduction, in the Cretaceous and since the Oligocene but there is no extensive accretionary record of subducted Hikurangi plateau rocks (Davy and others, 2008, Reyners and others, 2011). So, even though (meta)basalt occurrences with a LIP geochemical signature have been reported from accretionary fold-thrust belts (for example in the Pontides of northern Turkey (Can Genç, 2004), or in the North American Cordillera (Tardy and others, 2001, Wells and others, 2014)), LIPs appear to (eventually) subduct without leaving a geological record that is representative for its original paleogeographic dimension.

Recently, Wei and others (2020) claimed to have found evidence for such a subducted LIP in the subducted Kamchatka slab that is now located at the top of the lower mantle. They showed novel seismological results that reveal that part of the Kamchatka slab contains crust of more than 20 km thick. The along-slab distance to the trench suggests that this thick crust subducted in the middle to late Miocene, and Wei and others (2020) interpreted it as a LIP associated with the Hawaii-Emperor seamount chain (Figure 12), whose oldest seamounts are currently located close to the Kamchatka trench. They cited evidence for accreted Lower Cretaceous basaltic rocks known as the Kamchatka Mys ophiolite complex exposed in eastern Kamchatka, with a geochemistry consistent with plume-related magmatism (Portnyagin and others, 2008) as geological evidence for this LIP. However, these Kamchatka Mys ophiolites are widely interpreted to represent a late Cretaceous to Paleogene accretionary prism that formed below the Kronotsky intra-oceanic arc that was active between ~85 and 40 Ma and whose relics are found structurally above the Kamchatka Mys ophiolites (Khotin and Shapiro, 2006, Lander and Shapiro, 2007, Portnyagin and others, 2008) (Figure 13). In the early Late Miocene, the Kronotsky arc and the associated Kamchatka Mys accretionary prism accreted together to the Kamchatka accretionary prism (Levashova and others, 2000, Solov'ev and others, 2004), but subduction below the Kronotsky arc occurred 1000s of km to the east, within the Northern Pacific realm (Konstantinovskaia, 2001, Shapiro and Solov'ev, 2009), and the associated slab, which could contain a LIP associated with the Hawaii-Emperor hotspot chain, is not the Kamchatka slab, but the North Pacific slab which is located in the lower mantle 1000's of km east of Kamchatka (van der Meer and others, 2010, Domeier and others, 2017, van der Meer and others, 2018, Vaes and others, 2019) (Figures 12 and 13). The thick crust imaged by Wei and others (2020) in the Kamchatka slab more likely represents the subducted underpinnings of the Kronotsky intra-oceanic arc instead of a LIP (Figure 13), and whether or not the Hawaii-Emperor hotspot chain was ever associated with a now-subducted LIP remains to be demonstrated. Nonetheless, bathymetric features on the ocean floor such as seamounts, fossil arcs, and even large igneous provinces subduct without preserving an accretionary record, they may become 'ghost impactors' that may transfer stresses to the overriding plate and trigger deformation (Wan and others, 2020). Such ghost impactors could explain enigmatic orogenesis (for example, the Cretaceous Palmer Land orogenic event of the Antarctic Peninsula (Vaughan and others, 2012)), but we do not include any deformation associated with ghost impactors in our forward modeling scenarios.

We consider all fragments of continental crust on downgoing plates as 'accretable' and assume that of all subducting continental crust CPS will be accreted. In addition, we assume that extended continental crust (that is whole microcontinents or stretched continental margins) will subduct upon arrival in a subduction zone and that its CPS accretes, but that arrival of non-extended crust culminates in slab break-off and triggers the arrest of convergence. If convergence continues non-extended continental crust will horizontally underthrust the upper plate, with horizontal Indian underthrusting below Tibet as example (Nabelek and others, 2009) (Figure 6). For our thought experiment, we will use the somewhat arbitrary measure that we assume that submerged continental crust (that is continental margins, or microcontinents of the Mascarene Plateau (Seychelles, Mauritius) (Torsvik and others, 2013, Ashwal and others, 2017)) are sufficiently extended to subduct, whilst arrival of emergent continents such as Madagascar in a trench will lead to subduction arrest.

Finally, the leading edge of upper plate oceanic lithosphere will become preserved as ophiolites in an orogen if it is underthrusted by CPS or OPS nappes, and eventually a continent, followed by subduction arrest. Because after ophiolite obduction there is still oceanic crust present in the former upper plate, the eventual position of ophiolites in an orogen after full ocean closure depends on where subduction relocates after collision. If polarity reverses, such as in Kamchatka (see for example Konstantinovskaia, 2001) (Figures 12 and 13), forearc ophiolites and potentially the associated volcanic arc become incorporated as the highest structural unit of the orogen, in the upper plate of the younger active continental margin. If subduction transfers to the opposite continental margin, the ophiolite and underlying accreted OPS and CPS units may become a composite nappe in a younger accretionary fold-thrust belt, such as in the Balkan-Aegean orogen (for example, Schmid and others, 2020) (Figures 3 and 4).

Upper plate deformation is the result of the competition between absolute motions of the downgoing plate and the subducting slab (Şengör, 1990, Lallemand and others, 2005, 2008, Oncken and others, 2006, Sdrolias and Müller, 2006, Schellart and others, 2008, Cawood and others, 2009, Schepers and others, 2017) (Figure 8). One end-member scenario for upper plate shortening is the absolute advance of an upper plate outpacing roll-back of the subducting slab. In this case, the slab bend advances relative to the overriding plate (even if it may retreat relative to the mantle), and a flat subduction segment with enhanced plate contact area develops that increases friction at the plate contact, driving upper plate shortening. This is the classical case of the Andes (Oncken and others, 2006, Schellart and others, 2008) but probably also explains the Laramide orogeny in western North America (Boschman and others, 2018). The other end member is the opposite case where absolute advance of a slab outpaces upper plate retreat. A variation on this theme is where the downgoing plate carries a continent below an upper plate and does not subduct but underthrusts horizontally below the upper plate. In that case, continental edge advance (van Hinsbergen and others, 2020a) may be a better description than slab advance (Figure 8). Continental edge advance applies to the Neogene of Tibet, Iran, and eastern Anatolia, where following their respective arrivals at the southern Eurasian margin, continental lithosphere of India and Arabia advanced well beyond the original location of subduction and well beyond the suture, despite upper plate shortening that effectively led to upper plate retreat (Nabelek and others, 2009, Paul and others, 2010, Replumaz and others, 2010b, Agius and Lebedev, 2013, van der Meer and others, 2018, van Hinsbergen and others, 2019b). However, the last slab to break off India, currently residing in the upper mantle and top of the lower mantle below the Himalaya, is clearly overturned and offset northward, that is in the direction of Indian plate motion, relative to the deep lower mantle anomaly that is widely interpreted to contain most subducted Neotethyan lithosphere

(Van der Voo and others, 1999, Replumaz and others, 2010b, Parsons and others, 2020). This demonstrates that also prior to the arrival of buoyant Indian lithosphere the slab advanced, over a distance of some ~600 km, perhaps in response to interactions with the mantle transition zone, and likely caused flat slab subduction (van Hinsbergen and others, 2019b). Regardless of the interpreted dynamic drivers, upper plate shortening may correlate with lengthening of the plate contact and enhanced friction, of which the arrival of buoyant crust in a trench may be one, but certainly not the only driver.

Upper plate shortening is mostly accommodated by roughly trench-normal shortening, such as in the Andes (McQuarrie, 2002, Oncken and others, 2006, Ramos, 2009, Schepers and others, 2017), or in the North American Cordillera (DeCelles, 2004, Yonkee and Weil, 2015). Kinematic reconstructions of plateau shortening yielded estimates that after ~50-60% of upper plate shortening plateaus tend to grow outward instead of upward (England and Houseman, 1989, Tapponnier and others, 2001). Particularly in the Tethyan realm, however, some upper plate shortening is also accommodated by lateral, roughly trench-parallel extrusion, for example towards adjacent oceanic subduction zones. Such extrusion is well documented around the eastern Himalayan syntaxis in eastern Tibet and Indochina (Tapponnier and others, 1982, Leloup and others, 1995), in Anatolia (Dewey and Şengör, 1979, Sengör, 1979), and perhaps also around the western Himalayan syntaxis, towards Afghanistan, and eastern Iran (Tapponnier and others, 1981, Bagheri and Gol, 2020). Kinematic reconstructions of the effects of extrusion reveal that the contribution to accommodating shortening are limited: extrusion may have accommodated several hundred km of upper plate shortening in eastern Tibet, but this decreases rapidly westwards (Li and others, 2017) and extrusion of Anatolia accommodated no more than some tens of km of trench-normal shortening north of northwestern Arabia (van Hinsbergen and others, 2020b). In our constructions, we do not model extrusion, and as a rule of thumb, we apply a conservative maximum of 50% for upper plate shortening.

Deriving a quantitative relationship about the partitioning of slab advance relative to an upper plate, and upper plate shortening is more challenging. For many regions in the Andes, except for two flat slab segments of a few hundred kilometers wide, the Nazca slab bend is located close to the trench, suggesting that the ~1000 km of South American plate advance has been fully accommodated by the combined effect of slab roll-back and upper plate shortening. In Tibet, the last slab to break off, around 25-15 Ma is offset ~600 km northwards relative to a deeper slab that broke off ~40-35 Ma, revealing slab advance, yet is located directly below the Indus-Yarlung suture (Replumaz and others, 2010b, van

Hinsbergen and others, 2019b). This shows that much of the ~600 km of slab advance was accommodated by upper plate shortening. On the other hand, after the 25-15 Ma slab break-off episode, India has underthrusted subhorizontally below Tibet over a distance of up to ~800 km in the Miocene (Agius and Lebedev, 2013, van Hinsbergen and others, 2019b), during which time there was only a few hundred km of upper plate shortening (van Hinsbergen and others, 2011a). Hence, we derive no general rule for this partitioning at this stage, and our constructions merely display the expected style of deformation during phases of slab or upper plate advance.

Upper plate extension results from divergence between the slab and upper plate, with slab roll-back outpacing upper plate advance, or upper plate retreat outpacing slab advance as end-members (Lallemand and others, 2005, 2008, Sdrolias and Müller, 2006). For extending upper plate lithosphere consisting of continental crust or previously accreted fold-thrust belts, we apply the same rules of thumb as for continental break-up: formation of back-arc spreading ridges occurs following a phase of pre-drift extension, the amount of which depends on crustal thickness and may vary from ~300-500 km (Table 1), and may take tens of Ma (for example, (Gautier and others, 1999, McQuarrie and Wernicke, 2005, Jolivet and Brun, 2010, van Hinsbergen and Schmid, 2012). Upper plate extension may reactivate weak zones in the upper continental or oceanic plates, either within hot and weak arcs, or reactivating pre-existing weak zones, aided by local convection above subduction zones (for example, Sdrolias and Müller, 2006, Jolivet and others, 2009).

Where relative plate convergence occurs oblique to the margin, strain may partition over strike-slip faults and megathrusts (for example, Jarrard, 1986, Philippon and Corti, 2016). Like all subduction zones, oblique subduction zones may be associated with accretion of OPS or CPS, but the accretionary fold-thrust belt, and fragments of the upper plate lithosphere, may migrate laterally along the plate boundary (for example, in Sumatra (Malod and Kemal, 1996), or Myanmar (Morley and others, 2019) (Figure 6)). Oblique subduction may be associated with upper plate extension (for example, pre-Miocene Basin and Range (Schellart and others, 2010) or shortening (for example, in parts of the Andes (McQuarrie, 2002)), but the upper plate shortening and extension directions are in such cases often oblique to the trench (Figure 1). Lateral transport of forearc slivers may simply terminate in trench-trench-transform triple junctions, for example in the Sea of Java (Schlüter and others, 2002, Bradley and others, 2017), but may also result in margin-parallel extension (for example, the Andaman Sea (Curray, 2005)), or margin-parallel shortening forming fold-thrust belts at high angles to the trench (for example, in California along the San Andreas fault system (Kimura, 1996). In addition, major trench-parallel motion, on the order of 1000 km or more, may lead to large-scale buckling of the forearc sliver, forming oroclines (for example, in Alaska (Johnston, 2001, Shaw and Johnston, 2016) and eastern Australia (Cawood and others, 2011b, Rosenbaum, 2012)).

Finally, in addition to crustal deformation related to relative oblique plate motion, a recently realized additional phenomenon is slab dragging: the motion of a slab that is driven by absolute motion of a subducting plate, with the absolute motion component parallel to the slab as the most easily recognized form of dragging (Spakman and others, 2018). For instance even though the relative convergence direction between the Pacific and Australian plates at the Tonga trench is more or less trench-normal, the absolute motion of both plates share a strong northward component, which led to > 1000 km of trench-parallel slab dragging (van de Lagemaat and others, 2018) (Figure 8). Trench-parallel slab dragging must also affect the Burma slab that is subducting eastwards below the West Burma block in Myanmar (Figure 6), but that is attached to the rapidly northward moving Indian plate (Le Dain and others, 1984). The effects of slab dragging on the geological record are still poorly explored. Enigmatic slab-parallel shortening in Morocco (Capella and others, 2017), and poorly understood slab-parallel relative motion of mantle deduced from earthquakes around the Tonga slab (Giardini and Woodhouse, 1986) have been ascribed to trench-lateral slab dragging (Spakman and others, 2018, van de Lagemaat and others, 2018, Capella and others, 2020). Also, upper plate shortening in the northeastern Caribbean plate has been tentatively linked to the transition from trench-normal to trench-lateral absolute subducting plate motion (Philippon and others, 2020). It is at this stage too early to infer 'rules' for the effect of slab dragging, but such trench-parallel absolute slab motion may affect for example the propensity of slabs to roll back or advance (Chertova and others, 2014), and the examples above show that it may modify upper and lower plate deformation patterns.

3.2 A geological timescale of the future

In describing and portraying geological evolution, it is common and convenient to subdivide geological time in eons, eras, periods, and epochs. For the geological past, such timescales are primarily based on bio- or magnetostratigraphy (for example, (Gradstein and others, 2012), which is obviously an impossible basis for the future, but to stay on par with common geological literature, we defined for our thought experiment a geological timescale for the next 250 Ma (Figure 14). We color code isochrons in our tectonic maps according in accordance with the timescale. The 250 Ma long Eon of the 'Agnostozoic' refers to the unknown, the Eras are 100 Ma long Neozoic (new) and 150 Ma long Mellontozoic (future), the 50 Ma long Periods refer to circum-Indian Ocean languages, and the 10 Ma long Epochs to the numerals from one to five in these languages. The unit of time is Mega annum (Ma), but to indicate future time, we add 'future tempore', with abbreviation Maft.

3.3 Methods and boundary and initial conditions

For our construction of future orogens, we used GPlates plate reconstruction software (Müller and others, 2018). For the drift of major continents, we use rotations and polygons from Davies and others (2018) and added bathymetric and plate tectonic features of the modern Indian realm using polygons of Matthews and others (2016). Shape and rotation files of our modelled scenarios are provided in the supplementary information.

Davies and others (2018) constructed future supercontinents using three philosophies: introversion, extroversion and orthoversion, that make different assumptions about the nature of mantle convection on long geological timescales. Because the Indian Ocean contains irregular continental margins, as well as microcontinental realms and intervening ocean basins, we selected this region to apply the 'rules of orogenesis'. We therefore selected the 'extroversion' scenario of from Davies and others (2018), which creates the future supercontinent 'Novopangea', as basis for our thought experiment, in which the Indian Ocean closes and the Somali and Indian margins collide. In this scenario, the East African rift develops into an ocean and separates a plate that carries Somalia from Nubia in the Tinacene (Figure 14), at 25 Maft: while the Nubian continent continues its motion to the North, this fully developed Somalian plate, including Madagascar, drifts east to northeastward and converges with India. The model of Davies and others (2018) assumes that there is no future relative motion between India and Asia, and that both are part of a merged Indo-Eurasian plate. Australia keeps converging with Eurasia, and a plate boundary must exist in the eastern Indian Ocean, but we do not construct the eastern Indian Ocean in detail. The arrest of convergence between Somalia and Indo-Eurasia occurs at the end of the Swahilian (200 Maft).

Davies and others (2018) cast their constructions in a hypothetical absolute plate motion context and we use their choices on relative as well as absolute plate motions (east to northeastward for both Somalia and India) as boundary condition for our thought experiment. However, the models of Davies and others (2018) only display continental drift and define no plate boundaries. We thus add ridges and transforms in case of divergence and transcurrent motion, and subduction zones in case of convergence. To illustrate how different choices of initial subduction geometry lead to different orogenic architecture even with the same starting geography and bounding plate motions, we select two initial subduction zones in the Indian ocean: one starting along the modern Carlsberg Mid-oceanic ridge and one starting along the western Chagos-Laccadive Margin west of India. In addition, we added polygons of accretable units of the modern Indian ocean (Figure 15).

3.4 Initial conditions: modern geographical and geological architecture of (circum-) Indian Ocean

The Indian Ocean separates Nubia (Africa) and Arabia in the west, the Makran Subduction zone in the north, India in the northeast, Australia and the Sunda Subduction zone in the east, and Antarctica in the South (Figure 16). The Indian Ocean is not a single oceanic basin but rather displays a complex mosaic of smaller ocean basins separating (micro)continental blocks that presently span four different tectonic plates: the Arabian, Indo-Australian, Nubian, and Antarctic Plates. The latter three are separated by mid-oceanic spreading ridges that meet in a triple junction (Figure 15) (for example, McKenzie and Sclater, 1971). Arabia and Nubia are separated by the Red Sea Spreading ridge, Arabia and Somalia by the Gulf of Aden ridge, and Arabia and India by the Owen Fracture Zone (for example, Fournier and others, 2011). The latter two meet in a triple junction with the Carlsberg Mid-ocean ridge between India and Somalia (Figure 15). Because the Antarctic Plate diverges from the Indo-Eurasian, Somalian, and Nubian plates in the Novopangea construction, we do not consider the accretable units of this plate for our future orogens. We also do not construct a detailed geology for the between the diverging Nubian and Somalian continents, apart from a set of isochrons. In addition, Arabia does not play a key role in the closure of the Indian Ocean in the Novopangea scenario of Davies and others, (2018), and by the end of India-Somalia convergence there has not been interaction yet between the Australian continent and Somalia or Madagascar. We therefore simply assume the formation of the “Red Sea Orogen” as a result of Nubia-Arabia convergence and do not explicitly construct its orogenic architecture. It is geodynamically likely that the Sunda subduction zone below SE Asia (Figure 15) will roll-back, fragment, and consume Indian Ocean lithosphere in the future, and complex scenarios may be modeled similar to those that formed the Central Asian Orogenic Belt (Wakita and others, 2013). While such an exercise may serve as proof-of-concept for models to reconstruct Central Asia, this is beyond the scope of our study, and in our constructions, we assume that the Sunda Trench does not change its modern position relative to Indo-Eurasia. Our construction thus focuses on the Indian oceanic realm between India, Madagascar, and Somalia.

The Indian subcontinent contains a mosaic of Precambrian cratonic blocks and intervening Paleozoic or older former mobile belts inherited from the amalgamation of Gondwana and earlier supercontinents (Meert, 2003). Some of these intervening paleo-fault zones have been reactivated, are seismically active, and are potential locations for intra/upper plate deformation in our scenarios: these are the WSW-ENE Narmada-Son Fault Zone (Kumar and others, 2000, Rai and others, 2005) that runs approximately over most of the Indian continent, the NW trending Cambay Fault in the northwest (Yadav and others, 2011) and the Godavari and Mahanandi Rifts in the south (Rao, 2000, Mazumder and Eriksson, 2015) (Figure 15).

The Indian ocean to the south and west of India is characterized by several oceanic basins and large intervening bathymetric highs. Off the western margin of India lies the Laxmi Ridge, a microcontinental sliver that is separated from the Indian Continent by a narrow Paleocene ocean basin (Bhattacharya and others, 1994, Talwani and Reif, 1998). To the south and southwest of India lies the N-S trending Chagos-Laccadive Ridge that extends from 15°N to 10°S (Figure 15). The Laccadive Ridge in the north (15°N-8.5°N) contains extended continental crust (Nair and others, 2013) whereas the Chagos Ridge in the south (8.5°N-10°S) is thought to be volcanically thickened oceanic crust that may have resulted from interaction of the Reunion hotspot with the early Carlsberg ridge (Ashalatha and others, 1991, Henstock and Thompson, 2004, Nair and others, 2013). On the Somalian plate lies the bathymetric high of the arcuate Mascarene Plateau (Figure 11). The nature of the thickened crust is thought to mirror that of the Chagos-Laccadive Ridge: it is well established that the northernmost section of this plateau, the Seychelles bank, is continental in nature based on the presence of granitic rocks of Neoproterozoic age (~750 Ma) (Torsvik and others, 2001, Tucker and others, 2001) while it has long been thought that the southern part consists of thickened oceanic crust as a result of interaction between the Reunion Plume and the Carlsberg Ridge (for example, Bonneville and others, 1988, Mart, 1988). However, recent findings of zircon xenocrysts of Neoproterozoic age in upper Neogene basalts on Mauritius in the south of the Mascarene Plateau (Torsvik and others, 2013, Ashwal and others, 2017) show that the hotspot-related volcanics formed on a ridge of continental crust. Torsvik and others (2013) proposed that the Mascarene Plateau overlies a microcontinent with stretched Precambrian crust that was once contiguous with the Chagos-Laccadive Ridge before they were separated by a ridge jump from the Mascarene basin to the Carlsberg Ridge around 63 Ma (Collier and others, 2008, Ganerød and others, 2011).

Prior to ~63 Ma, the India-Africa plate boundary was located in the Mascarene Basin (Figures 15 and 16), which opened since the mid-Cretaceous (Schlich, 1974, Gaina and others, 2015), separating the Mascarene Ridge microcontinents, then still part of India, from Madagascar (Torsvik and others, 2013). Madagascar consist largely of Precambrian rocks related to Gondwana formation and older orogens, covered by Paleozoic to recent sediments, and intruded and overlain by a Cretaceous LIP (Windley and others, 1994, Torsvik and others, 1998). Madagascar was separated, together with India and Mascarene Microcontinents, from Africa by the opening of the oceanic Mozambique Channel between ~160 and 135 Ma (Storey and others, 1995, Gaina and others, 2013). In the north of the Mozambique Channel are the Comores islands that form part of a hotspot track (Emerick and Duncan, 1982) (Figures 15 and 16).

Finally, the African continent consists of cratonic blocks and intervening Paleozoic and older orogens that formed during assembly of Gondwana and earlier supercontinents (Lenoir and others, 1994, Stern, 1994, Kröner and Sassi, 1996). From the triple junction with the Red Sea and the Gulf of Aden to the south, the East African Rift system separates the Nubian and Somalian continents (Chorowicz, 2005, Corti, 2009) from where it connects as a diffuse plate boundary to the Nubia and Somalia-Antarctica ridges in the South Indian Ocean (Stamps and others, 2008) (Figure 15). In the Novopangea scenario of (Davies and others, 2018), the East African rift develops into an ocean basin, and this forms the western boundary of our thought experiment.

3.5 Results

3.5.1 Scenario 1: Subduction initiation at the Carlsberg Ridge

At the base of the Ekacene, at 0 Maft, subduction of the Somalian plate under the Indo-Eurasian plate is initiated at a location coinciding with the present-day Carlsberg mid-ocean ridge creating the intraoceanic *Hadiboh Subduction zone* (Figure 17). We model this trench as mantle stationary. As a result, the northeastward absolute motion of Indo-Eurasia prescribed by Davies and others (2018) requires upper plate extension. We accommodated this extension by the formation of the new *Kharif Supra-subduction zone spreading ridge* that develops in the forearc of the upper, Indo-Eurasian plate and migrates northeastward relative to the Hadiboh Trench at half-spreading rate. The Kharif Spreading ridge cuts a section from the Indian plate to create a new *Kharif Oceanic microplate*.

The Mascarene Plateau arrives obliquely at the Hadiboh Subduction zone in the Tinacene-Characene, between 28 to 33 Maft and subducts below the Kharif Microplate (Figure 17b), whereby its sedimentary cover accretes as the 1900 km wide *Mascarene Nappes*. This accretion uplifts the leading edge of the Kharif Oceanic microplate as the *Antsiranana Ophiolites*. This is followed by ongoing northeastward subduction consuming the Mascarene basin during which OPS may accrete. Farther north, the Somalian Continental margin arrives in the Hadiboh subduction zone in the Tinacene, at 28 Maft, also uplifts the forearc of the Kharif plate and forms the *Hobyo Ophiolites* below which CPS of the Somali passive margin accretes as the *Kismayo-Mogadishu Nappes* (Figure 17b). Following our general rule that unstretched, emergent continental crust will not subduct, its arrival in the Hadiboh Subduction zone stops subduction. We model that ongoing convergence is accommodated by a polarity reversal that consumes Kharif Plate lithosphere westward beneath the Somali margin, forming the *Ras Caseyr Subduction zone* (Figure 17b). At this subduction zone, OPS may accrete from the Kharif Plate, and after Kharif Ridge subduction, the Indo-Eurasian plate. The high angle of the Somali margin and the Hadiboh Subduction zone results in a diachronous obduction and polarity reversal starting in the Tinacene, at 28 Maft, in the north and ending at the end of the Panchacene, at 50 Maft, in the south (Figure 17b-d).

To the south, the Madagascar margin arrives in the Characene, around 40 Maft, at the Hadiboh Trench. This accretes Madagascar margin CPS as the *Toamasina nappes* below the Mascarene Nappes and possibly underlying OPS or mélange. Like in Somalia, we assume that the arrival of the Madagascar unstretched, emergent continent in the trench halts subduction of the Hadiboh Subduction zone, and leads to a polarity reversal, producing the *Ambre Subduction zone* along the eastern Madagascar margin. The obliquity of this margin dictates that this polarity reversal also propagates from north to south. The southern limit of the Mascarene Nappes, coinciding with the geographic location of Mauritius, are thrust upon central-eastern Madagascar. To the south of this, the *Farafangana* Ophiolites are not underlain by the Mascarene nappes, but only by OPS or mélange, and directly overlie the Toamasina nappes.

The polarity reversals along the Somali and Madagascar margins isolates an increasingly narrow east-dipping Hadiboh Subduction zone between the west-dipping Ras Caseyr and Ambre Subduction zones. Narrowing slabs have an increasing propensity to roll-back (for example, (Schellart and others, 2007) and we model Hadiboh Subduction roll-back around the northern tip of Madagascar into the north Mozambique Channel, whereby OPS from the Comores Seamounts may accrete below the Mascarene Nappes. This leads to ~180° counterclockwise rotation of the Mascarene Nappes and overlying Antsiranana Ophiolites, before they become emplaced over the northwestern margin of Madagascar in the Panchacene, between ~40 and 50 Maft. Emplacement drives accretion of CPS of the Madagascar margin as the Toamasina nappes and these nappes hence form a contiguous belt from western, to northern, to eastern Madagascar with a tight oroclinal shape (Figure 17d). However, whereas the Mascarene Nappes rotated up to a 180° from an original N-S position, the parallel striking Toamasina Nappes do not undergo significant rotations. In addition, the CPS of the Toamasina nappes of western Madagascar contain a much older (~180-160 Ma) passive margin sequence than those on eastern Madagascar (~100-80 Ma).

At the end of the Panchacene, around 50 Maft, the Hadiboh Subduction zone has everywhere collided with the Somali-Mozambique Margin. The roll-back of the subduction zone into the Mozambique Channel is associated with diachronous, southward propagating slab break-off along both the Mozambique Margin in the west and the western Madagascar Margin in the east, and the remaining subduction zone becomes progressively narrower as it rolls back southward. In our model, we assume the subduction zone does not propagate and widen into the south Mozambique Channel but breaks off when the trench arrives at the narrowest part of the channel. The result is a southward convex orocline, with ~180° counterclockwise rotated Antsiranana Ophiolites and Mascarene Nappes on western Madagascar, and not significantly rotated, but far displaced Mascarene Nappes and overlying ophiolites, together with perhaps accreted OPS from the Comores, overlying the *Dar-es-Salaam Nappes* that comprise CPS from the Mozambique Margin. Where the Mascarene Nappes no longer exist, the Dar-es-Salaam Nappes are directly overlain by the *Nyoka ophiolites* and possibly underlying OPS and mélange. The Nyoka Ophiolites are the northward continuation of the Farafangana Ophiolites and transition northward into the Hobyo Ophiolites. The Dar-es-Salaam Nappes transition northward transition into the Kismayo-Mogadishu Nappes (Figure 17d). The interaction of the Madagascar and east Somali Margins with the Hadiboh Subduction zone thus forms a belt of ophiolites that contains two sharp oroclines overlying passive margin CPS, and from Mozambique, along western and northern to central eastern Madagascar also contains the far-traveled Mascarene Nappes. The system is overlain by the Farafangana, Antsiranana, Nyoka and Hobyo Ophiolites, whose age of final emplacement on a continental margin occurred diachronously between the Tinacene and Panchacene, 28 to ~50 Maft. The north Mozambique Channel is underlain by back-arc basin crust that formed above the Hadiboh Subduction zone in the Panchacene, between ~40 and 50 Maft, whereas the southern Mozambique Channel is underlain by oceanic crust that formed during Jurassic separation of Madagascar and Africa. Upon arrest of the Hadiboh Subduction zone, spreading at the Kharif Spreading ridge ceases and after 50 Maft, the system returns to two plates, Somalia in the southwest, and Indo-Eurasia in the northeast. Spreading in the Kharif Forearc was nearly perpendicular to the mantle-stationary Hadiboh Trench from subduction initiation at 0 Maft onwards. Absolute Indo-Eurasian Plate motion of 3 cm / a (Davies and others, 2018) thus equals the spreading rate at the Kharif Forearc, and ophiolitic crust of the forearc recorded this at half-spreading rate of 1.5 cm / a or 15 km / Ma. In our construction, the width of the 5000 km long ophiolite belt is ~100 km, which would have formed in the first ~7 Ma after the onset of SSZ spreading, from 0-~7 Maft.

Following polarity reversal, we model that the Ras Caseyr and Ambre Trenches are connected through the *Mtwari Transfer Fault* (Figure 17d-f). The Somali plate undergoes eastward absolute plate motion and hence advances towards the west-dipping Ras Caseyr and Ambre Subduction zones. We assume that trench rollback velocity is lower than overriding plate advance, resulting in Andean-style overriding plate contraction and perhaps episodic flat slab subduction. This leads to uplift of the *Somali and Madagascar Plateaus* in response to upper plate shortening, which we assign an arbitrary 360 km of contraction from the Characene to the Efatracene (37-88 Maft) in northern Somalia decreasing to ~140 km from the Panchacene to the Layyocene (48-140 Maft) in the southern section of the Somalian continent, and ~100 km of contraction in Madagascar from the Panchacene to the Tanocene (40-200 Maft).

Upon closure of the Indian Ocean all ocean floor that had formed at the pre-subduction initiation Carlsberg Ridge in the Cenozoic (~63-0 Ma) (Collier and others, 2008) and subsequently at the supra-Hadiboh subduction Kharif Ridge in the Bengalian (0-50 Maft) has been consumed. The Indian margin first arrives in the Ras Caseyr Trench in the Efatracene (88 Maft). From this moment onward, the former Horn of Africa overrides the Indian continent around the Kathiawar Peninsula, creating the *Kathiawar Nappes* comprised of Indian margin CPS as well as remnants of the Deccan Traps-related volcanic complexes from the former Kathiawar Peninsula (Krishnan, 1963). The Kathiawar Collision zone subsequently forms a pivot for the Somali Plate that starts rotating counterclockwise relative to India (Davies and others, 2018). This moves the Kathiawar Nappes northward, whereby the previously underthrust West Indian Margin exhumes, or 'educts' (Andersen and others, 1991). The thus formed *West-Indian Gneiss Region* exposes metamorphosed India-derived nappes and crystalline basement (Figure 12). The Somalia-India rotation also diachronously closes the remaining Indian Ocean until the Mbilicene (170 Maft). While the associated, slow convergence may invite roll-back of the Ras Caseyr Slab and opening of back-arc basins within the Somali margin and overlying nappes OPS and CPS nappes and ophiolites, we do not add this complexity to our construction. Instead, we model a diachronous arrival of the Indian margin in the Ras Caseyr Subduction zone and the accretion of the CPS of the northern part of the Chagos-Laccadive Ridge and Indian Margin as the *Malabar Nappes* below the Somali margin (Figure 17e, f). In the central part of the collision zone, CPS of the Laxmi Ridge will accrete as a separate *Laxmi Nappe* separated by possibly accreting *Laxmi OPS or mélange* derived from the Laxmi Basin from the underlying Malabar Nappes but our maps simply display this as one coherent fold-thrust belt (Figure 17f, Figure 18b). By 200 Maft, convergence between Somalia and India comes to a halt, and has formed the *Somalaya Orogen*, with the east-verging, Mellontozoic (Myanmarian-Swahilian) (Figures 17, 18) India-derived nappes to the east and the Somali Plateau fringed by the west-verging, mostly Neozoic (mostly Bengalian) Hobyo Ophiolites and underlying Somali Nappes to the west, separated by the *Kilwa Suture zone* that may or may not contain OPS relics and subduction mélange (Figure 18a, b).

Finally, the relative India-Somali Plate rotation predict that the south Indian Margin arrives just north of the Mtwari Transfer Fault in the Ras Caseyr Subduction zone. To the south, the Laccadive Ridge arrives in the Ambre Subduction zone adjacent to the Madagascar Plateau. We model that this arrival accretes CPS of the *Chagos Nappes*, including extensive volcanic successions of the Chagos-Laccadive Ridge, to the east Madagascar Margin, after which westward subduction continues until the end of our modeled interval at 200 Maft (Figure 18c).

3.5.2 Scenario 2: initial continental margin subduction

In the second scenario, convergence between the Somali and Indo-Eurasian Plate initiates the *Malé Subduction zone* along the western margin of the Chagos-Laccadive Ridge/Chain. As in Scenario 1, we assume that this east-dipping subduction zone is initially mantle stationary. The ~3 cm / a northeastward absolute motion of the Indian Plate modeled by Davies and others (2018) then requires that the upper plate above the Malé Subduction zone undergoes extension. We choose to accommodate extension within the Indian Continent by interconnecting the reactivated Cambay fault zone, the Narmada-Son Fault zone, and the Mahanandi Rift zone (Figure 19). In the Duicene, by 12 Maft, this extension has exceeded 300 km, accommodated by pre-drift extension of the *Rewa Rift* within Indian continental crust, and marks the onset of formation of a slow-spreading *Rewa Spreading ridge*. As a consequence, the Indian continent is split into two, creating the *Dakshinapatha Plate (*and *Dakshinapatha Continent)* in the upper plate of the Malé Subduction zone, and the *Uttarapatha Subcontinent* that is part of the Indo-Eurasian plate (Figure 19a, b).

Keeping the Malé Subduction zone mantle stationary throughout the convergence history had as side-effect that the East Arabian Margin would start subducting in the northern part of the Malé Subduction zone. Because we intend to show what effect the initial subduction zone configuration has on orogenic architecture resulting from collision of the Indian and Somali Margins, we preferred to avoid this complication and chose to slowly migrate the Malé Subduction zone, and the Dakshinapatha Plate, southward such that the relative Dakshinapatha-Arabia motion is accommodated along a future version of the Owen Fracture Zone (Figure 19).

With this modification, the Mascarene Plateau arrives in the Malé Subduction zone in the Characene, between 31 to 37 Maft, and its lower crustal and lithospheric mantle underpinnings are diachronously subducted whereas its sedimentary cover is accreted as the 2300 km wide long *Mascarene Nappes* below the Laccadive Lithosphere in the upper plate. Following this accretion, oceanic subduction of the Mascarene Basin may be associated with OPS accretion below the Mascarene Nappes.

In the north, the former Horn of Africa arrives at the Malé Trench in the Characene, at 37 Maft, and starts subducting while accreting margin CPS as the *Punt Nappes* below the northern Dakshinapatha margin (and possibly below previously accreted OPS nappes or mélange) (Figure 19). Because it is unlikely that the thick continental crust of the Horn of Africa will subduct steeply into the mantle, and it is not kinematically possible to relocate subduction elsewhere, we assume that the Horn of Africa horizontally underthrusts Dakshinapatha. In response, Dakshinapatha is shortened to form the *Saurashtra Plateau*. In contrast, we assume that towards the south, where oceanic crust continues to subduct below Dakshinapatha along the Malé Subduction zone, no flat slab subduction occurs, and we model a neutral upper plate. To accommodate the relative motion of the northern and southern section of Dakshinapatha we reactivate the remaining section of the *Narmada Fault zone* (Figures 15 and 19) as a dextral strike-slip fault.

In the Panchacene, around 44 Maft, Madagascar arrives in the Malé Subduction zone, after subduction continues for 2 Ma until 150 km of the continental margin has been subducted. This leads to the accretion of the overlying CPS as the *Panganales Nappes*, below the Mascarene Nappes and possibly underlying OPS and mélange, and the Chagos-Laccadive Ridge in the upper plate. Arrival of unstretched Madagascar crust leads to arrest of subduction and slab break-off. Because the upper plate consists of (micro-)continental lithosphere, we choose in this scenario to accommodate ongoing convergence by initiating the *Qamar Subduction zone* along the western margin of Madagascar (Figure 19). To the north, the Malé Subduction zone remains unchanged, and connects with the new Qamar Subduction zone. This re-initiation of subduction leads to a temporary narrowing the Malé Slab, increasing its propensity to roll back. As a result, we let the Malé Subduction zone rotate clockwise, and the Qamar Subduction zone counterclockwise, towards the curved Somali Margin (Figure 19), which is followed by continental underthrusting of this margin at both subduction zones at the beginning of the Iraycene (50 Maft). This leads to accretion of CPS as the *Dar-es-Salaam Nappes* between Madagascar and the south Somali Continent establishing the *Mahajanga Suture* (Figures 19 and 20), and to emplacement of the *Kismayo Nappes* between the Chagos Margin and the north Somali Margin establishing the *Kanheri Suture* (Figures 19 and 20). The opposite rotations and oroclinal bending results in trench-parallel stretching of the Malé Subduction zone, and possibly the formation of a spreading ridge, of the Chagos-Laccadive Forearc. If margin-parallel stretching forms a spreading ridge,these may become preserved as ophiolites with Panchacene crustal ages, slightly older than 50 Maft, not much older than or even overlapping with the age of obduction and with spreading directions parallel to the trench.

Roll-back of the Malé Trench, and the associated clockwise rotation, triggers extension in the upper, Dakshinapatha Continent. We accommodate this by opening of two back-arc basins: the *Godavari Back-arc basin* separates Dakshinapatha into the *Deccan-Dharwar Block* and the *Bastar Block* and the *Mangalore Back-arc basin* separates the Chagos-Laccadive Ridge from the Deccan-Dharwar Margin. The Godavari Back-arc basin does not reach oceanic conditions within the Dakhinapatha Continent but propagates southwards into the ocean where it forms a spreading ridge. The Chagos-Laccadive Ridge/Chain also becomes oceanic southward where extension exceeds 300 km. Both basins end in a pivot point in the north and abut against the *Sri Lanka Transform fault* in the south. Opening of the Mangalore Back-arc basin ceases when the Somali continental margin arrives in the Malé Trench and subduction stops. This finalizes the formation of the *Mumbay Orogen* that separates the Chagos-Laccadive and Saurashtra Plateau upper plate from downgoing plate-derived, Mascarene and Kismayo Nappes that comprises Somali Margin CPS, and possibly OPS and mélange along the Kanheri Suture zone (Figures 19d and 20).

Post-50 Maft convergence is subsequently transferred to subduction of the Rewa Ocean along the southern margin of Uttarapatha and the western margin of Sundaland and continues into the late Neozoic and Mellontozoic, until the end of the assembly of Novopangea. Because we aim to compare the orogens between India, Somalia, and Madagascar between the two scenarios, we do not model the orogenesis due to the closure of the Rewa Ocean in any detail.

4. Discussion

Below, we evaluate to what extent our rules of orogenesis translate the modern geography of the Indian ocean and the plate kinematic scenario of Davies and others (2018) into sensible orogens with a similar architecture as modern orogens. But first, we briefly discuss some caveats of our thought experiment. First, the scenarios we model are only two examples of many possible initial subduction zone configurations, and there is no reason to assume one initial condition is more likely than the other. It is also possible to vary within each scenario, for example with other locations for subduction initiation, with the absolute motion of the subduction zone, or through slab segmentation. Such possibilities, however, are not limitations of the models that we produced but rather provide opportunities to explore the effects of a more complex evolution of plate boundaries than modeled here on final orogenic architecture. Second our constructions strictly follow the kinematic evolution of the Somali and Indo-Eurasian plates as in the scenario of Davies and others (2018). It is likely, however, that different initial subduction configurations would lead to different dynamic evolution of plates. For instance, the subduction polarity reversal in Scenario 1 would change the Indo-Eurasian plate from an upper to a lower plate position, and this process may have an effect on its absolute plate motion (for example, Domeier and others, 2017). Additionally, the southward motion of the Dakshinapatha plate during the Bengalian in Scenario 2 that we invoke to avoid the complexity of collision with the Arabian margin may not be geodynamically realistic in absence of a subduction zone in the south to drive such plate motion. For the purpose of our thought experiment, however, in which we simply aim to illustrate how the interplay between plate kinematics, subduction zone configuration, and paleogeography is reflected in orogenic architecture, such geodynamic considerations are not of importance – they would simply lead to a somewhat different kinematic history, and hence to a somewhat different orogenic architecture.

With these caveats in mind, we now explore similarities and differences between our model orogens and real orogens. Not surprisingly, the first-order architecture of the Somalaya and Mumbay orogens (Figures 18 and 20) are similar to known orogens: an accretionary fold-thrust belt derived from downgoing plate CPS and possibly OPS (equivalent to for example, the Himalaya or Zagros) separated by a suture zone from a deformed upper plate. The Somali plateau in Scenario 1 may be in part equivalent to for example the Tibetan or Iranian plateaus (Figure 6), even though it formed entirely prior to arrival of the Indian continental margin in the Ras Caseyr subduction zone, and the southern Tibetan Plateau is not overlain by ophiolites (those instead overlie the Himalaya). Somali plateau formation resulted entirely from overriding plate advance, whilst the Iranian and Tibetan plateaus appear more related to continental edge advance in the downgoing plate (Figure 8) – similar to the Saurashtra plateau of Scenario 2. Similarly, the Mangalore or Godavari back-arc basins behind the Mumbay orogen at 50 Maft may be equivalent to the Liguro-Provencal and Tyrrhenian back-arc basins, Figure 3) behind the Apennines (Faccenna and others, 2001), or the South Fiji and Lau basins in the upper plate adjacent to the Tonga trench (Karig, 1970, Seton and others, 2016).

Subduction in Scenario 1 initiates in an intra-oceanic position and results in the emplacement of a ~ 5000 km long, curvilinear belt along the Somali and Madagascar margins. The 100 km wide ophiolite belt contains crustal ages that cover a 7 Ma range. Such narrow age bands are commonly observed in long ophiolite belts (for example, Robertson, 2002, Dilek and Furnes, 2011, Dewey and Casey, 2013, Gaina and others, 2015) – and this range would be even narrower if our scenario would include slab roll-back shortly after subduction initiation, which would generate higher upper plate spreading rates. It is important to note that the Kharif supra-subduction zone spreading ridge remains active for 50 Ma, in this case until obduction and subduction polarity reversal is finalized. This illustrates that the age range of crust found in ophiolite belts is not representative for the longevity of supra-subduction zone spreading but is the result of the preservation of only a narrow strip of the total ocean floor produced at the SSZ ridge (for example, Maffione and van Hinsbergen, 2018)).

The ophiolites of Scenario 1 may all have the same oceanic crustal ages, but the arrival of continental crust below these ophiolites differs strongly along-strike. This is also a feature that is well-known from the geological record. In our example, the subduction of the

Mascarene ribbon continent and the accretion of the Mascarene nappes occurs diachronously between 28 and 33 Maft, after which the eastern Madagascar margin first arrives around 40 Maft, and roll-back and oroclinal bending leads to final emplacement of ophiolites around 50 Maft. The Madagascar and Mascarene scenario bears strong similarities to ophiolite obduction in the eastern Mediterranean region (even though there was no subduction polarity reversal in the Mediterranean case). The first continental crust to arrive below an Eastern Mediterranean belt of ophiolites with a narrow age range (94-90 Ma) comprises the now-rootless nappes decoupled from their original lithospheric underpinnings (Tavşanlı and Kırşehir massifs (Figures 3 and 5), equivalent to the Mascarene nappes) and occurred around 90-85 Ma (Whitney and Hamilton, 2004, Pourteau and others, 2019, Radwany and others, 2020). These were emplaced after subduction of a narrow oceanic basin that bounded the Tavşanlı-Kırşehir massifs to the south onto the margin of Greater Adria around 70 Ma (Pourteau and others, 2013), that is with a similar time delay as in our case of Scenario 1 (even though convergence rates for the eastern Mediterranean region were considerably lower, and paleogeographic width of the ocean basins narrower (van Hinsbergen and others, 2020b). East of the Kırşehir massif, oceanic subduction below ophiolites continued longer, until ~70 Ma (van Hinsbergen and others, 2020b), but the age of the first continental arrival below the ophiolites then gradually becomes older again to ~85 Ma on easternmost Greater Adria (Topuz and others, 2017) due to diachronous arrival of the continental margin in the trench, equivalent to the Somali margin in Scenario 1. Between Greater Adria and Arabia, the ophiolite belt was bent into a westward convex orocline (Figures 3b and 5) due to slab roll-back into the Eastern Mediterranean ocean (Maffione and others, 2017). As a result, it took ~20-25 Ma from formation until final emplacement of ophiolites on both margins of the eastern Mediterranean ocean around 70 Ma (Özgül, 1984, Al-Riyami and others, 2002, Kaymakci and others, 2010, McPhee and others, 2018, McPhee and van Hinsbergen, 2019), similar to the roll-back invasion of the north Mozambique channel in scenario 1 (Figure 17).

Orocline formation due to slab roll-back invading oceanic embayments is often interpreted from the geological record, for example, the late Cretaceous eastern Mediterranean example above, but also the Carpathians (Csontos and Vörös, 2004, Ustaszewski and others, 2008), or the Alboran region (Lonergan and White, 1997, Rosenbaum and others, 2002, van Hinsbergen and others, 2014) (Figure 3). Our construction illustrates that the Mozambique channel may provide a modern example of a geography that will be prone to the formation of such oroclines.

The polarity reversals along the Somali and Madagascar margins in Scenario 1 yield geological records that are commonly observed. The diachronous polarity reversal of Madagascar covers a similar time span, generates a similar orogenic architecture, and occurs over a similar distance as reconstructed from Kamchatka (Figures 12 and 13) (Konstantinovskaia, 2001, Shapiro and Solov'ev, 2009, Domeier and others, 2017, Vaes and others, 2019). And although we did not construct the Sunda trench in any detail in our thought experiment, this arc arrives in the Ambre subduction zone below Madagascar around 200 Maft, a situation reminiscent of the arrival of the Kronotsky arc below Kamchatka (Figures 12 and 13) (Shapiro and Solov'ev, 2009, Domeier and others, 2017, Vaes and others, 2019). The westward obduction followed by a subduction polarity reversal along the north Somali margin yields an orogenic architecture for the Somalaya orogen of Scenario 1 that bears similarities to the Balkanides and Hellenides architecture in the Mediterranean region. The Balkanides (and Rhodopes that likely formed structurally below the basal decollement of the Balkanides) formed first due to CPS accretion during southward continental margin subduction below oceanic crust preserved as the East Vardar Ophiolites, followed by a polarity reversal (Figures 3 and 4). After closure of the remaining ocean followed accretion of Greater Adriatic margin CPS in the latest Cretaceous and Cenozoic (van Hinsbergen and others, 2020b). The Hellenides are equivalent to the Malabar nappes, the Balkanides/Rhodopes and East Vardar ophiolites to the Kismayo and Dar-es-Salaam nappes and Hobyo ophiolites, respectively. What differs in the Mediterranean case is that the Greater Adriatic margin (equivalent to the west Indian margin) was prior to latest Cretaceous Sava ocean closure also obducted by ophiolites (with metamorphic soles, hence upper oceanic plate derived (for example, (Liati and others, 2004, Tremblay and others, 2015)), whereas the west Indian margin in Scenario 1 is not. For this reason, the paleogeographic reconstructions of the eastern Mediterranean region invoke two intra-oceanic subduction zones to account for emplacement of ophiolites on both continental margins (for example, (Schmid and others, 2008, 2020, van Hinsbergen and others, 2020b)).

The Mascarene nappes, derived from the modern microcontinental ribbon continent that stretches from the Seychelles to Mauritius, are in both scenarios incorporated earlier into an accretionary fold-thrust belt than the CPS units of the continental margins of Madagascar or Somalia. The geological expression of this time difference will be evident from the age of flysch deposited on the Mascarene nappes and if exhumed, of HP metamorphic rocks in deeply buried portions of these nappes, which will be significantly older than those of the Dar-es-Salaam, Kismayo, Toamasina and Panganales nappes of Somalia and Madagascar.

Such time delays between accretion of nappes are also known from modern orogens, such as the Himalaya (~59-54 Ma in the Tethyan Himalaya versus Miocene in the Lesser Himalaya (for example, (DeCelles and others, 2014), Figures 6 and 7), or the Briançonnais nappe (Paleocene-early Eocene) versus the Helvetic nappes (late Oligo-Miocene) versus the Helvetic nappes (late Oligocene) in the Alps (Figure 3) and illustrates that such delays may indicate that in intervening periods oceanic lithosphere subducted. For the Alps, this is evident, since OPS relics are found below and on top of the Briançonnais nappe (Schmid and others, 2004). We note, however, that the Briançonnais fragment of the Alps, and its westward paleogeographic continuation to Corsica and Sardinia, was only a small block of some 100s of km wide rather than the > 2000 km of the Mascarene Nappes, and may be better compared to the Laxmi nappe that forms the highest unit of the Malabar nappes in Scenario 1 (Figure 17). The Mascarene Nappes may also provide an equivalent of the Tethyan (and Greater) Himalaya nappes as portrayed in van Hinsbergen and others (2012). However, there are no relics of the lithosphere that subducted between the early Eocene and early Miocene in the Himalaya and the paleogeographic interpretation of the nature of this lithosphere cannot be directly constrained from accreted relics (Ingalls and others, 2016, Kapp and DeCelles, 2019, van Hinsbergen and others, 2019b). Nevertheless, our thought experiments may provide useful insights to further this paleogeographic debate.

The evolution of subduction zones in Madagascar in Scenario 2 is an example of a commonly interpreted feature in orogenic evolution scenarios: terrane accretion. We model that the whole Madagascar lithosphere accretes to the upper plate, facilitated by Hadiboh slab breakoff and Qamar subduction initiation. An alternative scenario would be subduction of a single slab through delamination of the Madagascar continent, as proposed for western Turkey, the Banda region, and the South America-derived continents in the Scotia back-arc (Spakman and Hall, 2010, van Hinsbergen and others, 2010, van de Lagemaat and others, 2021), but the size of Madagascar is much larger than those examples and we consider our modeled scenario more feasible. This history may thus form an equivalent of the commonly portrayed accretion history of the Lhasa block in southern Tibet (Yin and Harrison, 2000, Zhu and others, 2013, Kapp and DeCelles, 2019, Li and others, 2019), or of the Cimmerian blocks of Iran following Paleotethys closure and inception of Neotethys subduction (Şengör, 1984, Stampfli and Borel, 2002, Scotese, 2004, Muttoni and others, 2009). The histories of Madagascar and the Mascarene plateau in our scenarios illustrate the end-member behaviors between continental fragments as we identified in our 'rules' of orogenesis: they either subduct and leave their upper crust as nappes in the geological record, or they only accrete their passive margin CPS and then lead to arrest and relocation of subduction.

The above comparisons of the results of our thought experiments to modern geological records include our preferred interpretations of those geological records and will thus undoubtedly not be universally agreed upon. Nevertheless, our comparisons illustrate that the orogenic architecture that we produce by applying our rules of orogenesis to modern geography in combination with a future continental drift scenario (Davies and others, 2018) compares well with known orogens. Thought experiments like ours may thus be used as inspiration and proof-of-concept of paleogeographic interpretations (also with alternative rules).

Based on our experiments, we notice several features in our reconstruction that may be used as basis for future hypotheses on orogenic evolution. For example, in Scenario 1, the construction of Davies and others (2018) predicts that the Horn of Africa overrides the Indian continent, but because Somalia subsequently pivots around this initial collision zone, the previously underthrusted Indian continent is extensionally exhumed. We suggestively named the resulting exhumed Indian margin the ‘west-Indian gneiss region’, as it may provide a hypothetical equivalent to the Western Gneiss Region of the Norwegian Caledonides. There, the continental margin of Baltica was deeply underthrusted during collision with Laurentia in the Paleozoic, and subsequently ‘educted’, that is it exhumed as a HP-LT metamorphosed, but otherwise coherent continental crust overlain by accreted CPS and OPS nappes (Andersen and others, 1991). Such eduction is often viewed as the result of plate divergence following collision (Andersen and others, 1991, Brueckner and van Roermund, 2004, Duretz and others, 2012), but Andersen (1998) and Krabbendam and Dewey (1998) suggested that margin-oblique transtension may also have played a role. The scenario for the west-Indian gneiss region may illustrate how plate rotation and interaction of continental margins oblique to subduction zones could generate such transtension.

As noted above, the subduction termination and relocation from east to west Madagascar in Scenario 2 may be equivalent to the evolution of the Lhasa block upon its early Cretaceous collision with Tibet. In that context, it is interesting to note that the Malé subduction zone to the north of Madagascar remains unaffected by this jump and remains active. This may serve as an inspiration to infer that the subduction jump recorded around the Lhasa margins may not have affected the region where the Lhasa block ends in the west, which is currently in the region occupied by the Kohistan-Ladakh arcs (Figure 6) (Schwab and others, 2004). The plate tectonic evolution of the Kohistan region is debated (Khan and others, 2009, Hébert and others, 2012, Bouilhol and others, 2013, Borneman and others, 2015, Jagoutz and others, 2015, Martin and others, 2020) and reconstructing intra-oceanic subduction history from narrow sutures is notoriously difficult due to the scarcity of accreted relics. The example of the Madagascar evolution in Scenario 2 illustrates that the events associated with Lhasa-Qiangtang collision, and the associated arrest and relocation of subduction zones, may not have affected the Kohistan region, where instead subductionmay have continued much longer on the same subduction zones.

Finally, in Scenario 2, the Horn of Africa forms the downgoing plate and underthrusts the Dakshinapatha, leading to accretion of the Punt nappes and upper plate shortening making the Saurashtra plateau (Figure 19). It is interesting to note that such local oroclines forming the eastern and western Himalayan syntaxes (Figure 6) are located in the regions where horizontally underthrust Indian continental crust protrudes farthest below Tibet (Agius and Lebedev, 2013, van Hinsbergen and others, 2019b) and where the latest, Miocene phase of slab break-off likely occurred first Webb and others (2017). The underthrusting of the Horn of Africa promontory below the Dakshinapatha continent may thus provide a hypothetical example of syntaxis formation.

Our thought experiments illustrate that identical initial conditions with a different, but simple initial subduction zone configuration, lead to different orogenic architectures and evolutions. From this, we infer that orogenic architecture is sensitive to and allows reconstruction of the unique paleogeography and subduction configuration that led to its development. The initial position and polarity of subduction determines which margins generate accretionary fold-thrust belts, whether and where ophiolite belts form, and whether and where oroclines form. In addition, in our example the overall eastward absolute plate motion combined with the modeled subduction polarity determines the deformation history of the upper plate: in this particular case extensional above eastward dipping subduction zones and contractional above westward dipping subduction zones. Slab (or continental edge) advance only plays a role in our example for the Horn of Africa underthrusting below the Dakshinapatha continent. As a result of our assumption that eastward dipping subduction zones remain more or less mantle stationary, the final Somalia-India suturing differs by > 100 Ma between the two scenarios, and the second scenario will lead to another major orogen within modern India through closure of the Rewa ocean (Figure 19). This illustrates how final orogenic architecture is a sum of paleogeography, initial subduction zone geometry, and absolute plate motions of the plates involved.

Finally, we chose a relatively simple paleogeography, and a simple plate kinematic scenario for our thought experiments. Much more complex scenarios and orogenic architecture would result from for example a hypothetical convergence between Australia, Eurasia, and India, closure of the Mediterranean region between Africa and Eurasia, or closure of the Caribbean region between North and South America. Such exercises may generate sources of inspiration for the detailed reconstruction of complex, and resource-rich orogens such as the Central Asian Orogenic Belt, the Pan-African orogen, or the Variscan orogen. Thought experiments using the possibilities provided by GPlates plate reconstruction software, future supercontinent constructions like those of (Davies and others, 2018) and our (or alternative) rules of orogenesis may unlock the well-known modern geography for interpreting paleogeography from orogens that formed throughout Earth history.

5. Conclusions

In this paper, we review the relationships between orogenic architecture, subduction history, and paleogeography. We find that current concepts that link orogenic architecture and evolution to the oceanic or continental nature of the downgoing plate do not predict the evolution of Mesozoic-Cenozoic orogens well enough to use them as basis for paleogeographic reconstruction. In particular, widely assumed diagnostic features to date continental collision, such as upper plate deformation, plate motion change, or arrest of magmatism, also occurred during oceanic subduction, and do not always apply to continental collision zones. We propose an alternative view on analysis of orogenic history by separately analyzing the history of accretion of ocean and continent-derived nappes using Oceanic and Continental Plate Stratigraphy (OPS and CPS). The accretionary history provides arguments for the paleogeography of subducted lithosphere, and the timing of its subduction and accretion. Upper plate deformation results from the competition between absolute motions of the upper plate and downgoing slab, and is reconstructed separately based on kinematic criteria, independent from interpretations on relationships with the nature of the downgoing plate, and independent from the presence, absence, or nature of magmatism. We translate our views into a set of 'rules' (of thumb) or orogenesis that link the paleogeography of a downgoing plate and the absolute motion of an overriding plate and slab to resulting orogenic architecture (or vice versa). We illustrated the use of these rules by constructing orogens from the modern Indian Ocean, using a recently constructed continental drift scenario of a future supercontinent in which the Somali margin collides with India. We show that the resulting orogens bear strong similarities with existing orogens, and this way unlock modern geography as analogue for the study of paleogeography from orogenic architecture.

Epilogue

This seed for this paper was planted by several journalists who, when reporting on plate reconstructions of the past, often asked the first author whether it is also possible to predict the future. We realized that in order to do so, we needed the set of 'rules' that many scholars of tectonics and paleogeography may have developed for themselves, but that have not been explicitly formulated in the literature to our knowledge. We hope that formulating such rules, which are obviously open for discussion, will be useful for the scientific community, and we thank the science writers and journalists who translate the results of the scientific community to the public for sparking the idea that became this paper.

Acknowledgements

DJJvH acknowledges NWO Vici grant 865.17.001. We thank Nalan Lom for discussion and critical reading of the manuscript and Thomas van der Linden for developing the isochrons in the constructions of future plates. We thank Hannah Davies (University of Lisbon, Portugal) for kindly sharing her GPlates constructions of future continents that we used as basis for our thought experiment. We appreciated constructive reviews by Paul Kapp and Peter Cawood.

Figure captions

Figure 1: Conceptual map displaying the four possible combinations of continental and oceanic crust in upper and downgoing plates, upper plate deformation modes, and common terminology for orgenic systems. CPS = Continental Plate Stratigraphy; OPS = Oceanic Plate Stratigraphy

Figure 2: Accretable units from downgoing plates. Oceanic Plate Stratigraphy, overlying MORB crust, Large Igneous Provinces, or Ocean Island Basalts (or former intra-oceanic arcs together with associated accretionary prisms associated with an earlier subduction zone), may accrete at the subduction zone, but normally does not. Continental Plate Stratigraphy typically accretes to form nappes that decouple in weak horizons in the stratigraphy, around the sediment-basement interface, or more rarely, along decollements within or below the crystalline crust.

Figure 3 a: Schematic tectonic map of the Mediterranean orogens, and the first-order distribution of accreted CPS nappes and OPS nappes and mélanges. Ophiolites represent relics of upper plate oceanic lithosphere below which CPS and OPS was accreted. Aeg = Aegean region; Alb = Alboran region; Cal = Calabria; Cy = Cyprus; IAM = İzmir-Ankara mélange; Kı = Kırşehir Block; LP = Liguro-Provençal Basin; MM = Misis Mélange; Pan = Pannonian Basin Pyr = Pyrenees; Ta = Tavşanlı Zone; Tyr = Tyrrhenian Sea Basin. **B:** Paleogeographic map (in a Europe-fixed frame) around 120 Ma showing the outline of the now largely subducted Greater Adria continental domain. Dotted lines represent retreating trenches that rolled back into oceanic embayments between continental margins. Kı = Kırşehir Block; Ta = Tavşanlı Zone.

Figure 4: Schematic evolution in cross section of subduction, accretion, and upper plate deformation along a section across the Balkan orogen of Greece and Bulgaria. Simplified after Maffione and van Hinsbergen (2018), Schmid and others (2020), van Hinsbergen and others (2020b): the Rhodope nappes, that formed from the stratigraphic underpinnings of the Balkanide Nappes, are omitted from the section. The Pindos Zone, consisting of cherts and pelagic limestones, is indicated as OPS, although the nature of the original underlying basement may largely have been highly extended continental crust. Italic codes refer to slabs

listed on www.atlas-of-the-underworld.org (van der Meer and others, 2018). Aeg = Aegean Slab; Alg = Algeria Slab; Ap = Apulian Platform; Ba = Balkanide Nappes; Emp = Emporios Slab; EVa = East Vardar Ophiolites; Io = Ionian Zone; NT = Neotethys Ocean; Pe = Pelagonian Nappes; Pi = Pindos Zone; PT = Paleotethys Ocean; Sa = Sava Ocean/Suture; Tr = Tripoliza Zone; WVa = West Vardar Ophiolites.

Figure 5: Schematic evolution in cross section of subduction, accretion, and upper plate deformation from the Black Sea to Cyprus and Africa. Simplified after (Gürer and others, 2016, McPhee and van Hinsbergen, 2019, van Hinsbergen and others, 2020b). The Inner Tauride Basin is a conceptual, presumably oceanic basin of which there is no demonstrated geological record: it is inferred because of a 20 Ma gap in accretion during ongoing subduction during which there is arc magmatism in the upper plate (see (van Hinsbergen and others, 2016). The structural position of the Misis Mélange is indicated in section B-B', but is not exposed to the east of the line of section. Italic codes refer to slabs listed on www.atlas-of-the-underworld.org (van der Meer and others, 2018); the Egypt slab was defined in (van der Meer and others, 2010); the Pontides and Herodotus slabs were defined in (Gürer, 2017). AB = Aladağ and Bolkardağı (Afyon Zone) Nappes; An = Antalya Nappes; AO = Antalya Ophiolites; Bo = Bozdağ Zone/sub-ophiolitic mélange; BS = Black Sea; CAO = Central Anatolian Ophiolites; Çankırı Ophiolites; Cyp = Cyprus Slab; Egy = Egypt Slab; EMO = Eastern Mediterranean Ocean; EP = Eastern Pontides; Ge = Geyikdağı Nappe; Her = Herodotus Slabs; İA = İzmir-Ankara mélange; ITB = Inner Tauride Basin; Ka = Karakaya Zone; Ky = Kyrenia Ranges (Trype Unit); MO = Misis Ocean; Mi = Misis Mélange; NT = Neotethys Ocean; Pon – Pontides Slab; PT = Paleotethys Ocean; Ta = Tavşanlı Zone; Tf = Tauric Flysch (Crimea); TO = Troodos Ophiolite.

Figure 6: Schematic tectonic map of the Himalaya orogen and Tibetan Plateau, with the first-order distribution of accreted CPS nappes and OPS nappes and mélanges. Ophiolites represent relics of upper plate oceanic lithosphere below which CPS and OPS was accreted. BNS = Bangong-Nujianh Suture; ESyn = Eastern Syntaxis; GH = Greater Himalaya; IBR = Indo-Burman Ranges; IYSZ = Indus-Yarlung Suture Zone; KB = Kabul Block; LH = Lesser Himalaya; TH = Tethyan Himalaya; Wsyn = Western Syntaxis.

Figure 7: Schematic evolution in cross section of subduction, accretion, and upper plate deformation of the India-Asia convergence and collision zone, following scenarios of a) Kapp and DeCelles (2019) and b) van Hinsbergen and others (2019b). A key difference between the two scenarios is the location of the Indus-Yarlung Suture relative to the position of the Xigaze Ophiolite: Scenario (a) infers that the subduction zone finalizing the suture zone is structurally above the ophiolite, closing a back-arc basin, whilst scenario (b) infers that the Xigaze Ophiolite was always narrow (<150 km) and formed the margin of the Lhasa terrane; this scenario places the suture below the ophiolite and infers that the Gangdese Thrust accommodated moderate (<150 km) forearc shortening. In addition, scenario A infers that all convergence after 45 Ma was accommodated by continental subduction and upper plate shortening, whereby there is no CPS accretion between ~45 and 25 Ma. Scenario (b) infers oceanic subduction after short-lived accretion of the Tethyan and Greater Himalaya around 60-55 Ma, until ~25 Ma, such that all continental subduction is associated with CPS accretion. Scenario (a) thus infers that the Himalaya slab comprises continental lithosphere, whilst scenario (b) infers it is oceanic lithosphere. The MCT is in that case proposed as an out-of-sequence-thrust that buried a latest Oligocene-earliest Miocene suture zone. Italic codes refer to slabs listed on www.atlas-of-the-underworld.org (van der Meer and others, 2018). ATF = Altyn Tagh Fault; BNS = Bangong-Nujiang Suture; GA = Gangdese Arc; GaT = Gangdese Thrust; GH = Greater Himalaya; GIB = Greater India Basin; Him = Himalaya Slab; Ind = India Slab; IYS = Indus-Yarlung Suture; JS = Jinsha Suture; LH = Lesser Himalaya; Mal = Maldives Slab; MBT = Main Boundary Thrust; MCT = Main Central Thrust; S-G = Songpan-Garzi Terrane; STD = South Tibetan Detachment; STT = South Tibetan Thrust; TH = Tethyan Himalaya; XBAB = Xigaze Back-Arc Basin; XO = Xigaze Ophiolite;

Figure 8: Conceptual styles of upper plate deformation as a function of the competition between absolute motion of the slab bend and the upper plate, as detailed in Schepers and other (2017). Slab dragging is the component of slab motion relative to the mantle driven by the absolute motion of the downgoing plate, and is most prominently seen as trench-lateral absolute slab motion (Spakman and Hall, 2010, van de Lagemaat and others, 2018).

Figure 9: Schematic tectonic map of the Scotia Sea region and southern South America, highlighting the contributions of upper plate absolute motion and slab roll-back to upper plate deformation. Westward South America advance towards the east-dipping Nazca and

Antarctic plate slabs generates upper plate shortening of the Andes (see for example (Schepers and others, 2017)), whilst for the west-dipping South Sandwich subduction zone the same absolute South American plate motion constitutes upper plate retreat causing extension. Since ~25 Ma, South Sandwich slab roll-back started to contribute to upper plate extension, and upper plate retreat and slab roll-back have contributed nearly equally to the total amount of ~2000 km of cumulative extension accommodated in the Scotia Sea basins (van de Lagemaat and others, 2021). JaB = Jane Bank; SOr = South Orkney continent.

Figure 10: Cartoon indicating the relationships between basal and frontal accretion as well as lateral delamination (modified from van de Lagemaat and others, 2021). Displayed is the simplest case with a single decollement horizon, with multiple decollement levels, frontal accretion and basal accretion may occur simultaneously at different levels (see for example Tate and others, 2015). In the latter case, crust of a downgoing plate becomes incorporated in the upper plate without being thrusted, buried, or shortened, but by lateral expansion of a slab that peels off the mantle lithospheric portion of the downgoing plate (Spakman and Hall, 2010).

Figure 11: Schematic representation of Oceanic Plate Stratigraphy (following (Isozaki and others, 1990)) and Continental Plate Stratigraphy (this paper).

Figure 12 a: Schematic tectonic map of the NW Pacific region, with accreted intra-oceanic arc rocks. The Olyutorsky arc of Kamchatka (and equivalents on Sakhalin and Hokkaido) overthrusted the continental margin of Kamchatka following a period of southeastward subduction followed by a subduction polarity reversal. Remnants of the intra-oceanic Kronotsky arc accreted as downgoing plate-derived OPS nappes to southern Kamchatka as well as on the Komandorsky Islands. Modified from (Vaes and others, 2019). H-E chain = Hawaii-Emperor seamount chain; Hok = Hokkaido; Kom = Komandorsky Islands; Kro = Kronotsky arc; Oly = Olyutorsky arc; Sak = Sakhalin; The evolution of orogenic architecture along cross-section C-C' is given in Figure 13. **b**: Reconstructed subduction geometry and paleogeographic locations of the Olyutorsky and Kronotsky arcs of Kamchatka, at 70 Ma, based on the reconstruction of Vaes and others (2019) in the slab-fitted mantle reference frame of (van der Meer and others, 2010). Sections C-C' and C-C'' are indicated in Figure 13: Prior to 50 Ma, these sections develop as lateral equivalents at different intra-oceanic subduction zones. As a result of a ~50-45 Ma Pacific plate motion change from NW to W, the pre-Eocene records of the two sections become juxtaposed in the Kamchatka orogen (see Vaes and others (2019) and references therein).

Figure 13: Schematic evolution in cross section of the subduction, accretion, and upper plate deformation in Kamchatka, based on the reconstructions of Domeier and others (2017) and Vaes and others (2019). See Figure 12 for locations of sections. In the late Cretaceous, the Olyutorsky and Kronotsky arcs formed lateral equivalents that became in Miocene time juxtaposed in the Kamchatka accretionary fold-thrust belt. Italic codes refer to slabs listed on www.atlas-of-the-underworld.org (van der Meer and others, 2018). Aga = Agattu Slab; Emp = Emperor seamount chain; KaK = Kamchatka-Kuriles slab; KM = Kamchatka-Mys 'ophiolite' (OPS); Kp = Kamchatka accretionary prism; Kr = Kronotksy Arc; Ma = Malka Complex; NPa = North Pacific Slab; Ol = Olyutorsky arc; OlBab = Olyutorsky Back-arc basin; SOk = Sea of Okhotsk back-arc basin; Sr = Sredinny Complex; VG = Vetlovsky-Govena accretionary prism.

Figure 14: Geological timescale for the future.

Figure 15: Schematic tectonic map of the Indian Ocean realm. Mak = Makran block, CaF = Cambay Fault, NaF = Narmada Fault, MaF = Mahanandi Fault, GoF = Godavari Fault, Dec = Deccan volcanic province, CLC = Chagos-Laccadive Chain, Mas = Mascarene plateau, EAR = East African Rift

Figure 16: Geographic map of the Indian realm, with major landmasses, mid-oceanic ridges, microcontinents, and seamounts.

Figure 17: Snapshots of the plate-kinematic construction of the Indian realm in scenario 1 (see Figure 15 for initial conditions) from the present, 33, 42, 50, 100 and 200 Maft in the mantle reference frame of Davies and others (2018). AmS = Ambre subduction zone, AnO = Antsiranana ophiolites, ChN = Chagos nappes, CLC = Chagos-Laccadive chain, Com = Comores hotspot track, DSN = Dar-es-Salaam nappes FaO = Farafangana ophiolites, HaS = Hadiboh subduction zone, HoO = Hobyo ophiolites KaN = Kathiawar nappes, KhR = Kharif spreading ridge, KiF = Kilwa suture, Mad = Madagascar, Mak = Makran block, MlN = Malabar nappes, Msc = Mascarenes, MsN = Mascarene nappes, MoN = Mogadishu nappes,

MtT = Mtwari transfer fault, RCS = Ras Caseyr subduction zone, RSO = Red Sea orogen, ToN = Toamasina nappes.

Figure 18: Schematic cross sections through the Somalaya orogen (See Figure 17 for locations). AmS = Ambre subduction zone, AnO = Antsiranana ophiolites, ChN = Chagos nappes, CLC = Chagos-Laccadive chain, Com = Comores hotspot track, DSN = Dar-es-Salaam nappes FaO = Farafangana ophiolites, HaS = Hadiboh subduction zone, HoO = Hobyo ophiolites KaN = Kathiawar nappes, KhR = Kharif spreading ridge, KiF = Kilwa suture, Mad = Madagascar, Mak = Makran block, MlN = Malabar nappes, Msc = Mascarenes, MsN = Mascarene nappes, MoN = Mogadishu nappes, MtT = Mtwari transfer fault, OwT = Owens transform, RCS = Ras Caseyr subduction zone, RSO = Red Sea orogen, ToN = Toamasina nappes.

Figure 19: Snapshots of the plate-kinematic construction of the Indian realm in scenario 2 (see Figure 15 for initial conditions) from the present, 33, 42, 50, 100 and 200 Maft in the mantle reference frame of Davies and others (2018). Bas = Bastar block, CLC = Chagos-Laccadive chain, Com = Comores hotspot track, DeD = Deccan-Dharwar block, GoB = Godavari back-arc-basin, GoF = Godavari fault zone, HaM = Hamar metamorphic core complex, KaF = Kanheri thrust fault, , KiN = Kismayo nappes, Mad = Madagascar, Mak = Makran block, MgB = Mangalore back-arc basin, MjF = Mahajanga fault, Msc = Mascarenes, MsN = Mascarene nappes, OwT = Owens transform, PaN = Panganales nappes, PeO = Pemba ophiolite, QaS = Qamar subduction zone, ReR = Rewa spreading ridge, RSO = Red Sea Orogen, Sau = Saurasthra block, SLT = Sri Lanka transfer fault.

Figure 20: Schematic cross sections through the Mumbay orogen (See Figure 19 for locations). Bas = Bastar block, CLC = Chagos-Laccadive chain, Com = Comores hotspot track, DeD = Deccan-Dharwar block, GoB = Godavari back-arc-basin, GoF = Godavari fault zone, HaM = Hamar metamorphic core complex, KaF = Kanheri thrust fault, , KiN = Kismayo nappes, Mad = Madagascar, Mak = Makran block, MgB = Mangalore back-arc basin, MjF = Mahajanga fault, Msc = Mascarenes, MsN = Mascarene nappes, OwT = Owens transform, PaN = Panganales nappes, PeO = Pemba ophiolite, QaS = Qamar subduction zone, ReR = Rewa spreading ridge, RSO = Red Sea Orogen, Sau = Saurasthra block, SLT = Sri Lanka transfer fault.

Table 1: Ten rules (of thumb) of orogenesis.

6. References

Ackerman, L., Hajná, J., Žák, J., Erban, V., Sláma, J., Polák, L., Kachlík, V., Strnad, L., and Trubač, J., 2019, Architecture and composition of ocean floor subducted beneath northern Gondwana during Neoproterozoic to Cambrian: A palinspastic reconstruction based on Ocean Plate Stratigraphy (OPS): Gondwana Research, v. 76, p. 77-97.

Advokaat, E. L., van Hinsbergen, D. J. J., Kaymakcı, N., Vissers, R. L. M., and Hendriks, B. W. H., 2014, Late Cretaceous extension and Palaeogene rotation-related contraction in Central Anatolia recorded in the Ayhan-Büyükkışla basin: International Geology Review, v. 56, p. 1813-1836.

Agard, P., Omrani, J., Jolivet, L., and Mouthereau, F., 2005, Convergence history across Zagros (Iran): constraints from collisional and earlier deformation: International Journal of Earth Sciences, v. 94, p. 401-419.

Agard, P., Searle, M. P., Alsop, G. I., and Dubacq, B., 2010, Crustal stacking and expulsion tectonics during continental subduction: P-T deformation constraints from Oman: Tectonics, v. 29, p. n/a-n/a.

Agard, P., Yamato, P., Jolivet, L., and Burov, E., 2009, Exhumation of oceanic blueschists and eclogites in subduction zones: Timing and mechanisms: Earth-Science Reviews, v. 92, p. 53-79.

Agard, P., Yamato, P., Soret, M., Prigent, C., Guillot, S., Plunder, A., Dubacq, B., Chauvet, A., and Monié, P., 2016, Plate interface rheological switches during subduction infancy: Control on slab penetration and metamorphic sole formation: Earth and Planetary Science Letters, v. 451, p. 208-220.

Agard, P., Zuo, X., Funiciello, F., Bellahsen, N., Faccenna, C., and Savva, D., 2014, Obduction: Why, how and where. Clues from analog models: Earth and Planetary Science Letters, v. 393, p. 132-145.

Agius, M. R., and Lebedev, S., 2013, Tibetan and Indian lithospheres in the upper mantle beneath Tibet: Evidence from broadband surface-wave dispersion: Geochemistry, Geophysics, Geosystems, v. 14, p. 4260-4281.

Aitchison, J. C., Ali, J. R., and Davis, A. M., 2007, When and where did India and Asia collide?: Journal of Geophysical Research, v. 112.

Al-Riyami, K., Robertson, A., Dixon, J., and Xenophontos, C., 2002, Origin and emplacement of the Late Cretaceous Baer–Bassit ophiolite and its metamorphic sole in NW Syria: Lithos, v. 65, p. 225-260.

Alexeiev, D. V., Gaedicke, C., Tsukanov, N. V., and Freitag, R., 2006, Collision of the Kronotskiy arc at the NE Eurasia margin and structural evolution of the Kamchatka–Aleutian junction: International Journal of Earth Sciences, v. 95, p. 977-993.

Ali, J. R., and Aitchison, J. C., 2005, Greater India: Earth-Science Reviews, v. 72, p. 169-188.

Andersen, T. B., 1998, Extensional tectonics in the Caledonides of southern Norway, an overview, Tectonophysics, 285, 333-352.

Andersen, T. B., Jamtveit, B., Dewey, J. F., and Swensson, E., 1991, Subduction and eduction of continental crust: Major mechanisms during continent-continent collision and orogenic extensional collapse, a model based on the south Norwegian Caledonides: Terra Nova, v. 3, p. 303-310.

Anderson, R. S. (1994), Evolution of the Santa Cruz Mountains, California, through tectonic growth and geomorphic decay, Journal of Geophysical Research: Solid Earth, 99(B10), 20161-20179.

Anonymous, 1972, Penrose field conference on ophiolites: Geotimes, v. 17, p. 24-25.

Ashalatha, B., Subrahmanyam, C., and Singh, R., 1991, Origin and compensation of Chagos-Laccadive Ridge, Indian Ocean, from admittance analysis of gravity and bathymetry data: Earth and Planetary Science Letters, v. 105, p. 47-54.
Ashwal, L. D., Wiedenbeck, M., and Torsvik, T. H., 2017, Archaean zircons in Miocene oceanic hotspot rocks establish ancient continental crust beneath Mauritius: Nature Communications, v. 8, p. 14086.
Atwater, T., 1989, Plate tectonic history of the northeast Pacific and western North America: The eastern Pacific Ocean and Hawaii: Boulder, Colorado, Geological Society of America, Geology of North America, v. N, p. 21-72.
Auzemery, A., Willingshofer, E., Yamato, P., Duretz, T., and Sokoutis, D., 2020, Strain localization mechanisms for subduction initiation at passive margins: Global and Planetary Change, p. 103323.
Avigad, D., Garfunkel, Z., Jolivet, L., and Azañón, J. M., 1997, Back arc extension and denudation of Mediterranean eclogites: Tectonics, v. 16, p. 924-941.
Badarch, G., Cunningham, W. D., and Windley, B. F., 2002, A new terrane subdivision for Mongolia: implications for the Phanerozoic crustal growth of Central Asia: Journal of Asian Earth Sciences, v. 21, p. 87-110.
Baes, M., Govers, R., and Wortel, R., 2011, Subduction initiation along the inherited weakness zone at the edge of a slab: Insights from numerical models: Geophysical Journal International, v. 184, p. 991-1008.
Bagheri, S., and Gol, S. D., 2020, The Eastern Iranian Orocline: Earth-Science Reviews, p. 103322.
Bandyopadhyay, D., A. Ghosh, C. Guilmette, A. Plunder, F. Corfu, E. Advokaat, P. C. Bandopadhyay, and D. J. J. van Hinsbergen, 2020a, From back-arc to forearc: a geochemical and geochronological record of arc polarity reversal from the Andaman Ophiolite, SE Asia, Lithos, 105853.
Bandyopadhyay, D., van Hinsbergen, D. J. J., Plunder, A., Bandopadhyay, P. C., Advokaat, E., Chattopadhaya, S., Morishita, T., and Ghosh, B., 2020b, Andaman Ophiolite: An Overview, *in* Ray, J. S., and Radhakrishna, M., editors, The Andaman Islands and Adjoining Offshore: Geology, Tectonics and Palaeoclimate: Cham, Springer International Publishing, p. 1-17.
Barber, A., 2000, The origin of the Woyla Terranes in Sumatra and the Late Mesozoic evolution of the Sundaland margin: Journal of Asian Earth Sciences, v. 18, p. 713-738.
Bazhenov, M., Burtman, V., Krezhovskikh, O., and Shapiro, M., 1992, Paleomagnetism of Paleogene rocks of the Central—East Kamchatka and Komanorsky Islands: tectonic implications: Tectonophysics, v. 201, p. 157-173.
Béchennec, F., Le Metour, J., Rabu, D., Bourdillon-de-Grissac, C., De Wever, P., Beurrier, M., and Villey, M., 1990, The Hawasina Nappes: stratigraphy, palaeogeography and structural evolution of a fragment of the south-Tethyan passive continental margin: Geological Society, London, Special Publications, v. 49, p. 213-223.
Bhattacharya, G., Chaubey, A., Murty, G., Srinivas, K., Sarma, K., Subrahmanyam, V., and Krishna, K., 1994, Evidence for seafloor spreading in the Laxmi Basin, northeastern Arabian Sea: Earth and Planetary Science Letters, v. 125, p. 211-220.
Bilham, R., Larson, K., and Freymueller, J., 1997, GPS measurements of present-day convergence across the Nepal Himalaya: Nature, v. 386, p. 61-64.
Bonneville, A., Barriot, J. P., and Bayer, R., 1988, Evidence from geoid data of a hotspot origin for the southern Mascarene Plateau and Mascarene Islands (Indian Ocean): Journal of Geophysical Research: Solid Earth, v. 93, p. 4199-4212.

Borneman, N. L., Hodges, K. V., Van Soest, M. C., Bohon, W., Wartho, J. A., Cronk, S. S., and Ahmad, T., 2015, Age and structure of the Shyok suture in the Ladakh region of northwestern India: implications for slip on the Karakoram fault system: Tectonics, v. 34, p. 2011-2033.
Boschman, L. M., Van Hinsbergen, D. J., Kimbrough, D. L., Langereis, C. G., and Spakman, W., 2018, The dynamic history of 220 million years of subduction below Mexico: a correlation between slab geometry and overriding plate deformation based on geology, paleomagnetism, and seismic tomography: Geochemistry, Geophysics, Geosystems, v. 19, p. 4649-4672.
Boschman, L. M., and van Hinsbergen, D. J. J., 2016, On the enigmatic birth of the Pacific Plate within the Panthalassa Ocean: Science Advances, v. 2, p. e1600022.
Boschman, L. M., van Hinsbergen, D. J. J., Langereis, C. G., Flores, K. E., Kamp, P. J. J., Kimbrough, D. L., Ueda, H., van de Lagemaat, S. H. A., van der Wiel, E., and Spakman, W., 2021a, Reconstructing lost plates and plate boundaries of the Panthalassa Ocean from circum-Pacific accretionary orogens: American Journal of Science, v. submitted.
Boschman, L. M., van Hinsbergen, D. J. J., Langereis, C. G., and Spakman, W., 2021b, Reconstructing Jurassic-Cretaceous intra-oceanic subduction evolution in the northwestern Panthalassa Ocean using Ocean Plate Stratigraphy from Hokkaido, Japan: Tectonics, v. submitted.
Boschman, L. M., van Hinsbergen, D. J. J., Torsvik, T. H., Spakman, W., and Pindell, J. L., 2014, Kinematic reconstruction of the Caribbean region since the Early Jurassic: Earth-Science Reviews, v. 138, p. 102-136.
Bouilhol, P., Jagoutz, O., Hanchar, J. M., and Dudas, F. O., 2013, Dating the India–Eurasia collision through arc magmatic records: Earth and Planetary Science Letters, v. 366, p. 163-175.
Boutelier, D., Chemenda, A., and Burg, J.-P., 2003, Subduction versus accretion of intra-oceanic volcanic arcs: insight from thermo-mechanical analogue experiments: Earth and Planetary Science Letters, v. 212, p. 31-45.
Bozkurt, E., Satır, M., and Buğdaycıoğlu, Ç., 2011, Surprisingly young Rb/Sr ages from the Simav extensional detachment fault zone, northern Menderes Massif, Turkey: Journal of Geodynamics, v. 52, p. 406-431.
Bradley, K. E., Feng, L., Hill, E. M., Natawidjaja, D., and Sieh, K., 2017, Implications of the diffuse deformation of the Indian Ocean lithosphere for slip partitioning of oblique plate convergence in Sumatra: Journal of Geophysical Research: Solid Earth, v. 122, p. 572-591.
Brede, R., Hauptmann, M., and Herbig, H.-G., 1992, Plate tectonics and intracratonic mountain ranges in Morocco-The Mesozoic-Cenozoic development of the Central High Atlas and the Middle Atlas: Geologische Rundschau, v. 81, p. 127-141.
Brown, M., 2007, Metamorphic conditions in orogenic belts: a record of secular change: International Geology Review, v. 49, p. 193-234.
Brown, M., 2009, Metamorphic patterns in orogenic systems and the geological record: Geological Society, London, Special Publications, v. 318, p. 37-74.
Brueckner, H. K., and van Roermund, H. L., 2004, Dunk tectonics: A multiple subduction/eduction model for the evolution of the Scandinavian Caledonides: Tectonics, v. 23.
Brun, J.-P., and Faccenna, C., 2008, Exhumation of high-pressure rocks driven by slab rollback: Earth and Planetary Science Letters, v. 272, p. 1-7.

Brunet, C., Monié, P., Jolivet, L., and Cadet, J. P., 2000, Migration of compression and extension in the Tyrrhenian Sea, insights from 40Ar/39Ar ages on micas along a transect from Corsica to Tuscany: Tectonophysics, v. 321, p. 127-155.
Buiter, S. J., and Torsvik, T. H., 2014, A review of Wilson Cycle plate margins: A role for mantle plumes in continental break-up along sutures?: Gondwana Research, v. 26, p. 627-653.
Burke, K., and Dewey, J., 1973, Plume-generated triple junctions: key indicators in applying plate tectonics to old rocks: The Journal of Geology, v. 81, p. 406-433.
Cai, F., Ding, L., Laskowski, A. K., Kapp, P., Wang, H., Xu, Q., and Zhang, L., 2016, Late Triassic paleogeographic reconstruction along the Neo–Tethyan Ocean margins, southern Tibet: Earth and Planetary Science Letters, v. 435, p. 105-114.
Caldwell, J., and Turcotte, D., 1979, Dependence of the thickness of the elastic oceanic lithosphere on age: Journal of Geophysical Research: Solid Earth, v. 84, p. 7572-7576.
Can Genç, Ş., 2004, A Triassic large igneous province in the Pontides, northern Turkey: geochemical data for its tectonic setting: Journal of Asian Earth Sciences, v. 22, p. 503-516.
Capella, W., Matenco, L., Dmitrieva, E., Roest, W. M. J., Hessels, S., Hssain, M., Chakor-Alami, A., Sierro, F. J., and Krijgsman, W., 2017, Thick-skinned tectonics closing the Rifian Corridor: Tectonophysics, v. 710-711, p. 249-265.
Capella, W., Spakman, W., van Hinsbergen, D. J., Chertova, M. V., and Krijgsman, W., 2020, Mantle resistance against Gibraltar slab dragging as a key cause of the Messinian Salinity Crisis: Terra Nova, v. 32, p. 141-150.
Capitanio, F. A., Morra, G., Goes, S., Weinberg, R. F., and Moresi, L., 2010, India–Asia convergence driven by the subduction of the Greater Indian continent: Nature Geoscience, v. 3, p. 136-139.
Cavazza, W., Cattò, S., Zattin, M., Okay, A. I., and Reiners, P., 2018, Thermochronology of the Miocene Arabia-Eurasia collision zone of southeastern Turkey: Geosphere, v. 14, p. 2277-2293.
Cawood, P., Leitch, E., Merle, R. E., and Nemchin, A., 2011a, Orogenesis without collision: Stabilizing the Terra Australis accretionary orogen, eastern Australia: Geological Society of America Bulletin, v. 123, p. 2240-2255.
Cawood, P., Pisarevsky, S. A., and Leitch, E., 2011b, Unraveling the New England orocline, east Gondwana accretionary margin: Tectonics, v. 30.
Cawood, P. A., 1982, Structural relations in the subduction complex of the Paleozoic New England Fold Belt, eastern Australia: The Journal of Geology, v. 90, p. 381-392.
-, 2005, Terra Australis Orogen: Rodinia breakup and development of the Pacific and Iapetus margins of Gondwana during the Neoproterozoic and Paleozoic: Earth-Science Reviews, v. 69, p. 249-279.
Cawood, P. A., and Buchan, C., 2007, Linking accretionary orogenesis with supercontinent assembly: Earth-Science Reviews, v. 82, p. 217-256.
Cawood, P. A., Hawkesworth, C., and Dhuime, B., 2013, The continental record and the generation of continental crust: Geological Society of America Bulletin, v. 125, p. 14-32.
Cawood, P. A., and Hawkesworth, C. J., 2019, Continental crustal volume, thickness and area, and their geodynamic implications: Gondwana Research, v. 66, p. 116-125.
Cawood, P. A., Kröner, A., Collins, W. J., Kusky, T. M., Mooney, W. D., and Windley, B. F., 2009, Accretionary orogens through Earth history: Geological Society, London, Special Publications, v. 318, p. 1-36.

Cawood, P. A., and Suhr, G., 1992, Generation and obduction of ophiolites: constraints from the Bay of Islands Complex, western Newfoundland: Tectonics, v. 11, p. 884-897.
Chemenda, A. I., Mattauer, M., Malavieille, J., and Bokun, A. N., 1995, A mechanism for syn-collisional rock exhumation and associated normal faulting: results from physical modelling: Earth and Planetary Science Letters, v. 132, p. 225-232.
Chertova, M. V., Spakman, W., van den Berg, A. P., and van Hinsbergen, D. J. J., 2014, Absolute plate motions and regional subduction evolution: Geochemistry, Geophysics, Geosystems, v. 15, p. 3780-3792.
Chorowicz, J., 2005, The east African rift system: Journal of African Earth Sciences, v. 43, p. 379-410.
Cloos, M., 1993, Lithospheric buoyancy and collisional orogenesis: Subduction of oceanic plateaus, continental margins, island arcs, spreading ridges, and seamounts: Geological Society of America Bulletin, v. 105, p. 715-737.
Cloos, M., and Shreve, R. L., 1988, Subduction-channel model of prism accretion, melange formation, sediment subduction, and subduction erosion at convergent plate margins: 1. Background and description: Pure and Applied Geophysics, v. 128, p. 455-500.
Cocks, L., and Torsvik, T., 2002, Earth geography from 500 to 400 million years ago: a faunal and palaeomagnetic review: Journal of the Geological Society, v. 159, p. 631-644.
Collier, J. S., Sansom, V., Ishizuka, O., Taylor, R. N., Minshull, T. A., and Whitmarsh, R. B., 2008, Age of Seychelles–India break-up: Earth and Planetary Science Letters, v. 272, p. 264-277.
Collins, A. S., and Pisarevsky, S. A., 2005, Amalgamating eastern Gondwana: The evolution of the Circum-Indian Orogens: Earth-Science Reviews, v. 71, p. 229-270.
Copley, A., Avouac, J.-P., and Royer, J.-Y., 2010, India-Asia collision and the Cenozoic slowdown of the Indian plate: Implications for the forces driving plate motions: Journal of Geophysical Research, v. 115.
Corti, G., 2009, Continental rift evolution: from rift initiation to incipient break-up in the Main Ethiopian Rift, East Africa: Earth-Science Reviews, v. 96, p. 1-53.
Cox, A., and Hart, R. B., 1986, Plate tectonics: how it works, John Wiley & Sons.
Csontos, L., and Vörös, A., 2004, Mesozoic plate tectonic reconstruction of the Carpathian region: Palaeogeography, Palaeoclimatology, Palaeoecology, v. 210, p. 1-56.
Cunningham, D., 2005, Active intracontinental transpressional mountain building in the Mongolian Altai: Defining a new class of orogen: Earth and Planetary Science Letters, v. 240, p. 436-444.
Curray, J. R., 2005, Tectonics and history of the Andaman Sea region: Journal of Asian Earth Sciences, v. 25, p. 187-232.
Dalziel, I. W., 1997, OVERVIEW: Neoproterozoic-Paleozoic geography and tectonics: Review, hypothesis, environmental speculation: Geological Society of America Bulletin, v. 109, p. 16-42.
Darin, M., Umhoefer, P. J., and Thomson, S., 2018, Rapid late Eocene exhumation of the Sivas Basin (Central Anatolia) driven by initial Arabia-Eurasia collision: Tectonics, v. 37, p. 3805-3833.
Davies, H. S., Green, J. A. M., and Duarte, J. C., 2018, Back to the future: Testing different scenarios for the next supercontinent gathering: Global and Planetary Change, v. 169, p. 133-144.
Davies, J. H., and von Blanckenburg, F., 1995, Slab breakoff: a model of lithosphere detachment and its test in the magmatism and deformation of collisional orogens: Earth and Planetary Science Letters, v. 129, p. 85-102.

Davy, B., Hoernle, K., and Werner, R., 2008, Hikurangi Plateau: Crustal structure, rifted formation, and Gondwana subduction history: Geochemistry, Geophysics, Geosystems, v. 9.
de Sigoyer, J., Chavagnac, V., Blichert-Toft, J., Villa, I. M., Luais, B., Guillot, S., Cosca, M., and Mascle, G., 2000, Dating the Indian continental subduction and collisional thickening in the northwest Himalaya: Multichronology of the Tso Morari eclogites: Geology, v. 28, p. 487-490.
DeCelles, P. G., 2004, Late Jurassic to Eocene evolution of the Cordilleran thrust belt and foreland basin system, western USA: American Journal of Science, v. 304, p. 105-168.
DeCelles, P. G., and Giles, K. A., 1996, Foreland basin systems: Basin Research, v. 8, p. 105-123.
DeCelles, P. G., and Horton, B. K., 2003, Early to middle Tertiary foreland basin development and the history of Andean crustal shortening in Bolivia: Geological Society of America Bulletin, v. 115, p. 58-77.
DeCelles, P. G., Kapp, P., Ding, L., and Gehrels, G. E., 2007, Late Cretaceous to middle Tertiary basin evolution in the central Tibetan Plateau: Changing environments in response to tectonic partitioning, aridification, and regional elevation gain: Geological Society of America Bulletin, v. 119, p. 654-680.
DeCelles, P. G., Kapp, P., Gehrels, G. E., and Ding, L., 2014, Paleocene-Eocene foreland basin evolution in the Himalaya of southern Tibet and Nepal: Implications for the age of initial India-Asia collision: Tectonics, v. 33, p. 824-849.
Dercourt, J., et al., Zonenshain, L. P., Ricou, L. E., Kazmin, V. G., Le Pichon, X., Knipper, A. L., Grandjacquet, C., Sbortshikov, I. M., Geyssant, J., and Lepvrier, C., 1986, Geological evolution of the Tethys belt from the Atlantic to the Pamirs since the Lias: Tectonophysics, v. 123, p. 241-315.
Dewey, J., and Şengör, A. M. C., 1979, Aegean and surrounding regions: complex multiplate and continuum tectonics in a convergent zone: Geological Society of America Bulletin, v. 90, p. 84-92.
Dewey, J. F., 1969, Evolution of the Appalachian/Caledonian orogen: Nature, v. 222, p. 124-129.
Dewey, J. F., 1976, Ophiolite obduction: Tectonophysics, v. 31, p. 93-120.
-, 2005, Orogeny can be very short: Proceedings of the National Academy of Sciences, v. 102, p. 15286-15293.
Dewey, J. F., and Bird, J. M., 1970, Mountain belts and the new global tectonics: Journal of Geophysical Research, v. 75, p. 2625-2647.
Dewey, J. F., and Burke, K. C., 1973, Tibetan, Variscan, and Precambrian basement reactivation: products of continental collision: The Journal of Geology, v. 81, p. 683-692.
Dewey, J. F., and Casey, J. F., 2013, The sole of an ophiolite: the Ordovician Bay of Islands Complex, Newfoundland: Journal of the Geological Society, v. 170, p. 715-722.
Dilek, Y., and Furnes, H., 2011, Ophiolite genesis and global tectonics: Geochemical and tectonic fingerprinting of ancient oceanic lithosphere: Geological Society of America Bulletin, v. 123, p. 387-411.
Ding, L., Kapp, P., and Wan, X., 2005, Paleocene-Eocene record of ophiolite obduction and initial India-Asia collision, south central Tibet: Tectonics, v. 24, p. n/a-n/a.
Ding, L., Qasim, M., Jadoon, I. A. K., Khan, M. A., Xu, Q., Cai, F., Wang, H., Baral, U., and Yue, Y., 2016, The India–Asia collision in north Pakistan: Insight from the U–Pb detrital zircon provenance of Cenozoic foreland basin: Earth and Planetary Science Letters, v. 455, p. 49-61.

Domeier, M., Shephard, G. E., Jakob, J., Gaina, C., Doubrovine, P. V., and Torsvik, T. H., 2017, Intraoceanic subduction spanned the Pacific in the Late Cretaceous–Paleocene: Science Advances, v. 3, p. eaao2303.
Domeier, M., and Torsvik, T. H., 2019, Full-plate modelling in pre-Jurassic time: Geological Magazine, v. 156, p. 261-280.
Duretz, T., Gerya, T., Kaus, B., and Andersen, T., 2012, Thermomechanical modeling of slab eduction: Journal of Geophysical Research: Solid Earth, v. 117.
Duretz, T., Gerya, T. V., and May, D. A., 2011, Numerical modelling of spontaneous slab breakoff and subsequent topographic response: Tectonophysics, v. 502, p. 244-256.
Duretz, T., Gerya, T. V., and Spakman, W., 2014, Slab detachment in laterally varying subduction zones: 3-D numerical modeling: Geophysical Research Letters, v. 41, p. 1951-1956.
Eagles, G., 2016, Plate kinematics of the Rocas Verdes Basin and Patagonian orocline: Gondwana Research, v. 37, p. 98-109.
Eagles, G., and Jokat, W., 2014, Tectonic reconstructions for paleobathymetry in Drake Passage: Tectonophysics, v. 611, p. 28-50.
Eagles, G., and Livermore, R., 2002, Opening history of Powell Basin, Antarctic Peninsula: Marine Geology, v. 185, p. 195-205.
Eichelberger, N., and McQuarrie, N., 2015, Kinematic reconstruction of the Bolivian orocline: Geosphere, v. 11, p. 445-462.
Emerick, C., and Duncan, R., 1982, Age progressive volcanism in the Comores Archipelago, western Indian Ocean and implications for Somali plate tectonics: Earth and Planetary Science Letters, v. 60, p. 415-428.
Endrun, B., Lebedev, S., Meier, T., Tirel, C., and Friederich, W., 2011, Complex layered deformation within the Aegean crust and mantle revealed by seismic anisotropy: Nature Geoscience, v. 4, p. 203-207.
England, P., and Houseman, G., 1989, Extension during continental convergence, with application to the Tibetan Plateau: Journal of Geophysical Research: Solid Earth, v. 94, p. 17561-17579.
Faccenna, C., Becker, T. W., Auer, L., Billi, A., Boschi, L., Brun, J. P., Capitanio, F. A., Funiciello, F., Horvàth, F., and Jolivet, L., 2014, Mantle dynamics in the Mediterranean: Reviews of Geophysics, v. 52, p. 283-332.
Faccenna, C., Becker, T. W., Lucente, F. P., Jolivet, L., and Rossetti, F., 2001, History of subduction and back arc extension in the Central Mediterranean: Geophysical Journal International, v. 145, p. 809-820.
Faccenna, C., Oncken, O., Holt, A. F., and Becker, T. W., 2017, Initiation of the Andean orogeny by lower mantle subduction: Earth and Planetary Science Letters, v. 463, p. 189-201.
Faccenna, C., Piromallo, C., Crespo-Blanc, A., Jolivet, L., and Rossetti, F., 2004, Lateral slab deformation and the origin of the western Mediterranean arcs: Tectonics, v. 23, p. n/a-n/a.
Festa, A., Pini, G. A., Dilek, Y., and Codegone, G., 2010, Mélanges and mélange-forming processes: a historical overview and new concepts: International Geology Review, v. 52, p. 1040-1105.
Floyd, P., Kelling, G., Gökçen, S., and Gökçen, N., 1991, Geochemistry and tectonic environment of basaltic rocks from the Misis ophiolitic mélange, south Turkey: Chemical Geology, v. 89, p. 263-280.
-, 1992, Arc-related origin of volcaniclastic sequences in the Misis Complex, Southern Turkey: The Journal of Geology, v. 100, p. 221-230.

Fournier, M., Chamot-Rooke, N., Rodriguez, M., Huchon, P., Petit, C., Beslier, M.-O., and Zaragosi, S., 2011, Owen fracture zone: the Arabia–India plate boundary unveiled: Earth and Planetary Science Letters, v. 302, p. 247-252.

Frisch, W., 1979, Tectonic progradation and plate tectonic evolution of the Alps: Tectonophysics, v. 60, p. 121-139.

Gaetani, M., Casnedi, R., Fois, E., Garzanti, E., Jadoul, F., Nicora, A., and Tintori, A., 1986, Stratigraphy of the Tethys Himalaya in Zanskar, Ladakh: Rivista Italiana di Paleontologia e Stratigrafia, v. 91, p. 443-478.

Gągała, Ł., Vergés, J., Saura, E., Malata, T., Ringenbach, J.-C., Werner, P., and Krzywiec, P., 2012, Architecture and orogenic evolution of the northeastern Outer Carpathians from cross-section balancing and forward modeling: Tectonophysics, v. 532, p. 223-241.

Gaina, C., Torsvik, T. H., van Hinsbergen, D. J. J., Medvedev, S., Werner, S. C., and Labails, C., 2013, The African Plate: A history of oceanic crust accretion and subduction since the Jurassic: Tectonophysics, v. 604, p. 4-25.

Gaina, C., van Hinsbergen, D. J. J., and Spakman, W., 2015, Tectonic interactions between India and Arabia since the Jurassic reconstructed from marine geophysics, ophiolite geology, and seismic tomography: Tectonics, v. 34, p. 875-906.

Ganerød, M., Torsvik, T. H., van Hinsbergen, D. J. J., Gaina, C., Corfu, F., Werner, S., Owen-Smith, T. M., Ashwal, L. D., Webb, S. J., and Hendriks, B. W. H., 2011, Palaeoposition of the Seychelles microcontinent in relation to the Deccan Traps and the Plume Generation Zone in Late Cretaceous-Early Palaeogene time: Geological Society, London, Special Publications, v. 357, p. 229-252.

Garzanti, E., 1999, Stratigraphy and sedimentary history of the Nepal Tethys Himalaya passive margin: Journal of Asian Earth Sciences, v. 17, p. 805-827.

Garzanti, E., Le Fort, P., and Sciunnach, D., 1999, First report of Lower Permian basalts in South Tibet: tholeiitic magmatism during break-up and incipient opening of Neotethys: Journal of Asian Earth Sciences, v. 17, p. 533-546.

Gautier, P., Brun, J.-P., Moriceau, R., Sokoutis, D., Martinod, J., and Jolivet, L., 1999, Timing, kinematics and cause of Aegean extension: a scenario based on a comparison with simple analogue experiments: Tectonophysics, v. 315, p. 31-72.

Geersen, J., Voelker, D., and Behrmann, J. H., 2018, Oceanic trenches, Submarine Geomorphology, Springer, p. 409-424.

Gerya, T. V., Stöckhert, B., and Perchuk, A. L., 2002, Exhumation of high-pressure metamorphic rocks in a subduction channel: A numerical simulation: Tectonics, v. 21, p. 6-1-6-19.

Giardini, D., and Woodhouse, J., 1986, Horizontal shear flow in the mantle beneath the Tonga arc: Nature, v. 319, p. 551-555.

Gibbons, A. D., Barckhausen, U., van den Bogaard, P., Hoernle, K., Werner, R., Whittaker, J. M., and Müller, R. D., 2012, Constraining the Jurassic extent of Greater India: Tectonic evolution of the West Australian margin: Geochemistry Geophysics Geosystems, v. 13.

Gill, J. B., 1981, Orogenic andesites and plate tectonics, v. 16, Springer Science & Business Media, 391 p.

Golonka, J., Ross, M., and Scotese, C., 1994, Phanerozoic paleogeographic and paleoclimatic modeling maps.

Govers, R., and Wortel, M., 2005, Lithosphere tearing at STEP faults: Response to edges of subduction zones: Earth and Planetary Science Letters, v. 236, p. 505-523.

Gradstein, F. M., Ogg, J. G., Schmitz, M., and Ogg, G., 2012, The geologic time scale 2012, elsevier.

Groves, D. I., Goldfarb, R. J., Gebre-Mariam, M., Hagemann, S., and Robert, F., 1998, Orogenic gold deposits: a proposed classification in the context of their crustal distribution and relationship to other gold deposit types: Ore Geology Reviews, v. 13, p. 7-27.
Guilmette, C., Smit, M. A., van Hinsbergen, D. J., Gürer, D., Corfu, F., Charette, B., Maffione, M., Rabeau, O., and Savard, D., 2018, Forced subduction initiation recorded in the sole and crust of the Semail Ophiolite of Oman: Nature Geoscience, v. 11, p. 688-695.
Gülscher, A., Beaussier, S. J., and Gerya, T. V., 2019, On the formation of oceanic detachment faults and their influence on intra-oceanic subduction initiation: 3D thermomechanical modeling: Earth and Planetary Science Letters, v. 506, p. 195-208.
Gülyüz, E., Kaymakci, N., Meijers, M. J. M., van Hinsbergen, D. J. J., Lefebvre, C., Vissers, R. L. M., Hendriks, B. W. H., and Peynircioğlu, A. A., 2013, Late Eocene evolution of the Çiçekdağı Basin (central Turkey): Syn-sedimentary compression during microcontinent–continent collision in central Anatolia: Tectonophysics, v. 602, p. 286-299.
Gürer, D., Granot, R., and van Hinsbergen, D. J. J., 2021, Noise in the Cretaceous Quiet Zone reveals plate tectonic chain reaction: Nature Geoscience, v. submitted.
Gürer, D., Plunder, A., Kirst, F., Corfu, F., Schmid, S. M., and van Hinsbergen, D. J. J., 2018, A long-lived Late Cretaceous–early Eocene extensional province in Anatolia? Structural evidence from the Ivriz Detachment, southern central Turkey: Earth and Planetary Science Letters, v. 481, p. 111-124.
Gürer, D., and van Hinsbergen, D. J. J., 2019, Diachronous demise of the Neotethys Ocean as a driver for non-cylindrical orogenesis in Anatolia: Tectonophysics, v. 760, p. 95-106.
Gürer, D., van Hinsbergen, D. J. J., Matenco, L., Corfu, F., and Cascella, A., 2016, Kinematics of a former oceanic plate of the Neotethys revealed by deformation in the Ulukışla basin (Turkey): Tectonics, v. 35, p. 2385-2416.
Gürer, M. D., 2017, Subduction evolution in the Anatolian region: the rise, demise, and fate of the Anadolu Plate: University Utrecht, 239 p.
Gurnis, M., Hall, C., and Lavier, L., 2004, Evolving force balance during incipient subduction: Geochemistry, Geophysics, Geosystems, v. 5.
Gurnis, M., Yang, T., Cannon, J., Turner, M., Williams, S., Flament, N., and Müller, R. D., 2018, Global tectonic reconstructions with continuously deforming and evolving rigid plates: Computers & Geosciences, v. 116, p. 32-41.
Hacker, B., Mosenfelder, J., and Gnos, E., 1996, Rapid emplacement of the Oman ophiolite: Thermal and geochronologic constraints: Tectonics, v. 15, p. 1230-1247.
Hacker, B. R., 1994, Rapid emplacement of young oceanic lithosphere: argon geochronology of the Oman ophiolite: Science, v. 265, p. 1563-1565.
Hacker, B. R., and Gnos, E., 1997, The conundrum of Samail: explaining the metamorphic history: Tectonophysics, v. 279, p. 215-226.
Hafkenscheid, E., Wortel, M. J. R., and Spakman, W., 2006, Subduction history of the Tethyan region derived from seismic tomography and tectonic reconstructions: Journal of Geophysical Research, v. 111.
Hall, C. E., Gurnis, M., Sdrolias, M., Lavier, L. L., and Müller, R. D., 2003, Catastrophic initiation of subduction following forced convergence across fracture zones: Earth and Planetary Science Letters, v. 212, p. 15-30.
Hall, R., 2002, Cenozoic geological and plate tectonic evolution of SE Asia and the SW Pacific: computer-based reconstructions, model and animations: Journal of Asian Earth Sciences, v. 20, p. 353-431.

-, 2012, Late Jurassic–Cenozoic reconstructions of the Indonesian region and the Indian Ocean: Tectonophysics, v. 570-571, p. 1-41.
Handy, M. R., Schmid, S. M., Bousquet, R., Kissling, E., and Bernoulli, D., 2010, Reconciling plate-tectonic reconstructions of Alpine Tethys with the geological–geophysical record of spreading and subduction in the Alps: Earth-Science Reviews, v. 102, p. 121-158.
Harris, R., 2011, The nature of the Banda Arc–continent collision in the Timor region, Arc-Continent Collision, Springer, p. 163-211.
Hawkesworth, C., Cawood, P. A., and Dhuime, B., 2019, Rates of generation and growth of the continental crust: Geoscience Frontiers, v. 10, p. 165-173.
Hawkesworth, C. J., Dhuime, B., Pietranik, A., Cawood, P., Kemp, A. I., and Storey, C., 2010, The generation and evolution of the continental crust: Journal of the Geological Society, v. 167, p. 229-248.
Hébert, R., Bezard, R., Guilmette, C., Dostal, J., Wang, C. S., and Liu, Z. F., 2012, The Indus–Yarlung Zangbo ophiolites from Nanga Parbat to Namche Barwa syntaxes, southern Tibet: First synthesis of petrology, geochemistry, and geochronology with incidences on geodynamic reconstructions of Neo-Tethys: Gondwana Research, v. 22, p. 377-397.
Heine, C., Müller, R. D., Gaina, C., and Clift, P., 2004, Reconstructing the lost eastern Tethys ocean basin: convergence history of the SE Asian margin and marine gateways: Continent-Ocean Interactions Within East Asian Marginal Seas, Geophys. Monogr. Ser, v. 149, p. 37-54.
Henstock, T. J., and Thompson, P. J., 2004, Self-consistent modeling of crustal thickness at Chagos–Laccadive ridge from bathymetry and gravity data: Earth and Planetary Science Letters, v. 224, p. 325-336.
Horton, B. K., 2018, Sedimentary record of Andean mountain building: Earth-Science Reviews, v. 178, p. 279-309.
Hsü, K. J., Guitang, P., and Sengör, A. M. C., 1995, Tectonic Evolution of the Tibetan Plateau: A Working Hypothesis Based on the Archipelago Model of Orogenesis: International Geology Review, v. 37, p. 473-508.
Hu, X., Garzanti, E., Moore, T., and Raffi, I., 2015, Direct stratigraphic dating of India-Asia collision onset at the Selandian (middle Paleocene, 59 ± 1 Ma): Geology, v. 43, p. 859-862.
Hu, X., Garzanti, E., Wang, J., Huang, W., An, W., and Webb, A., 2016, The timing of India-Asia collision onset – Facts, theories, controversies: Earth-Science Reviews, v. 160, p. 264-299.
Hüsing, S. K., Zachariasse, W.-J., van Hinsbergen, D. J. J., Krijgsman, W., Inceöz, M., Harzhauser, M., Mandic, O., and Kroh, A., 2009, Oligocene–Miocene basin evolution in SE Anatolia, Turkey: constraints on the closure of the eastern Tethys gateway: Geological Society, London, Special Publications, v. 311, p. 107-132.
Ingalls, M., Rowley, D. B., Currie, B., and Colman, A. S., 2016, Large-scale subduction of continental crust implied by India–Asia mass-balance calculation: Nature Geoscience, v. 9, p. 848-853.
Isozaki, Y., 1996, Anatomy and genesis of a subduction-related orogen: A new view of geotectonic subdivision and evolution of the Japanese Islands: Island Arc, v. 5, p. 289-320.
Isozaki, Y., Aoki, K., Nakama, T., and Yanai, S., 2010, New insight into a subduction-related orogen: A reappraisal of the geotectonic framework and evolution of the Japanese Islands: Gondwana Research, v. 18, p. 82-105.

Isozaki, Y., Maruyama, S., and Furuoka, F., 1990, Accreted oceanic materials in Japan: Tectonophysics, v. 181, p. 179-205.
Iturralde-Vinent, M., Díaz Otero, C., García-Casco, A., and van Hinsbergen, D. J. J., 2008, Paleogene Foredeep Basin Deposits of North-Central Cuba: A Record of Arc-Continent Collision between the Caribbean and North American Plates: International Geology Review, v. 40, p. 1-22.
Jagoutz, O., Royden, L., Holt, A. F., and Becker, T. W., 2015, Anomalously fast convergence of India and Eurasia caused by double subduction: Nature Geoscience, v. 8, p. 475-478.
Jamieson, R. A., 1980, Formation of rnetamorphic aureoles beneath ophiolites— Evidence from the St. Anthony Complex, Newfoundland: Geology, v. 8.
Jarrard, R. D., 1986, Terrane motion by strike-slip faulting of forearc slivers: Geology, v. 14, p. 780-783.
Johnston, S. T., 2001, The Great Alaskan Terrane Wreck: reconciliation of paleomagnetic and geological data in the northern Cordillera: Earth and Planetary Science Letters, v. 193, p. 259-272.
Jolivet, L., and Brun, J.-P., 2010, Cenozoic geodynamic evolution of the Aegean: International Journal of Earth Sciences, v. 99, p. 109-138.
Jolivet, L., and Faccenna, C., 2000, Mediterranean extension and the Africa-Eurasia collision: Tectonics, v. 19, p. 1095-1106.
Jolivet, L., Faccenna, C., Goffé, B., Burov, E., and Agard, P., 2003, Subduction tectonics and exhumation of high-pressure metamorphic rocks in the Mediterranean orogens: American Journal of Science, v. 303, p. 353-409.
Jolivet, L., Faccenna, C., and Piromallo, C., 2009, From mantle to crust: Stretching the Mediterranean: Earth and Planetary Science Letters, v. 285, p. 198-209.
Jolivet, M., Dominguez, S., Charreau, J., Chen, Y., Li, Y., and Wang, Q., 2010, Mesozoic and Cenozoic tectonic history of the central Chinese Tian Shan: Reactivated tectonic structures and active deformation: Tectonics, v. 29, p. n/a-n/a.
Kapp, P., and DeCelles, P. G., 2019, Mesozoic–Cenozoic geological evolution of the Himalayan-Tibetan orogen and working tectonic hypotheses: American Journal of Science, v. 319, p. 159-254.
Kapp, P., DeCelles, P. G., Leier, A., Fabijanic, J., He, S., Pullen, A., Gehrels, G. E., and Ding, L., 2007, The Gangdese retroarc thrust belt revealed: GSA Today, v. 17, p. 4.
Karig, D. E., 1970, Ridges and basins of the Tonga-Kermadec island arc system: Journal of Geophysical Research, v. 75, p. 239-254.
Kästle, E. D., Rosenberg, C., Boschi, L., Bellahsen, N., Meier, T., and El-Sharkawy, A., 2020, Slab break-offs in the Alpine subduction zone: International Journal of Earth Sciences, p. 1-17.
Kaymakci, N., Inceöz, M., Ertepinar, P., and Koç, A., 2010, Late Cretaceous to Recent kinematics of SE Anatolia (Turkey): Geological Society, London, Special Publications, v. 340, p. 409-435.
Kerr, A. C., 2003, Oceanic plateaus: TrGeo, v. 3, p. 659.
Keskin, M., 2003, Magma generation by slab steepening and breakoff beneath a subduction-accretion complex: An alternative model for collision-related volcanism in Eastern Anatolia, Turkey: Geophysical Research Letters, v. 30.
Khan, S. D., Walker, D. J., Hall, S. A., Burke, K. C., Shah, M. T., and Stockli, L., 2009, Did the Kohistan-Ladakh island arc collide first with India?: Geological Society of America Bulletin, v. 121, p. 366-384.

Khotin, M. Y., and Shapiro, M., 2006, Ophiolites of the Kamchatsky Mys Peninsula, eastern Kamchatka: Structure, composition, and geodynamic setting: Geotectonics, v. 40, p. 297-320.
Kimura, G., 1996, Collision orogeny at arc-arc junctions in the Japanese Islands: Island Arc, v. 5, p. 262-275.
Konstantinovskaia, E., 2001, Arc–continent collision and subduction reversal in the Cenozoic evolution of the Northwest Pacific: an example from Kamchatka (NE Russia): Tectonophysics, v. 333, p. 75-94.
Krabbendam, M., and Dewey, J. F., 1998, Exhumation of UHP rocks by transtension in the Western Gneiss Region, Scandinavian Caledonides: Geological Society, London, Special Publications, v. 135, p. 159-181.
Krishnan, M., 1963, Deccan trap volcanism: Bulletin Volcanologique, v. 26, p. 387.
Kröner, A., Kovach, V., Belousova, E., Hegner, E., Armstrong, R., Dolgopolova, A., Seltmann, R., Alexeiev, D., Hoffmann, J., and Wong, J., 2014, Reassessment of continental growth during the accretionary history of the Central Asian Orogenic Belt: Gondwana Research, v. 25, p. 103-125.
Kröner, A., and Sassi, F., 1996, Evolution of the northern Somali basement: new constraints from zircon ages: Journal of African Earth Sciences, v. 22, p. 1-15.
Kumar, P., Tewari, H., and Khandekar, G., 2000, An anomalous high-velocity layer at shallow crustal depths in the Narmada zone, India: Geophysical Journal International, v. 142, p. 95-107.
Kusky, T., Windley, B., Safonova, I., Wakita, K., Wakabayashi, J., Polat, A., and Santosh, M., 2013, Recognition of ocean plate stratigraphy in accretionary orogens through Earth history: A record of 3.8 billion years of sea floor spreading, subduction, and accretion: Gondwana Research, v. 24, p. 501-547.
Lagabrielle, Y., Goddéris, Y., Donnadieu, Y., Malavieille, J., and Suarez, M., 2009, The tectonic history of Drake Passage and its possible impacts on global climate: Earth and Planetary Science Letters, v. 279, p. 197-211.
Lallemand, S., Heuret, A., and Boutelier, D., 2005, On the relationships between slab dip, back-arc stress, upper plate absolute motion, and crustal nature in subduction zones: Geochemistry, Geophysics, Geosystems, v. 6, p. n/a-n/a.
Lallemand, S., Heuret, A., Faccenna, C., and Funiciello, F., 2008, Subduction dynamics as revealed by trench migration: Tectonics, v. 27, p. n/a-n/a.
Lander, A. V., and Shapiro, M. N., 2007, The origin of the modern Kamchatka subduction zone: GMS, v. 172, p. 57-64.
Le Dain, A. Y., Tapponnier, P., and Molnar, P., 1984, Active faulting and tectonics of Burma and surrounding regions: Journal of Geophysical Research, v. 89.
Lee, C.-T. A., Luffi, P., and Chin, E. J., 2011, Building and destroying continental mantle: Annual Review of Earth and Planetary Sciences, v. 39, p. 59-90.
Leech, M., Singh, S., Jain, A., Klemperer, S., and Manickavasagam, R., 2005, The onset of India–Asia continental collision: Early, steep subduction required by the timing of UHP metamorphism in the western Himalaya: Earth and Planetary Science Letters, v. 234, p. 83-97.
Lefebvre, C., Meijers, M. J. M., Kaymakci, N., Peynircioğlu, A., Langereis, C. G., and van Hinsbergen, D. J. J., 2013, Reconstructing the geometry of central Anatolia during the late Cretaceous: Large-scale Cenozoic rotations and deformation between the Pontides and Taurides: Earth and Planetary Science Letters, v. 366, p. 83-98.
Legg, M. R., C. Goldfinger, M. Kamerling, J. Chaytor, and D. Einstein (2007), Morphology, structure and evolution of California Continental Borderland restraining bends, Geological Society, London, Special Publications, 290(1), 143-168.

Leloup, P. H., Lacassin, R., Tapponnier, P., Schärer, U., Zhong, D., Liu, X., Zhang, L., Ji, S., and Trinh, P. T., 1995, The Ailao Shan-Red river shear zone (Yunnan, China), tertiary transform boundary of Indochina: Tectonophysics, v. 251, p. 3-84.
Leng, W., and Gurnis, M., 2011, Dynamics of subduction initiation with different evolutionary pathways: Geochemistry, Geophysics, Geosystems, v. 12, p. n/a-n/a.
Lenoir, J.-L., Liégeois, J.-P., Küster, D., Utke, A., Matheis, G., and Haider, A., 1994, Origin and regional significance of late Precambrian and early Palaeozoic granitoids in the Pan-African belt of Somalia: Geologische Rundschau, v. 83, p. 624-641.
Levashova, N. M., Shapiro, M. N., Beniamovsky, V. N., and Bazhenov, M. L., 2000, Paleomagnetism and geochronology of the Late Cretaceous-Paleogene island arc complex of the Kronotsky Peninsula, Kamchatka, Russia: Kinematic implications: Tectonics, v. 19, p. 834-851.
Li, S., Advokaat, E. L., van Hinsbergen, D. J. J., Koymans, M., Deng, C., and Zhu, R., 2017, Paleomagnetic constraints on the Mesozoic-Cenozoic paleolatitudinal and rotational history of Indochina and South China: Review and updated kinematic reconstruction: Earth-Science Reviews, v. 171, p. 58-77.
Li, S., van Hinsbergen, D. J., Najman, Y., Liu-Zeng, J., Deng, C., and Zhu, R., 2020a, Does pulsed Tibetan deformation correlate with Indian plate motion changes?: Earth and Planetary Science Letters, v. 536, p. 116144.
Li, S., van Hinsbergen, D. J. J., Shen, Z., Najman, Y., Deng, C., and Zhu, R., 2020b, Anisotropy of magnetic susceptibility (AMS) analysis of the Gonjo Basin as an independent constraint to date Tibetan shortening pulses: Geophysical Research Letters, v. 47, p. e2020GL087531.
Li, S., Yin, C., Guilmette, C., Ding, L., and Zhang, J., 2019, Birth and demise of the Bangong-Nujiang Tethyan Ocean: A review from the Gerze area of central Tibet: Earth-Science Reviews, v. 198, p. 102907.
Li, Z.-X., Bogdanova, S., Collins, A., Davidson, A., De Waele, B., Ernst, R., Fitzsimons, I., Fuck, R., Gladkochub, D., and Jacobs, J., 2008, Assembly, configuration, and break-up history of Rodinia: a synthesis: Precambrian Research, v. 160, p. 179-210.
Li, Z.-X., and Li, X.-H., 2007, Formation of the 1300-km-wide intracontinental orogen and postorogenic magmatic province in Mesozoic South China: A flat-slab subduction model: Geology, v. 35.
Liati, A., Gebauer, D., and Fanning, C. M., 2004, The age of ophiolitic rocks of the Hellenides (Vourinos, Pindos, Crete): first U–Pb ion microprobe (SHRIMP) zircon ages: Chemical Geology, v. 207, p. 171-188.
Liberi, F., Morten, L., and Piluso, E., 2006, Geodynamic significance of ophiolites within the Calabrian Arc: Island Arc, v. 15, p. 26-43.
Livermore, R., Nankivell, A. P., Eagles, G., and Morris, P., 2005, Paleogene opening of Drake Passage: Earth and Planetary Science Letters, v. 236, p. 459-470.
Lonergan, L., and White, N., 1997, Origin of the Betic-Rif mountain belt: Tectonics, v. 16, p. 504-522.
Long, S., McQuarrie, N., Tobgay, T., and Grujic, D., 2011, Geometry and crustal shortening of the Himalayan fold-thrust belt, eastern and central Bhutan: Geological Society of America Bulletin, v. 123, p. 1427-1447.
Luth, S., Willingshofer, E., Sokoutis, D., and Cloetingh, S., 2010, Analogue modelling of continental collision: Influence of plate coupling on mantle lithosphere subduction, crustal deformation and surface topography: Tectonophysics, v. 484, p. 87-102.
Maffione, M., Thieulot, C., van Hinsbergen, D. J. J., Morris, A., Plümper, O., and Spakman, W., 2015a, Dynamics of intraoceanic subduction initiation: 1. Oceanic detachment

fault inversion and the formation of supra-subduction zone ophiolites: Geochemistry, Geophysics, Geosystems, v. 16, p. 1753-1770.
Maffione, M., and van Hinsbergen, D. J. J., 2018, Reconstructing plate boundaries in the Jurassic Neo-Tethys from the East and West Vardar Ophiolites (Greece, Serbia): Tectonics.
Maffione, M., van Hinsbergen, D. J. J., de Gelder, G. I. N. O., van der Goes, F. C., and Morris, A., 2017, Kinematics of Late Cretaceous subduction initiation in the Neo-Tethys Ocean reconstructed from ophiolites of Turkey, Cyprus, and Syria: Journal of Geophysical Research: Solid Earth, v. 122, p. 3953-3976.
Maffione, M., van Hinsbergen, D. J. J., Koornneef, L. M. T., Guilmette, C., Hodges, K., Borneman, N., Huang, W., Ding, L., and Kapp, P., 2015b, Forearc hyperextension dismembered the south Tibetan ophiolites: Geology, v. 43, p. 475-478.
Maldonado, A., Bohoyo, F., Galindo-Zaldívar, J., Hernández-Molina, F. J., Lobo, F. J., Lodolo, E., Martos, Y. M., Pérez, L. F., Schreider, A. A., and Somoza, L., 2014, A model of oceanic development by ridge jumping: Opening of the Scotia Sea: Global and Planetary Change, v. 123, p. 152-173.
Malod, J. A., and Kemal, B. M., 1996, The Sumatra margin: oblique subduction and lateral displacement of the accretionary prism: Geological Society, London, Special Publications, v. 106, p. 19-28.
Mamberti, M., Lapierre, H., Bosch, D., Jaillard, E., Ethien, R., Hernandez, J., and Polvé, M., 2003, Accreted fragments of the Late Cretaceous Caribbean–Colombian Plateau in Ecuador: Lithos, v. 66, p. 173-199.
Mart, Y., 1988, The tectonic setting of the Seychelles, Mascarene and Amirante plateaus in the western equatorial Indian Ocean: Marine Geology, v. 79, p. 261-274.
Martin, C. R., Jagoutz, O., Upadhyay, R., Royden, L. H., Eddy, M. P., Bailey, E., Nichols, C. I., and Weiss, B. P., 2020, Paleocene latitude of the Kohistan–Ladakh arc indicates multistage India–Eurasia collision: Proceedings of the National Academy of Sciences, v. 117, p. 29487-29494.
Martini, M., Solari, L., and López-Martínez, M., 2014, Correlating the Arperos Basin from Guanajuato, central Mexico, to Santo Tomás, southern Mexico: Implications for the paleogeography and origin of the Guerrero terrane: Geosphere, v. 10, p. 1385-1401.
Maruyama, S., 1997, Pacific-type orogeny revisited: Miyashiro-type orogeny proposed: Island Arc, v. 6, p. 91-120.
Maruyama, S., Kawai, T., and Windley, B., 2010, Ocean plate stratigraphy and its imbrication in an accretionary orogen: the Mona complex, Anglesey–Lleyn, Wales, UK: Geological Society, London, Special Publications, v. 338, p. 55-75.
Maruyama, S., Liou, J., and Terabayashi, M., 1996, Blueschists and eclogites of the world and their exhumation: International Geology Review, v. 38, p. 485-594.
Matte, P., Tapponnier, P., Arnaud, N., Bourjot, L., Avouac, J., Vidal, P., Qing, L., Yusheng, P., and Yi, W., 1996, Tectonics of Western Tibet, between the Tarim and the Indus: Earth and Planetary Science Letters, v. 142, p. 311-330.
Matthews, K. J., Maloney, K. T., Zahirovic, S., Williams, S. E., Seton, M., and Müller, R. D., 2016, Global plate boundary evolution and kinematics since the late Paleozoic: Global and Planetary Change, v. 146, p. 226-250.
Mazumder, R., and Eriksson, P. G., 2015, Precambrian basins of India: stratigraphic and tectonic context: Geological Society, London, Memoirs, v. 43, p. 1-4.
McKenzie, D., and Sclater, J. G., 1971, The evolution of the Indian Ocean since the Late Cretaceous: Geophysical Journal International, v. 24, p. 437-528.

McPhee, P. J., Altıner, D., and van Hinsbergen, D. J., 2018, First Balanced Cross Section Across the Taurides Fold-Thrust Belt: Geological Constraints on the Subduction History of the Antalya Slab in Southern Anatolia: Tectonics.
McPhee, P. J., and van Hinsbergen, D. J. J., 2019, Tectonic reconstruction of Cyprus reveals Late Miocene continental collision between Africa and Anatolia: Gondwana Research, v. 68, p. 158-173.
McQuarrie, N., 2002, Initial plate geometry, shortening variations, and evolution of the Bolivian orocline: Geology, v. 30, p. 867-870.
McQuarrie, N., Horton, B. K., Zandt, G., Beck, S., and DeCelles, P. G., 2005, Lithospheric evolution of the Andean fold–thrust belt, Bolivia, and the origin of the central Andean plateau: Tectonophysics, v. 399, p. 15-37.
McQuarrie, N., Stock, J. M., Verdel, C., and Wernicke, B. P., 2003, Cenozoic evolution of Neotethys and implications for the causes of plate motions: Geophysical Research Letters, v. 30, p. n/a-n/a.
McQuarrie, N., and van Hinsbergen, D. J. J., 2013, Retrodeforming the Arabia-Eurasia collision zone: Age of collision versus magnitude of continental subduction: Geology, v. 41, p. 315-318.
McQuarrie, N., and Wernicke, B. P., 2005, An animated tectonic reconstruction of southwestern North America since 36 Ma: Geosphere, v. 1, p. 147-172.
Meert, J. G., 2003, A synopsis of events related to the assembly of eastern Gondwana: Tectonophysics, v. 362, p. 1-40.
Meert, J. G., Van der Voo, R., Powell, C. M., Li, Z.-X., McElhinny, M. W., Chen, Z., and Symons, D., 1993, A plate-tectonic speed limit?: Nature, v. 363, p. 216-217.
Menant, A., Jolivet, L., and Vrielynck, B., 2016, Kinematic reconstructions and magmatic evolution illuminating crustal and mantle dynamics of the eastern Mediterranean region since the late Cretaceous: Tectonophysics, v. 675, p. 103-140.
Merdith, A. S., Collins, A. S., Williams, S. E., Pisarevsky, S., Foden, J. D., Archibald, D. B., Blades, M. L., Alessio, B. L., Armistead, S., and Plavsa, D., 2017, A full-plate global reconstruction of the Neoproterozoic: Gondwana Research, v. 50, p. 84-134.
Merdith, A. S., Williams, S. E., Collins, A. S., Tetley, M. G., Mulder, J. A., Blades, M. L., Young, A., Armistead, S. E., Cannon, J., and Zahirovic, S., 2020, Extending full-plate tectonic models into deep time: Linking the neoproterozoic and the phanerozoic: Earth-Science Reviews, p. 103477.
Meyer, B., Tapponnier, P., Bourjot, L., Metivier, F., Gaudemer, Y., Peltzer, G., Shunmin, G., and Zhitai, C., 1998, Crustal thickening in Gansu-Qinghai, lithospheric mantle subduction, and oblique, strike-slip controlled growth of the Tibet plateau: Geophysical Journal International, v. 135, p. 1-47.
Mittelstaedt, E., Ito, G., and Behn, M. D., 2008, Mid-ocean ridge jumps associated with hotspot magmatism: Earth and Planetary Science Letters, v. 266, p. 256-270.
Molnar, P., and Stock, J. M., 2009, Slowing of India's convergence with Eurasia since 20 Ma and its implications for Tibetan mantle dynamics: Tectonics, v. 28, p. n/a-n/a.
Molnar, P., and Tapponnier, P., 1975, Cenozoic tectonics of Asia: effects of a continental collision: Science, v. 189, p. 419-426.
Morley, C., 2018, Understanding Sibumasu in the context of ribbon continents: Gondwana Research, v. 64, p. 184-215.
Morley, C., Naing, T. T., Searle, M., and Robinson, S., 2019, Structural and tectonic development of the Indo-Burma Ranges: Earth-Science Reviews, p. 102992.
Mortimer, N., Campbell, H. J., Tulloch, A. J., King, P. R., Stagpoole, V. M., Wood, R. A., Rattenbury, M. S., Sutherland, R., Adams, C. J., and Collot, J., 2017, Zealandia: Earth's hidden continent: GSA Today, v. 27, p. 27-35.

Mouthereau, F., 2011, Timing of uplift in the Zagros belt/Iranian plateau and accommodation of late Cenozoic Arabia–Eurasia convergence: Geological Magazine, v. 148, p. 726-738.
Müller, R. D., Cannon, J., Qin, X., Watson, R. J., Gurnis, M., Williams, S., Pfaffelmoser, T., Seton, M., Russell, S. H., and Zahirovic, S., 2018, GPlates: building a virtual Earth through deep time: Geochemistry, Geophysics, Geosystems, v. 19, p. 2243-2261.
Müller, R. D., Zahirovic, S., Williams, S. E., Cannon, J., Seton, M., Bower, D. J., Tetley, M. G., Heine, C., Le Breton, E., and Liu, S., 2019, A global plate model including lithospheric deformation along major rifts and orogens since the Triassic: Tectonics.
Murphy, M. A., Yin, A., Harrison, T. M., Dürr, S. B., Z, C., Ryerson, F. J., Kidd, W. S. F., X, W., and X, Z., 1997, Did the Indo-Asian collision alone create the Tibetan plateau?: Geology, v. 25.
Muttoni, G., Mattei, M., Balini, M., Zanchi, A., Gaetani, M., and Berra, F., 2009, The drift history of Iran from the Ordovician to the Triassic: Geological Society, London, Special Publications, v. 312, p. 7-29.
Nabelek, J., Hetenyi, G., Vergne, J., Sapkota, S., Kafle, B., Jiang, M., Su, H., Chen, J., Huang, B. S., and Hi, C. T., 2009, Underplating in the Himalaya-Tibet collision zone revealed by the Hi-CLIMB experiment: Science, v. 325, p. 1371-4.
Nair, N., Anand, S., and Rajaram, M., 2013, Tectonic framework of laccadive Ridge in western Continental margin of India: Marine Geology, v. 346, p. 79-90.
Najman, Y., Appel, E., Boudagher-Fadel, M., Bown, P., Carter, A., Garzanti, E., Godin, L., Han, J., Liebke, U., Oliver, G., Parrish, R., and Vezzoli, G., 2010, Timing of India-Asia collision: Geological, biostratigraphic, and palaeomagnetic constraints: Journal of Geophysical Research, v. 115.
Neill, I., Kerr, A. C., Hastie, A. R., Stanek, K. P., and Millar, I. L., 2011, Origin of the Aves Ridge and Dutch-Venezuelan Antilles: interaction of the Cretaceous 'Great Arc' and Caribbean-Colombian Oceanic Plateau?: Journal of the Geological Society, v. 168, p. 333-348.
Nikolaeva, K., Gerya, T., and Marques, F., 2010, Subduction initiation at passive margins: numerical modeling: Journal of Geophysical Research: Solid Earth, v. 115.
Okay, A. I., Zattin, M., and Cavazza, W., 2010, Apatite fission-track data for the Miocene Arabia-Eurasia collision: Geology, v. 38, p. 35-38.
Oncken, O., Hindle, D., Kley, J., Elger, K., Victor, P., and Schemmann, K., 2006, Deformation of the central Andean upper plate system—Facts, fiction, and constraints for plateau models, The Andes, Springer, p. 3-27.
Orme, D. A., Carrapa, B., and Kapp, P., 2015, Sedimentology, provenance and geochronology of the upper Cretaceous-lower Eocene western Xigaze forearc basin, southern Tibet: Basin Research, v. 27, p. 387-411.
Özgül, N., 1984, Stratigraphy and tectonic evolution of the Central Taurides: Geology of the Taurus belt, p. 77-90.
Pandey, D. K., Pandey, A., and Whattam, S. A., 2019, Relict subduction initiation along a passive margin in the northwest Indian Ocean: Nature Communications, v. 10, p. 1-10.
Parkash, B., Sharma, R., and Roy, A., 1980, The Siwalik Group (molasse)—sediments shed by collision of continental plates: Sedimentary Geology, v. 25, p. 127-159.
Parlak, O., 2016, The tauride ophiolites of Anatolia (Turkey): A review: Journal of Earth Science, v. 27, p. 901-934.
Parsons, A. J., Hosseini, K., Palin, R., and Sigloch, K., 2020, Geological, geophysical and plate kinematic constraints for models of the India-Asia collision and the post-Triassic central Tethys oceans: Earth-Science Reviews, p. 103084.

Patriat, P., and Achache, J., 1984, India-Eurasia collision chronology has implications for crustal shortening and driving mechanism of plates: Nature, v. 311, p. 615-621.
Paul, A., Hatzfeld, D., Kaviani, A., Tatar, M., and Péquegnat, C., 2010, Seismic imaging of the lithospheric structure of the Zagros mountain belt (Iran): Geological Society, London, Special Publications, v. 330, p. 5-18.
Pearce, J. A., Lippard, S., and Roberts, S., 1984, Characteristics and tectonic significance of supra-subduction zone ophiolites: Geological Society, London, Special Publications, v. 16, p. 77-94.
Peters, K., van Hinsbergen, D., Smit, M., van Roermund, H., Brouwer, F., Plunder, A., and Guilmette, C., 2018, Magnitude and meaning of time lags between the formation and cooling of Neotethyan metamorphic soles from multi-chronology: EGUGA, p. 11957.
Peters, T., and Mercolli, I., 1998, Extremely thin oceanic crust in the Proto-Indian Ocean: Evidence from the Masirah Ophiolite, Sultanate of Oman: Journal of Geophysical Research: Solid Earth, v. 103, p. 677-689.
Philippon, M., Cornée, J.-J., Münch, P., van Hinsbergen, D. J., BouDagher-Fadel, M., Gailler, L., Boschman, L. M., Quillevere, F., Montheil, L., and Gay, A., 2020, Eocene intra-plate shortening responsible for the rise of a faunal pathway in the northeastern Caribbean realm: PLoS One, v. 15, p. e0241000.
Philippon, M., and Corti, G., 2016, Obliquity along plate boundaries: Tectonophysics, v. 693, p. 171-182.
Pindell, J., and Dewey, J. F., 1982, Permo-Triassic reconstruction of western Pangea and the evolution of the Gulf of Mexico/Caribbean region: Tectonics, v. 1, p. 179-211.
Platt, J., 1993, Exhumation of high-pressure rocks: A review of concepts and processes: Terra Nova, v. 5, p. 119-133.
Plunder, A., Bandyopadhyay, D., Ganerød, M., Advokaat, E. L., Ghosh, B., Bandopadhyay, P., and van Hinsbergen, D. J., 2020, History of subduction polarity reversal during arc-continent collision: constraints from the Andaman Ophiolite and its metamorphic sole: Tectonics, p. e2019TC005762.
Plunder, A., Thieulot, C., and van Hinsbergen, D. J., 2018, The effect of obliquity on temperature in subduction zones: insights from 3-D numerical modeling: Solid Earth, v. 9, p. 759-776.
Poblete, F., Dupont-Nivet, G., Licht, A., van Hinsbergen, D. J. J., Roperch, P., Mihalynuk, M. G., Johnston, S. T., Guillocheau, F., Baby, G., Fluteau, F., Robin, C., van der Linden, T. J. M., and Baatsen, M., 2021, Towards interactive global paleogeographic maps, new reconstructions at 60, 40 and 20 Ma,: Earth-Science Reviews, 103508.
Portnyagin, M., Savelyev, D., Hoernle, K., Hauff, F., and Garbe-Schönberg, D., 2008, Mid-Cretaceous Hawaiian tholeiites preserved in Kamchatka: Geology, v. 36, p. 903-906.
Pourteau, A., Scherer, E. E., Schorn, S., Bast, R., Schmidt, A., and Ebert, L., 2019, Thermal evolution of an ancient subduction interface revealed by Lu–Hf garnet geochronology, Halilbağı Complex (Anatolia): Geoscience Frontiers, v. 10, p. 127-148.
Pourteau, A., Sudo, M., Candan, O., Lanari, P., Vidal, O., and Oberhänsli, R., 2013, Neotethys closure history of Anatolia: insights from 40Ar-39Ar geochronology andP-Testimation in high-pressure metasedimentary rocks: Journal of Metamorphic Geology, v. 31, p. 585-606.
Pownall, J. M., Hall, R., and Armstrong, R. A., 2017, Hot lherzolite exhumation, UHT migmatite formation, and acid volcanism driven by Miocene rollback of the Banda Arc, eastern Indonesia: Gondwana Research, v. 51, p. 92-117.

Pownall, J. M., Hall, R., and Watkinson, I. M., 2013, Extreme extension across Seram and Ambon, eastern Indonesia: evidence for Banda slab rollback: Solid Earth, v. 4, p. 277-314.
Pusok, A., and Kaus, B. J., 2015, Development of topography in 3-D continental-collision models: Geochemistry, Geophysics, Geosystems, v. 16, p. 1378-1400.
Radwany, M., Morgan, L. E., and Whitney, D. L., 2020, Conditions and timing of incorporation of ophiolite into orogenic crust during oblique convergence, Central Anatolia: International Journal of Earth Sciences, p. 1-14.
Rai, S., Vijay Kumar, T., and Jagadeesh, S., 2005, Seismic evidence for significant crustal thickening beneath Jabalpur earthquake, 21 May 1997, source region in Narmada–Son lineament, central India: Geophysical Research Letters, v. 32.
Ramos, V. A., 2009, Anatomy and global context of the Andes: Main geologic features and the Andean orogenic cycle: Geological Society of America Memoirs, v. 204, p. 31-65.
Ranero, C. R., and von Huene, R., 2000, Subduction erosion along the Middle America convergent margin: Nature, v. 404, p. 748-752.
Rao, B. R., 2000, Historical seismicity and deformation rates in the Indian peninsular shield: Journal of Seismology, v. 4, p. 247-258.
Replumaz, A., Negredo, A. M., Guillot, S., and Villaseñor, A., 2010a, Multiple episodes of continental subduction during India/Asia convergence: Insight from seismic tomography and tectonic reconstruction: Tectonophysics, v. 483, p. 125-134.
Replumaz, A., Negredo, A. M., Villaseñor, A., and Guillot, S., 2010b, Indian continental subduction and slab break-off during Tertiary collision: Terra Nova, v. 22, p. 290-296.
Reyners, M., Eberhart-Phillips, D., and Bannister, S., 2011, Tracking repeated subduction of the Hikurangi Plateau beneath New Zealand: Earth and Planetary Science Letters, v. 311, p. 165-171.
Richards, J. P., 2009, Postsubduction porphyry Cu-Au and epithermal Au deposits: Products of remelting of subduction-modified lithosphere: Geology, v. 37, p. 247-250.
Richter, M., Nebel, O., Maas, R., Mather, B., Nebel-Jacobsen, Y., Capitanio, F. A., Dick, H. J., and Cawood, P. A., 2020, An Early Cretaceous subduction-modified mantle underneath the ultraslow spreading Gakkel Ridge, Arctic Ocean: Science Advances, v. 6, p. eabb4340.
Ring, U., 1994, The influence of preexisting structure on the evolution of the Cenozoic Malawi rift (East African rift system): Tectonics, v. 13, p. 313-326.
Rioux, M., Bowring, S., Kelemen, P., Gordon, S., Miller, R., and Dudás, F., 2013, Tectonic development of the Samail ophiolite: High-precision U-Pb zircon geochronology and Sm-Nd isotopic constraints on crustal growth and emplacement: Journal of Geophysical Research: Solid Earth, v. 118, p. 2085-2101.
Rioux, M., Garber, J., Bauer, A., Bowring, S., Searle, M., Kelemen, P., and Hacker, B., 2016, Synchronous formation of the metamorphic sole and igneous crust of the Semail ophiolite: New constraints on the tectonic evolution during ophiolite formation from high-precision U–Pb zircon geochronology: Earth and Planetary Science Letters, v. 451, p. 185-195.
Robertson, A. H. F. (2002), Overview of the genesis and emplacement of Mesozoic ophiolites in the Eastern Mediterranean Tethyan region, Lithos, 65, 1-67.
Robertson, A.H.F., Ü. C.., Unlügenç, Ü. C., İnan, N., and Taśli, K., 2004, The Misis–Andırın Complex: a Mid-Tertiary melange related to late-stage subduction of the Southern Neotethys in S Turkey: Journal of Asian Earth Sciences, v. 22, p. 413-453.
Robertson, A. H. F., 2002, Overview of the genesis and emplacement of Mesozoic ophiolites in the Eastern Mediterranean Tethyan region: Lithos, v. 65, p. 1-67.

Romagny, A., Jolivet, L., Menant, A., Bessière, E., Maillard, A., Canva, A., Gorini, C., and Augier, R., 2020, Detailed tectonic reconstructions of the Western Mediterranean region for the last 35 Ma, insights on driving mechanismsReconstructions détaillées de la Méditerranée occidentale depuis 35 Ma, implications en terme de mécanismes moteur: Bulletin de la Société Géologique de France, v. 191.
Rosenbaum, G., 2012, Oroclines of the southern New England orogen, eastern Australia: Episodes, v. 35, p. 187-194.
Rosenbaum, G., Lister, G. S., and Duboz, C., 2002, Reconstruction of the tectonic evolution of the western Mediterranean since the Oligocene: Journal of the Virtual Explorer, v. 8, p. 107-130.
Rossetti, F., Faccenna, C., Goffé, B., Monié, P., Argentieri, A., Funiciello, R., and Mattei, M., 2001, Alpine structural and metamorphic signature of the Sila Piccola Massif nappe stack (Calabria, Italy): Insights for the tectonic evolution of the Calabrian Arc: Tectonics, v. 20, p. 112-133.
Royden, L., and Faccenna, C., 2018, Subduction orogeny and the Late Cenozoic evolution of the mediterranean arcs: Annual Review of Earth and Planetary Sciences, v. 46, p. 261-289.
Safonova, I., Maruyama, S., Kojima, S., Komiya, T., Krivonogov, S., and Koshida, K., 2016, Recognizing OIB and MORB in accretionary complexes: A new approach based on ocean plate stratigraphy, petrology and geochemistry: Gondwana Research, v. 33, p. 92-114.
Safonova, I. Y., and Santosh, M., 2014, Accretionary complexes in the Asia-Pacific region: tracing archives of ocean plate stratigraphy and tracking mantle plumes: Gondwana Research, v. 25, p. 126-158.
Sarıfakıoğlu, E., Dilek, Y., and Sevin, M., 2017, New synthesis of the Izmir-Ankara-Erzincan suture zone and the Ankara mélange in northern Anatolia based on new geochemical and geochronological constraints: Tectonic Evolution, Collision, and Seismicity of Southwest Asia: In Honor of Manuel Berberian's Forty-Five Years of Research Contributions. Geological Society of America Special Paper, v. 525.
Schellart, W., Stegman, D., Farrington, R., Freeman, J., and Moresi, L., 2010, Cenozoic tectonics of western North America controlled by evolving width of Farallon slab: Science, v. 329, p. 316-319.
Schellart, W. P., 2008, Overriding plate shortening and extension above subduction zones: A parametric study to explain formation of the Andes Mountains: Geological Society of America Bulletin, v. 120, p. 1441-1454.
-, 2017, Andean mountain building and magmatic arc migration driven by subduction-induced whole mantle flow: Nature Communications, v. 8:2010.
Schellart, W. P., Freeman, J., Stegman, D. R., Moresi, L., and May, D., 2007, Evolution and diversity of subduction zones controlled by slab width: Nature, v. 446, p. 308-11.
Schellart, W. P., Stegman, D. R., and Freeman, J., 2008, Global trench migration velocities and slab migration induced upper mantle volume fluxes: Constraints to find an Earth reference frame based on minimizing viscous dissipation: Earth-Science Reviews, v. 88, p. 118-144.
Schepers, G., van Hinsbergen, D. J. J., Spakman, W., Kosters, M. E., Boschman, L. M., and McQuarrie, N., 2017, South-American plate advance and forced Andean trench retreat as drivers for transient flat subduction episodes: Nat Commun, v. 8, p. 15249.
Scherreiks, R., Meléndez, G., BouDagher-Fadel, M., Fermeli, G., and Bosence, D., 2014, Stratigraphy and tectonics of a time-transgressive ophiolite obduction onto the eastern margin of the Pelagonian platform from Late Bathonian until Valanginian time,

exemplified in northern Evvoia, Greece: International Journal of Earth Sciences, v. 103, p. 2191-2216.
Schleiffarth, W., Darin, M., Reid, M., and Umhoefer, P. J., 2018, Dynamics of episodic Late Cretaceous–Cenozoic magmatism across Central to Eastern Anatolia: New insights from an extensive geochronology compilation: Geosphere, v. 14, p. 1990-2008.
Schlich, R., 1974, Sea-floor spreading history and deep-sea drilling results in the Madagascar and Mascarene Basins, western Indian Ocean, Initial reports of the deep sea drilling project, US Government Printing Office Washington, DC, p. 663-678.
Schlüter, H. U., Gaedicke, C., Roeser, H. A., Schreckenberger, B., Meyer, H., Reichert, C., Djajadihardja, Y., and Prexl, A., 2002, Tectonic features of the southern Sumatra-western Java forearc of Indonesia: Tectonics, v. 21, p. 11-1-11-15.
Schmid, S. M., Bernoulli, D., Fügenschuh, B., Georgiev, N., Kounov, A., Matenco, L., Oberhänsli, R., Pleuger, J., Schefer, S., Schuster, R., Tomljenović, B., Ustaszewski, K., and van Hinsbergen, D. J. J., 2020, Tectonic units of the Alpine collision zone between Eastern Alps and Western Turkey: Gondwana Research, v. 78, p. 308-374.
Schmid, S. M., Bernoulli, D., Fügenschuh, B., Matenco, L., Schefer, S., Schuster, R., Tischler, M., and Ustaszewski, K., 2008, The Alpine-Carpathian-Dinaridic orogenic system: correlation and evolution of tectonic units: Swiss Journal of Geosciences, v. 101, p. 139-183.
Schmid, S. M., F□genschuh, B., Kissling, E., and Schuster, R., 2004, Tectonic map and overall architecture of the Alpine orogen: Eclogae Geologicae Helvetiae, v. 97, p. 93-117.
Schmidt, A., Pourteau, A., Candan, O., and Oberhänsli, R., 2015, Lu–Hf geochronology on cm-sized garnets using microsampling: New constraints on garnet growth rates and duration of metamorphism during continental collision (Menderes Massif, Turkey): Earth and Planetary Science Letters, v. 432, p. 24-35.
Scholl, D. W., and von Huene, R., 2009, Implications of estimated magmatic additions and recycling losses at the subduction zones of accretionary (non-collisional) and collisional (suturing) orogens: Geological Society, London, Special Publications, v. 318, p. 105-125.
Scholl, D. W., von Huene, R., Hatcher, R., Carlson, M., McBride, J., and Catalán, J., 2007, Exploring the implications for continental basement tectonics if estimated rates of crustal removal (recycling) at Cenozoic subduction zones are applied to Phanerozoic and Precambrian convergent ocean margins: HATCHER, RD JR, CARLSON, MP, MCBRIDE, JH & CATALÁ N, JM (eds), p. 9-32.
Schwab, M., Ratschbacher, L., Siebel, W., McWilliams, M., Minaev, V., Lutkov, V., Chen, F., Stanek, K., Nelson, B., Frisch, W., and Wooden, J. L., 2004, Assembly of the Pamirs: Age and origin of magmatic belts from the southern Tien Shan to the southern Pamirs and their relation to Tibet: Tectonics, v. 23, p. n/a-n/a.
Scotese, C. R., 2004, A continental drift flipbook: The Journal of Geology, v. 112, p. 729-741.
Sdrolias, M., and Müller, R. D., 2006, Controls on back-arc basin formation: Geochemistry, Geophysics, Geosystems, v. 7.
Searle, M. P., 2018, Timing of subduction initiation, arc formation, ophiolite obduction and India–Asia collision in the Himalaya: Geological Society, London, Special Publications, v. 483, p. SP483. 8.
Sengör, A., 1979, The North Anatolian transform fault: its age, offset and tectonic significance: Journal of the Geological Society, v. 136, p. 269-282.
Şengör, A. M. C., 1984, The Cimmeride orogenic system and the tectonics of Eurasia: Geological Society of America Special Paper, v. 195, p. 82.

-, 1987, Tectonics of the Tethysides: Orogenic Collage Development in a Collisional Setting: Annual Review of Earth and Planetary Sciences, v. 15, p. 213-244.
-, 1990, Plate tectonics and orogenic research after 25 years: A Tethyan perspective: Earth-Science Reviews, v. 27, p. 1-201.
Şengör, A. M. C., Özeren, M., Genç, T., and Zor, E., 2003, East Anatolian High Plateau as a mantle-supported, north-south shortened domal structure: Geophysical Research Letters, v. 30, p. 8050.
Şengör, A. M. C., Özeren, M. S., Keskin, M., Sakınç, M., Özbakır, A. D., and Kayan, İ., 2008, Eastern Turkish high plateau as a small Turkic-type orogen: Implications for post-collisional crust-forming processes in Turkic-type orogens: Earth-Science Reviews, v. 90, p. 1-48.
Şengör, A. M. C., and Yilmaz, Y., 1981, Tethyan evolution of Turkey: A plate tectonic approach: Tectonophysics, v. 75, p. 181-241.
Seton, M., Mortimer, N., Williams, S., Quilty, P., Gans, P., Meffre, S., Micklethwaite, S., Zahirovic, S., Moore, J., and Matthews, K. J., 2016, Melanesian back-arc basin and arc development: Constraints from the eastern Coral Sea: Gondwana Research, v. 39, p. 77-95.
Seton, M., Müller, R. D., Zahirovic, S., Gaina, C., Torsvik, T., Shephard, G., Talsma, A., Gurnis, M., Turner, M., Maus, S., and Chandler, M., 2012, Global continental and ocean basin reconstructions since 200Ma: Earth-Science Reviews, v. 113, p. 212-270.
Sevastjanova, I., Hall, R., Rittner, M., Paw, S. M. T. L., Naing, T. T., Alderton, D. H., and Comfort, G., 2016, Myanmar and Asia united, Australia left behind long ago: Gondwana Research, v. 32, p. 24-40.
Shapiro, M. N., and Solov'ev, A. V., 2009, Formation of the Olyutorsky–Kamchatka foldbelt: a kinematic model: Russian Geology and Geophysics, v. 50, p. 668-681.
Shaw, J., and Johnston, S. T., 2016, Terrane wrecks (coupled oroclines) and paleomagnetic inclination anomalies: Earth-Science Reviews, v. 154, p. 191-209.
Shervais, J. W., 2001, Birth, death, and resurrection: The life cycle of suprasubduction zone ophiolites: Geochemistry, Geophysics, Geosystems, v. 2.
Smewing, J. D., Abbotts, I. L., Dunne, L. A., and Rex, D. C., 1991, Formation and emplacement ages of the Masirah ophiolite, Sultanate of Oman: Geology, v. 19.
Sobel, E., Chen, J., and Heermance, R., 2006, Late Oligocene–Early Miocene initiation of shortening in the Southwestern Chinese Tian Shan: Implications for Neogene shortening rate variations: Earth and Planetary Science Letters, v. 247, p. 70-81.
Solov'ev, A., Shapiro, M., Garver, J., and Lander, A., 2004, Formation of the east Kamchatkan accretionary prism based on fission-track dating of detrital zircons from terrigene rocks: Russian Geology and Geophysics, v. 45, p. 1237-1247.
Soret, M., Agard, P., Dubacq, B., Plunder, A., and Yamato, P., 2017, Petrological evidence for stepwise accretion of metamorphic soles during subduction infancy (Semail ophiolite, Oman and UAE): Journal of Metamorphic Geology, v. 35, p. 1051-1080.
Spakman, W., Chertova, M. V., van den Berg, A., and van Hinsbergen, D. J. J., 2018, Puzzling features of western Mediterranean tectonics explained by slab dragging: Nature Geoscience, v. 11, p. 211-216.
Spakman, W., and Hall, R., 2010, Surface deformation and slab–mantle interaction during Banda arc subduction rollback: Nature Geoscience, v. 3, p. 562-566.
Spakman, W., and Wortel, R., 2004, A Tomographic View on Western Mediterranean Geodynamics, *in* Cavazza, W., Roure, F., Spakman, W., Stampfli, G. M., and Ziegler, P. A., editors, The TRANSMED Atlas. The Mediterranean Region from Crust to Mantle: Geological and Geophysical Framework of the Mediterranean and the Surrounding Areas: Berlin, Heidelberg, Springer Berlin Heidelberg, p. 31-52.

Spencer, C., Roberts, N., and Santosh, M., 2017, Growth, destruction, and preservation of Earth's continental crust: Earth-Science Reviews, v. 172, p. 87-106.
Stampfli, G., Marcoux, J., and Baud, A., 1991, Tethyan margins in space and time: Palaeogeography, Palaeoclimatology, Palaeoecology, v. 87, p. 373-409.
Stampfli, G. M., and Borel, G., 2002, A plate tectonic model for the Paleozoic and Mesozoic constrained by dynamic plate boundaries and restored synthetic oceanic isochrons: Earth and Planetary Science Letters, v. 196, p. 17-33.
Stampfli, G. M., and Hochard, C., 2009, Plate tectonics of the Alpine realm: Geological Society, London, Special Publications, v. 327, p. 89-111.
Stamps, D. S., Calais, E., Saria, E., Hartnady, C., Nocquet, J. M., Ebinger, C. J., and Fernandes, R. M., 2008, A kinematic model for the East African Rift: Geophysical Research Letters, v. 35.
Stern, C. R., 2011, Subduction erosion: rates, mechanisms, and its role in arc magmatism and the evolution of the continental crust and mantle: Gondwana Research, v. 20, p. 284-308.
Stern, R. J., 1994, Arc assembly and continental collision in the Neoproterozoic East African Orogen: implications for the consolidation of Gondwanaland: Annual Review of Earth and Planetary Sciences, v. 22, p. 319-351.
Stern, R. J., 2004, Subduction initiation: spontaneous and induced: Earth and Planetary Science Letters, v. 226, p. 275-292.
Storey, M., Mahoney, J. J., Saunders, A. D., Duncan, R. A., Kelley, S. P., and Coffin, M. F., 1995, Timing of hot spot—related volcanism and the breakup of Madagascar and India: Science, v. 267, p. 852-855.
Talwani, M., and Reif, C., 1998, Laxmi Ridge–A continental sliver in the Arabian Sea: Marine Geophysical Researches, v. 20, p. 259-271.
Tapponnier, P., Mattauer, M., Proust, F., and Cassaigneau, C., 1981, Mesozoic ophiolites, sutures, and arge-scale tectonic movements in Afghanistan: Earth and Planetary Science Letters, v. 52, p. 355-371.
Tapponnier, P., Peltzer, G., Le Dain, A. Y., Armijo, R., and Cobbold, P., 1982, Propagating extrusion tectonics in Asia: New insights from simple experiments with plasticine: Geology, v. 10.
Tapponnier, P., Zhiqin, X., Roger, F., Meyer, B., Arnaud, N., Wittlinger, G., and Jingsui, Y., 2001, Oblique stepwise rise and growth of the Tibet plateau: Science, v. 294, p. 1671-7.
Tardy, M., Lapierre, H., Struik, L., Bosch, D., and Brunet, P., 2001, The influence of mantle plume in the genesis of the Cache Creek oceanic igneous rocks: implications for the geodynamic evolution of the inner accreted terranes of the Canadian Cordillera: Canadian Journal of Earth Sciences, v. 38, p. 515-534.
Tate, G. W., McQuarrie, N., Tiranda, H., van Hinsbergen, D. J. J., Harris, R., Zachariasse, W. J., Fellin, M. G., Reiners, P. W., and Willett, S. D., 2017, Reconciling regional continuity with local variability in structure, uplift and exhumation of the Timor orogen: Gondwana Research, v. 49, p. 364-386.
Tate, G. W., McQuarrie, N., van Hinsbergen, D. J. J., Bakker, R. R., Harris, R., and Jiang, H., 2015, Australia going down under: Quantifying continental subduction during arc-continent accretion in Timor-Leste: Geosphere, v. 11, p. 1860-1883.
Tatsumi, Y., and Eggins, S., 1995, Subduction zone magmatism, v. 1, Wiley.
Tekin, U. K., Göncüoğlu, M. C., and Turhan, N., 2002, First evidence of Late Carnian radiolarians from the Izmir–Ankara suture complex, central Sakarya, Turkey: implications for the opening age of the Izmir–Ankara branch of Neo-Tethys: Geobios, v. 35, p. 127-135.

Tetreault, J., and Buiter, S., 2014, Future accreted terranes: a compilation of island arcs, oceanic plateaus, submarine ridges, seamounts, and continental fragments: Solid Earth, v. 5, p. 1243-1275.
Tetreault, J. L., and Buiter, S., 2012, Geodynamic models of terrane accretion: Testing the fate of island arcs, oceanic plateaus, and continental fragments in subduction zones: Journal of Geophysical Research: Solid Earth, v. 117.
Theunissen, K., Klerkx, J., Melnikov, A., and Mruma, A., 1996, Mechanisms of inheritance of rift faulting in the western branch of the East African Rift, Tanzania: Tectonics, v. 15, p. 776-790.
Thompson, A. B., Schulmann, K., and Jezek, J., 1997, Thermal evolution and exhumation in obliquely convergent (transpressive) orogens: Tectonophysics, v. 280, p. 171-184.
Tirel, C., Brun, J. P., Burov, E., Wortel, M. J. R., and Lebedev, S., 2013, A plate tectonics oddity: Caterpillar-walk exhumation of subducted continental crust: Geology, v. 41, p. 555-558.
Tirel, C., F. Gueydan, C. Tiberi, and J.-P. Brun (2004), Aegean crustal thickness inferred from gravity inversion. Geodynamical implications, Earth and Planetary Science Letters, 228(3-4), 267-280, doi: 10.1016/j.epsl.2004.10.023.
Topuz, G., Candan, O., Zack, T., and Yılmaz, A., 2017, East Anatolian plateau constructed over a continental basement: No evidence for the East Anatolian accretionary complex: Geology, v. 45, p. 791-794.
Torsvik, T., Ashwal, L., Tucker, R., and Eide, E., 2001, Neoproterozoic geochronology and palaeogeography of the Seychelles microcontinent: the India link: Precambrian Research, v. 110, p. 47-59.
Torsvik, T., Smethurst, M., Meert, J. G., Van der Voo, R., McKerrow, W., Brasier, M., Sturt, B., and Walderhaug, H., 1996, Continental break-up and collision in the Neoproterozoic and Palaeozoic—a tale of Baltica and Laurentia: Earth-Science Reviews, v. 40, p. 229-258.
Torsvik, T., Tucker, R., Ashwal, L., Eide, E., Rakotosolofo, N., and De Wit, M., 1998, Late Cretaceous magmatism in Madagascar: palaeomagnetic evidence for a stationary Marion hotspot: Earth and Planetary Science Letters, v. 164, p. 221-232.
Torsvik, T. H., Amundsen, H., Hartz, E. H., Corfu, F., Kusznir, N., Gaina, C., Doubrovine, P. V., Steinberger, B., Ashwal, L. D., and Jamtveit, B., 2013, A Precambrian microcontinent in the Indian Ocean: Nature Geoscience, v. 6, p. 223-227.
Torsvik, T. H., and Cocks, L. R. M., 2017, Earth history and palaeogeography, Cambridge University Press.
Torsvik, T. H., Müller, R. D., Van der Voo, R., Steinberger, B., and Gaina, C., 2008, Global plate motion frames: Toward a unified model: Reviews of Geophysics, v. 46.
Torsvik, T. H., Steinberger, B., Gurnis, M., and Gaina, C., 2010, Plate tectonics and net lithosphere rotation over the past 150My: Earth and Planetary Science Letters, v. 291, p. 106-112.
Toussaint, G., Burov, E., and Avouac, J. P., 2004, Tectonic evolution of a continental collision zone: A thermomechanical numerical model: Tectonics, v. 23.
Tremblay, A., Meshi, A., Deschamps, T., Goulet, F., and Goulet, N., 2015, The Vardar zone as a suture for the Mirdita ophiolites, Albania: Constraints from the structural analysis of the Korabi-Pelagonia zone: Tectonics, v. 34, p. 352-375.
Tucker, R., Ashwal, L., and Torsvik, T., 2001, U–Pb geochronology of Seychelles granitoids: a Neoproterozoic continental arc fragment: Earth and Planetary Science Letters, v. 187, p. 27-38.

Ueda, H., and Miyashita, S., 2005, Tectonic accretion of a subducted intraoceanic remnant arc in Cretaceous Hokkaido, Japan, and implications for evolution of the Pacific northwest: Island Arc, v. 14, p. 582-598.
Ustaszewski, K., Schmid, S. M., Fügenschuh, B., Tischler, M., Kissling, E., and Spakman, W., 2008, A map-view restoration of the Alpine-Carpathian-Dinaridic system for the Early Miocene: Swiss Journal of Geosciences, v. 101, p. 273-294.
Vaes, B., van Hinsbergen, D. J., and Boschman, L. M., 2019, Reconstruction of subduction and back-arc spreading in the NW Pacific and Aleutian Basin: Clues to causes of Cretaceous and Eocene plate reorganizations: Tectonics, v. 38, p. 1367-1413.
van Benthem, S., R. Govers, and R. Wortel (2014), What drives microplate motion and deformation in the northeastern Caribbean plate boundary region?, Tectonics, 33, 850-873, doi: 10.1002/2013tc003402.
van de Lagemaat, S. H., van Hinsbergen, D. J., Boschman, L. M., Kamp, P. J., and Spakman, W., 2018, Southwest Pacific absolute plate kinematic reconstruction reveals major Cenozoic Tonga-Kermadec slab dragging: Tectonics, v. 37, p. 2647-2674.
van de Lagemaat, S. H. A., Swart, M. L. A., Kosters, M. E., Vaes, B., Boschman, L. M., Burton-Johnson, A., Bijl, P. K., Spakman, W., and van Hinsbergen, D. J. J., 2021, From subduction initiation to extension in the Scotia Sea region and the opening of the Drake Passage: when and why?: Earth-Science Reviews, v. submitted.
van der Hilst, R., and Mann, P., 1994, Tectonic implications of tomographic images of subducted lithosphere beneath northwestern South America: Geology, v. 22, p. 451-454.
van der Meer, D. G., Spakman, W., van Hinsbergen, D. J. J., Amaru, M. L., and Torsvik, T. H., 2010, Towards absolute plate motions constrained by lower-mantle slab remnants: Nature Geoscience, v. 3, p. 36-40.
van der Meer, D. G., Torsvik, T. H., Spakman, W., van Hinsbergen, D. J. J., and Amaru, M. L., 2012, Intra-Panthalassa Ocean subduction zones revealed by fossil arcs and mantle structure: Nature Geoscience, v. 5, p. 215-219.
van der Meer, D. G., van Hinsbergen, D. J. J., and Spakman, W., 2018, Atlas of the underworld: Slab remnants in the mantle, their sinking history, and a new outlook on lower mantle viscosity: Tectonophysics, v. 723, p. 309-448.
Van der Voo, R., Spakman, W., and Bijwaard, H., 1999, Tethyan subducted slabs under India: Earth and Planetary Science Letters, v. 171, p. 7-20.
Van Gelder, I., Willingshofer, E., Sokoutis, D., and Cloetingh, S., 2017, The interplay between subduction and lateral extrusion: A case study for the European Eastern Alps based on analogue models: Earth and Planetary Science Letters, v. 472, p. 82-94.
van Gool, J. A., and Cawood, P. A., 1994, Frontal vs. basal accretion and contrasting particle paths in metamorphic thrust belts: Geology, v. 22, p. 51-54.
van Hinsbergen, D. J., Maffione, M., Koornneef, L. M., and Guilmette, C., 2019a, Kinematic and paleomagnetic restoration of the Semail ophiolite (Oman) reveals subduction initiation along an ancient Neotethyan fracture zone: Earth and Planetary Science Letters, v. 518, p. 183-196.
van Hinsbergen, D. J., Vissers, R. L., and Spakman, W., 2014, Origin and consequences of western Mediterranean subduction, rollback, and slab segmentation: Tectonics, v. 33, p. 393-419.
van Hinsbergen, D. J. J., 2010, A key extensional metamorphic complex reviewed and restored: The Menderes Massif of western Turkey: Earth-Science Reviews, v. 102, p. 60-76.
van Hinsbergen, D. J. J., Cunningham, D., Straathof, G. B., Ganerød, M., Hendriks, B. W. H., and Dijkstra, A. H., 2015a, Triassic to Cenozoic multi-stage intra-plate deformation

focused near the Bogd Fault system, Gobi Altai, Mongolia: Geoscience Frontiers, v. 6, p. 723-740.
van Hinsbergen, D. J. J., Hafkenscheid, E., Spakman, W., Meulenkamp, J. E., and Wortel, R., 2005a, Nappe stacking resulting from subduction of oceanic and continental lithosphere below Greece: Geology, v. 33.
van Hinsbergen, D. J. J., Kapp, P., Dupont-Nivet, G., Lippert, P. C., DeCelles, P. G., and Torsvik, T. H., 2011a, Restoration of Cenozoic deformation in Asia and the size of Greater India: Tectonics, v. 30, p. n/a-n/a.
van Hinsbergen, D. J. J., Kaymakci, N., Spakman, W., and Torsvik, T. H., 2010, Reconciling the geological history of western Turkey with plate circuits and mantle tomography: Earth and Planetary Science Letters, v. 297, p. 674-686.
van Hinsbergen, D. J. J., Lippert, P. C., Dupont-Nivet, G., McQuarrie, N., Doubrovine, P. V., Spakman, W., and Torsvik, T. H., 2012, Greater India Basin hypothesis and a two-stage Cenozoic collision between India and Asia: Proc Natl Acad Sci U S A, v. 109, p. 7659-64.
van Hinsbergen, D. J. J., Lippert, P. C., Li, S., Huang, W., Advokaat, E. L., and Spakman, W., 2019b, Reconstructing Greater India: Paleogeographic, kinematic, and geodynamic perspectives: Tectonophysics, v. 760, p. 69-94.
van Hinsbergen, D. J. J., Maffione, M., Plunder, A., Kaymakci, N., Ganerød, M., Hendriks, B. W. H., Corfu, F., Gürer, D., de Gelder, G. I. N. O., Peters, K., McPhee, P. J., Brouwer, F. M., Advokaat, E. L., and Vissers, R. L. M., 2016, Tectonic evolution and paleogeography of the Kırşehir Block and the Central Anatolian Ophiolites, Turkey: Tectonics, v. 35, p. 983-1014.
van Hinsbergen, D. J. J., Peters, K., Maffione, M., Spakman, W., Guilmette, C., Thieulot, C., Plümper, O., Gürer, D., Brouwer, F. M., Aldanmaz, E., and Kaymakcı, N., 2015b, Dynamics of intraoceanic subduction initiation: 2. Suprasubduction zone ophiolite formation and metamorphic sole exhumation in context of absolute plate motions: Geochemistry, Geophysics, Geosystems, v. 16, p. 1771-1785.
van Hinsbergen, D. J. J., and Schmid, S. M., 2012, Map view restoration of Aegean-West Anatolian accretion and extension since the Eocene: Tectonics, v. 31, p. n/a-n/a.
van Hinsbergen, D. J. J., Spakman, W., de Boorder, H., van Dongen, M., Jowitt, S. M., and Mason, P. R., 2020a, Arc-type magmatism due to continental-edge plowing through ancient subduction-enriched mantle: Geophysical Research Letters, v. 47, p. e2020GL087484.
van Hinsbergen, D. J. J., Steinberger, B., Doubrovine, P. V., and Gassmöller, R., 2011b, Acceleration and deceleration of India-Asia convergence since the Cretaceous: Roles of mantle plumes and continental collision: Journal of Geophysical Research, v. 116.
van Hinsbergen, D. J. J., Steinberger, B., Guilmette, C., Maffione, M., Gürer, D., Peters, K., Plunder, A., McPhee, P. J., Gaina, C., Advokaat, E. L., Vissers, R. L. M., and Spakman, W., 2021, A record of plume-induced plate rotation triggering seafloor spreading and subduction initiation: Nature Geoscience, accepted pending revision.
van Hinsbergen, D. J. J., Torsvik, T., Schmid, S. M., Matenco, L., Maffione, M., Vissers, R. L. M., Gürer, D., and Spakman, W., 2020b, Orogenic architecture of the Mediterranean region and kinematic reconstruction of its tectonic evolution since the Triassic: Gondwana Research, v. 81, p. 79-229.
van Hinsbergen, D. J. J., Zachariasse, W. J., Wortel, M. J. R., and Meulenkamp, J. E., 2005b, Underthrusting and exhumation: A comparison between the External Hellenides and the “hot” Cycladic and “cold” South Aegean core complexes (Greece): Tectonics, v. 24, p. n/a-n/a.

van Hunen, J., and Allen, M. B., 2011, Continental collision and slab break-off: A comparison of 3-D numerical models with observations: Earth and Planetary Science Letters, v. 302, p. 27-37.
Vaughan, A. P., Eagles, G., and Flowerdew, M. J., 2012, Evidence for a two-phase Palmer Land event from crosscutting structural relationships and emplacement timing of the Lassiter Coast Intrusive Suite, Antarctic Peninsula: Implications for mid-Cretaceous Southern Ocean plate configuration: Tectonics, v. 31.
Veevers, J., Powell, C. M., and Roots, S., 1991, Review of seafloor spreading around Australia. I. Synthesis of the patterns of spreading: Australian Journal of Earth Sciences, v. 38, p. 373-389.
Vérard, C., Flores, K., and Stampfli, G., 2012, Geodynamic reconstructions of the South America–Antarctica plate system: Journal of Geodynamics, v. 53, p. 43-60.
Vincent, S. J., Morton, A. C., Carter, A., Gibbs, S., and Barabadze, T. G., 2007, Oligocene uplift of the Western Greater Caucasus: an effect of initial Arabia–Eurasia collision: Terra Nova, v. 19, p. 160-166.
Vissers, R. L. M., van Hinsbergen, D. J. J., Meijer, P. T., and Piccardo, G. B., 2013, Kinematics of Jurassic ultra-slow spreading in the Piemonte Ligurian ocean: Earth and Planetary Science Letters, v. 380, p. 138-150.
Vitale Brovarone, A., Agard, P., Monie, P., Chauvet, A., and Rabaute, A., 2018, Tectonic and metamorphic architecture of the HP belt of New Caledonia: Earth-Science Reviews, v. 178, p. 48-67.
von Huene, R., and Scholl, D. W., 1991, Observations at convergent margins concerning sediment subduction, subduction erosion, and the growth of continental crust: Reviews of Geophysics, v. 29, p. 279-316.
von Quadt, A., Moritz, R., Peytcheva, I., and Heinrich, C. A., 2005, 3: Geochronology and geodynamics of Late Cretaceous magmatism and Cu–Au mineralization in the Panagyurishte region of the Apuseni–Banat–Timok–Srednogorie belt, Bulgaria: Ore Geology Reviews, v. 27, p. 95-126.
Wakabayashi, J., 1992, Nappes, tectonics of oblique plate convergence, and metamorphic evolution related to 140 million years of continuous subduction, Franciscan Complex, California: The Journal of Geology, v. 100, p. 19-40.
-, 2015, Anatomy of a subduction complex: architecture of the Franciscan Complex, California, at multiple length and time scales: International Geology Review, v. 57, p. 669-746.
Wakabayashi, J., and Dilek, Y., 2003, What constitutes 'emplacement' of an ophiolite?: Mechanisms and relationship to subduction initiation and formation of metamorphic soles: Geological Society, London, Special Publications, v. 218, p. 427-447.
Wakabayashi, J., Ghatak, A., and Basu, A. R., 2010, Suprasubduction-zone ophiolite generation, emplacement, and initiation of subduction: A perspective from geochemistry, metamorphism, geochronology, and regional geology: Geological Society of America Bulletin, v. 122, p. 1548-1568.
Wakita, K., and Metcalfe, I., 2005, Ocean plate stratigraphy in East and Southeast Asia: Journal of Asian Earth Sciences, v. 24, p. 679-702.
Wakita, K., Pubellier, M., and Windley, B. F., 2013, Tectonic processes, from rifting to collision via subduction, in SE Asia and the western Pacific: A key to understanding the architecture of the Central Asian Orogenic Belt: Lithosphere, v. 5, p. 265-276.
Wan, B., Wang, X., Liu, X., Cai, K., Xiao, W., and Mitchell, R. N., 2020, Long-lived seamount subduction in ancient orogens: Evidence from the Paleozoic South Tianshan: Geology.

Warners-Ruckstuhl, K. N., Meijer, P. T., Govers, R., and Wortel, M. J. R., 2010, A lithosphere-dynamics constraint on mantle flow: Analysis of the Eurasian plate: Geophysical Research Letters, v. 37, p. n/a-n/a.
Webb, A. A. G., Guo, H., Clift, P. D., Husson, L., Müller, T., Costantino, D., Yin, A., Xu, Z., Cao, H., and Wang, Q., 2017, The Himalaya in 3D: Slab dynamics controlled mountain building and monsoon intensification: Lithosphere.
Wei, S. S., Shearer, P. M., Lithgow-Bertelloni, C., Stixrude, L., and Tian, D., 2020, Oceanic plateau of the Hawaiian mantle plume head subducted to the uppermost lower mantle: Science, v. 370, p. 983-987.
Wells, R., Bukry, D., Friedman, R., Pyle, D., Duncan, R., Haeussler, P., and Wooden, J., 2014, Geologic history of Siletzia, a large igneous province in the Oregon and Washington Coast Range: Correlation to the geomagnetic polarity time scale and implications for a long-lived Yellowstone hotspot: Geosphere, v. 10, p. 692-719.
Whitney, D. L., and Hamilton, M. A., 2004, Timing of high-grade metamorphism in central Turkey and the assembly of Anatolia: Journal of the Geological Society, v. 161, p. 823-828.
Wilson, J. T., 1966, Did the Atlantic close and then re-open?: Nature, v. 211, p. 676-681.
Windley, B., Razafiniparany, A., Razakamanana, T., and Ackermand, D., 1994, Tectonic framework of the Precambrian of Madagascar and its Gondwana connections: a review and reappraisal: Geologische Rundschau, v. 83, p. 642-659.
Windley, B. F., Alexeiev, D., Xiao, W., Kröner, A., and Badarch, G., 2007, Tectonic models for accretion of the Central Asian Orogenic Belt: Journal of the Geological Society, v. 164, p. 31-47.
Wortel, M. J. R., and Spakman, W., 2000, Subduction and slab detachment in the Mediterranean-Carpathian region: Science, v. 290, p. 1910-1917.
Wu, J. T.-J., and Wu, J., 2019, Izanagi-Pacific ridge subduction revealed by a 56 to 46 Ma magmatic gap along the northeast Asian margin: Geology, v. 47, p. 953-957.
Xenophontos, C., and Osozawa, S., 2004, Travel time of accreted igneous assemblages in western Pacific orogenic belts and their associated sedimentary rocks: Tectonophysics, v. 393, p. 241-261.
Xiao, W., Huang, B., Han, C., Sun, S., and Li, J., 2010, A review of the western part of the Altaids: A key to understanding the architecture of accretionary orogens: Gondwana Research, v. 18, p. 253-273.
Xiao, W., Windley, B. F., Sun, S., Li, J., Huang, B., Han, C., Yuan, C., Sun, M., and Chen, H., 2015, A Tale of Amalgamation of Three Permo-Triassic Collage Systems in Central Asia: Oroclines, Sutures, and Terminal Accretion: Annual Review of Earth and Planetary Sciences, v. 43, p. 477-507.
Xiao, W. J., Windley, B. F., Huang, B. C., Han, C. M., Yuan, C., Chen, H. L., Sun, M., Sun, S., and Li, J. L., 2009, End-Permian to mid-Triassic termination of the accretionary processes of the southern Altaids: implications for the geodynamic evolution, Phanerozoic continental growth, and metallogeny of Central Asia: International Journal of Earth Sciences, v. 98, p. 1189-1217.
Xu, Y.-J., Cawood, P. A., and Du, Y.-S., 2016, Intraplate orogenesis in response to Gondwana assembly: Kwangsian orogeny, South China: American Journal of Science, v. 316, p. 329-362.
Yadav, R., Papadimitriou, E., Karakostas, V., Shanker, D., Rastogi, B., Chopra, S., Singh, A., and Kumar, S., 2011, The 2007 Talala, Saurashtra, western India earthquake sequence: tectonic implications and seismicity triggering: Journal of Asian Earth Sciences, v. 40, p. 303-314.

Yang, G., Li, Y., Tong, L., Wang, Z., Duan, F., Xu, Q., and Li, H., 2019, An overview of oceanic island basalts in accretionary complexes and seamounts accretion in the western Central Asian Orogenic Belt: Journal of Asian Earth Sciences, v. 179, p. 385-398.

Yao, W., Ding, L., Cai, F., Wang, H., Xu, Q., and Zaw, T., 2017, Origin and tectonic evolution of upper Triassic Turbidites in the Indo-Burman ranges, West Myanmar: Tectonophysics, v. 721, p. 90-105.

Yin, A., and Harrison, T. M., 2000, Geologic evolution of the Himalayan-Tibetan orogen: Annual Review of Earth and Planetary Sciences, v. 28, p. 211-280.

Yonkee, W. A., and Weil, A. B., 2015, Tectonic evolution of the Sevier and Laramide belts within the North American Cordillera orogenic system: Earth-Science Reviews, v. 150, p. 531-593.

Yuan, J., Yang, Z., Deng, C., Krijgsman, W., Hu, X., Li, S., Shen, Z., Qin, H., An, W., and He, H., 2020, Rapid drift of the Tethyan Himalaya terrane before two-stage India-Asia collision: National Science Review.

Zahirovic, S., Müller, R. D., Seton, M., and Flament, N., 2015, Tectonic speed limits from plate kinematic reconstructions: Earth and Planetary Science Letters, v. 418, p. 40-52.

Zhang, X., Chung, S.-L., Tang, J.-T., Maulana, A., Mawaleda, M., Oo, T., Tien, C.-Y., and Lee, H.-Y., 2020, Tracing Argoland in eastern Tethys and implications for India-Asia convergence: Geological Society of America Bulletin.

Zhang, Z., Xiao, W., Majidifard, M. R., Zhu, R., Wan, B., Ao, S., Chen, L., Rezaeian, M., and Esmaeili, R., 2017, Detrital zircon provenance analysis in the Zagros Orogen, SW Iran: implications for the amalgamation history of the Neo-Tethys: International Journal of Earth Sciences, v. 106, p. 1223-1238.

Zhu, D.-C., Zhao, Z.-D., Niu, Y., Dilek, Y., Hou, Z.-Q., and Mo, X.-X., 2013, The origin and pre-Cenozoic evolution of the Tibetan Plateau: Gondwana Research, v. 23, p. 1429-1454.

Zhu, D. C., Wang, Q., Zhao, Z. D., Chung, S. L., Cawood, P. A., Niu, Y., Liu, S. A., Wu, F. Y., and Mo, X. X., 2015, Magmatic record of India-Asia collision: Sci Rep, v. 5, p. 14289.

Zimmerman, A., Stein, H. J., Hannah, J. L., Koželj, D., Bogdanov, K., and Berza, T., 2007, Tectonic configuration of the Apuseni–Banat—Timok–Srednogorie belt, Balkans-South Carpathians, constrained by high precision Re–Os molybdenite ages: Mineralium Deposita, v. 43, p. 1-21.

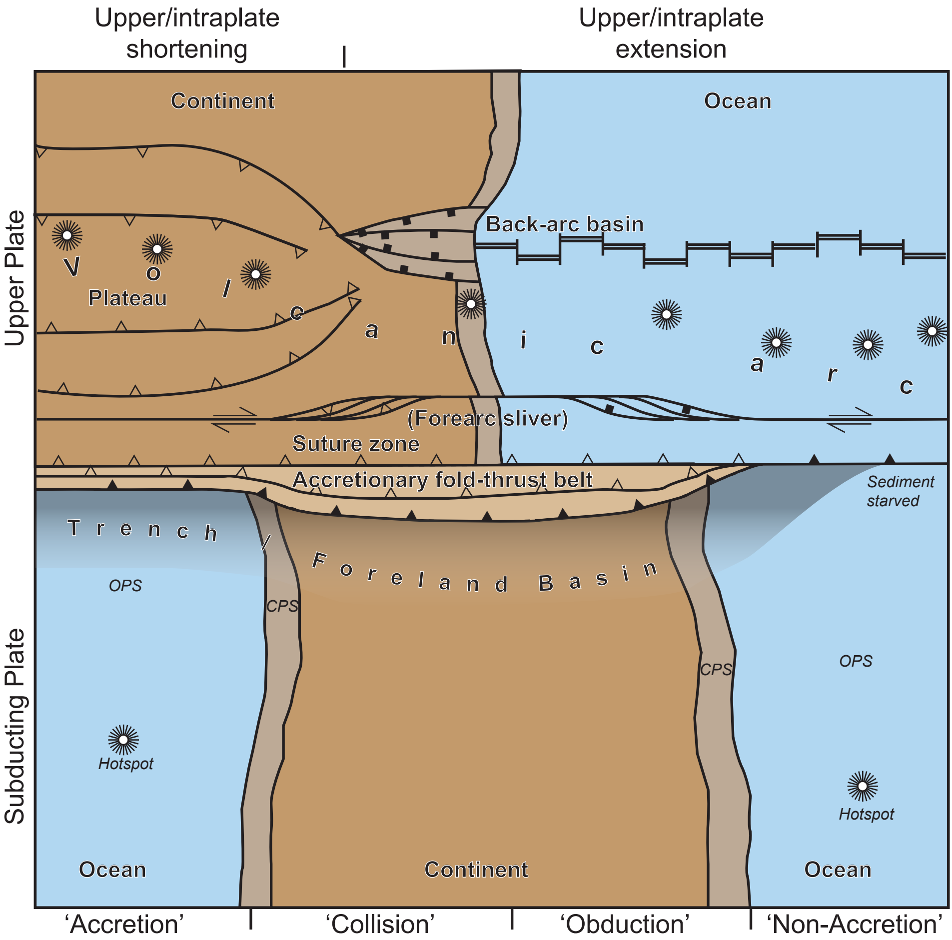

Upper/intraplate shortening
Upper/intraplate extension
Upper Plate
Continent
Ocean
Back-arc basin
Plateau
V o l c a n i c a r c
(Forearc sliver)
Suture zone
Accretionary fold-thrust belt
Sediment starved
T r e n c h / F o r e l a n d B a s i n
OPS
CPS
Subducting Plate
Hotspot
Ocean
Continent
Ocean
CPS
OPS
Hotspot
'Accretion'
'Collision'
'Obduction'
'Non-Accretion'

Figure 1

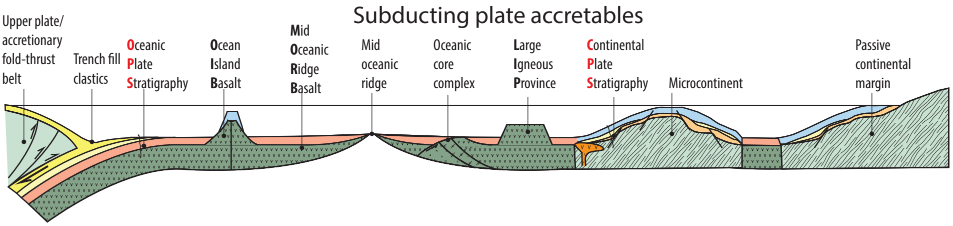
Subducting plate accretables
Upper plate/ accretionary fold-thrust belt
Trench fill clastics
Oceanic Plate Stratigraphy
Ocean Island Basalt
Mid Oceanic Ridge Basalt
Mid oceanic ridge
Oceanic core complex
Large Igneous Province
Continental Plate Stratigraphy
Microcontinent
Passive continental margin

Figure 2

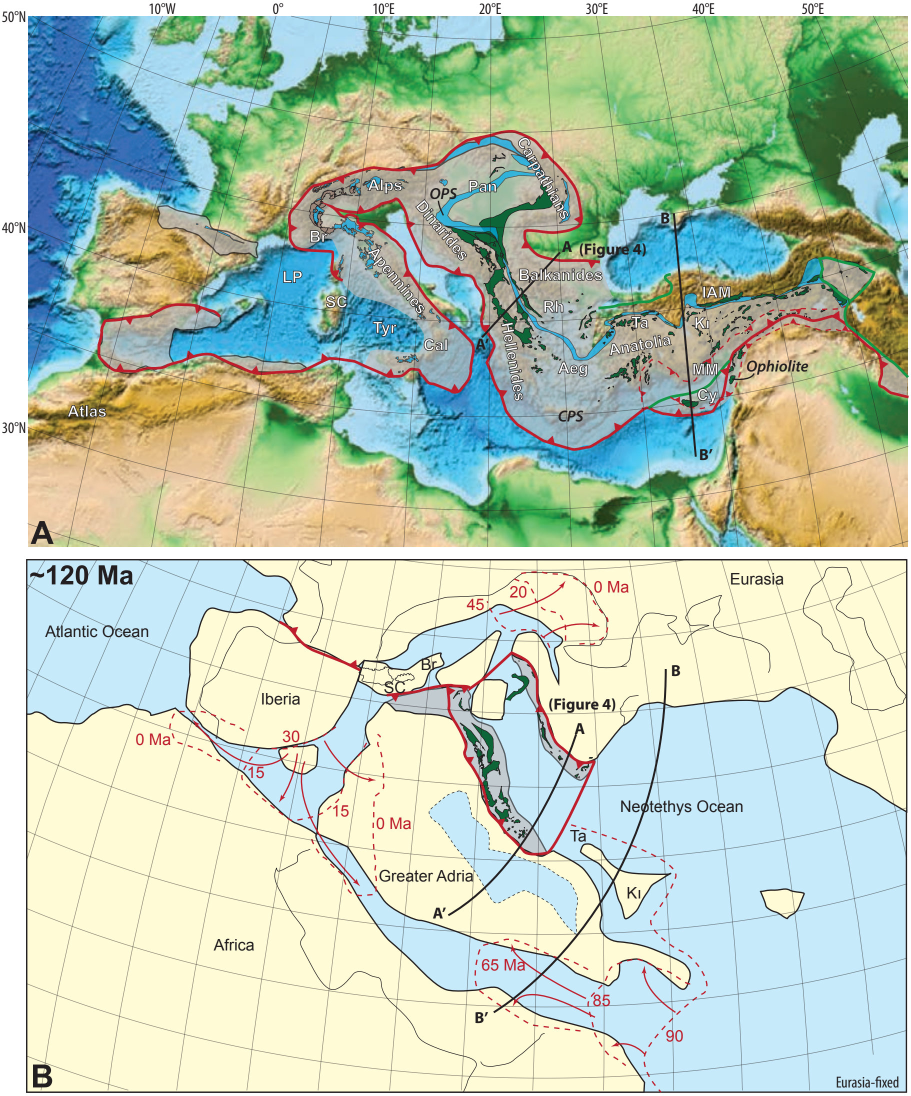
50°N
10°W
0°
10°E
20°E
30°E
40°E
50°E
40°N
30°N
Alps
Carpathians
Pan
OPS
Dinarides
Br
Apennines
LP
SC
Tyr
Cal
A
(Figure 4)
A'
Balkanides
Rh
Hellenides
Aeg
CPS
B
B'
IAM
Ta
Kı
Anatolia
MM
Cy
Ophiolite
Atlas
A
~120 Ma
Atlantic Ocean
Eurasia
45
20
0 Ma
Iberia
Br
SC
(Figure 4)
0 Ma
30
15
15
0 Ma
Neotethys Ocean
Ta
Kı
Greater Adria
Africa
65 Ma
85
90
B
Eurasia-fixed

Figure 3

Interpreted evolution of orogenic architecture of the Hellenide-Balkanide orogen

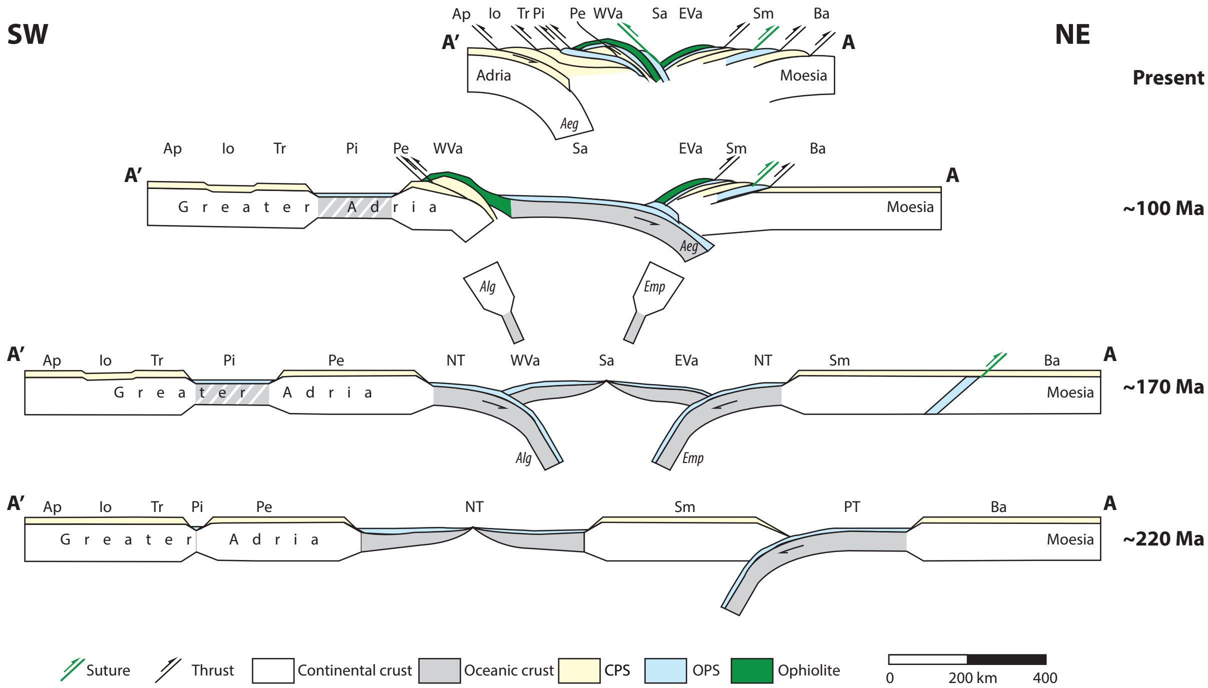

Figure 4

Interpreted evolution of orogenic architecture of the Anatolia-Cyprus orogen

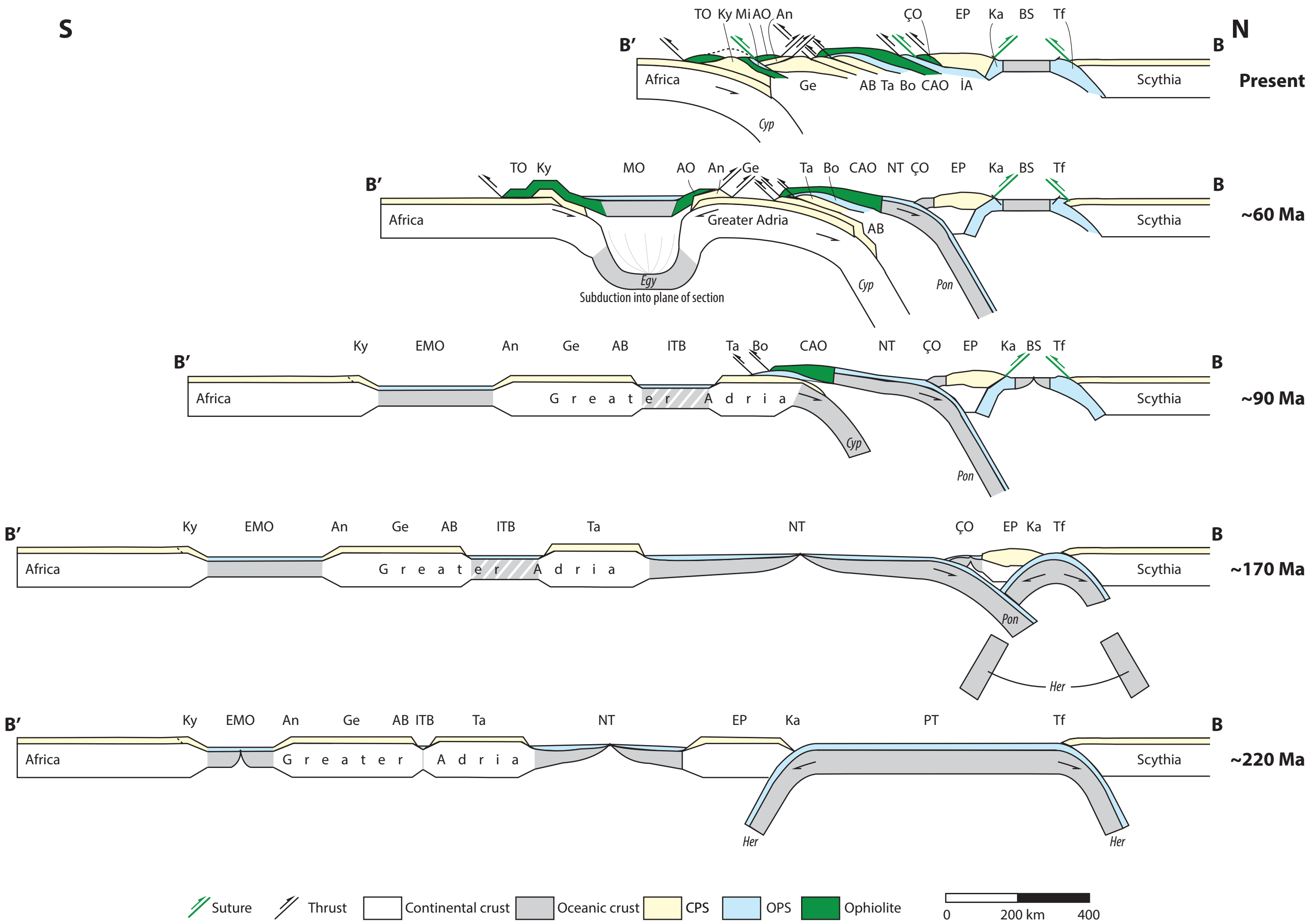

Figure 5

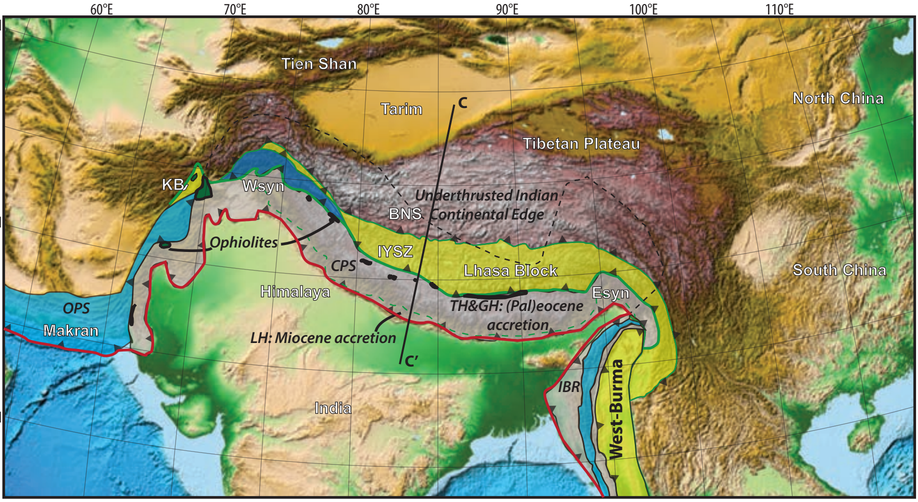
60°E
70°E
80°E
90°E
100°E
110°E
40°N
30°N
20°N
Tien Shan
Tarim
North China
Tibetan Plateau
C
KB
Wsyn
Underthrusted Indian
Continental Edge
BNS
Ophiolites
IYSZ
CPS
Lhasa Block
South China
Himalaya
Esyn
TH&GH: (Pal)eocene
accretion
OPS
Makran
LH: Miocene accretion
C'
IBR
West-Burma
India

Figure 6

Interpreted evolution of orogenic architecture of the Himalaya-Tibet orogen

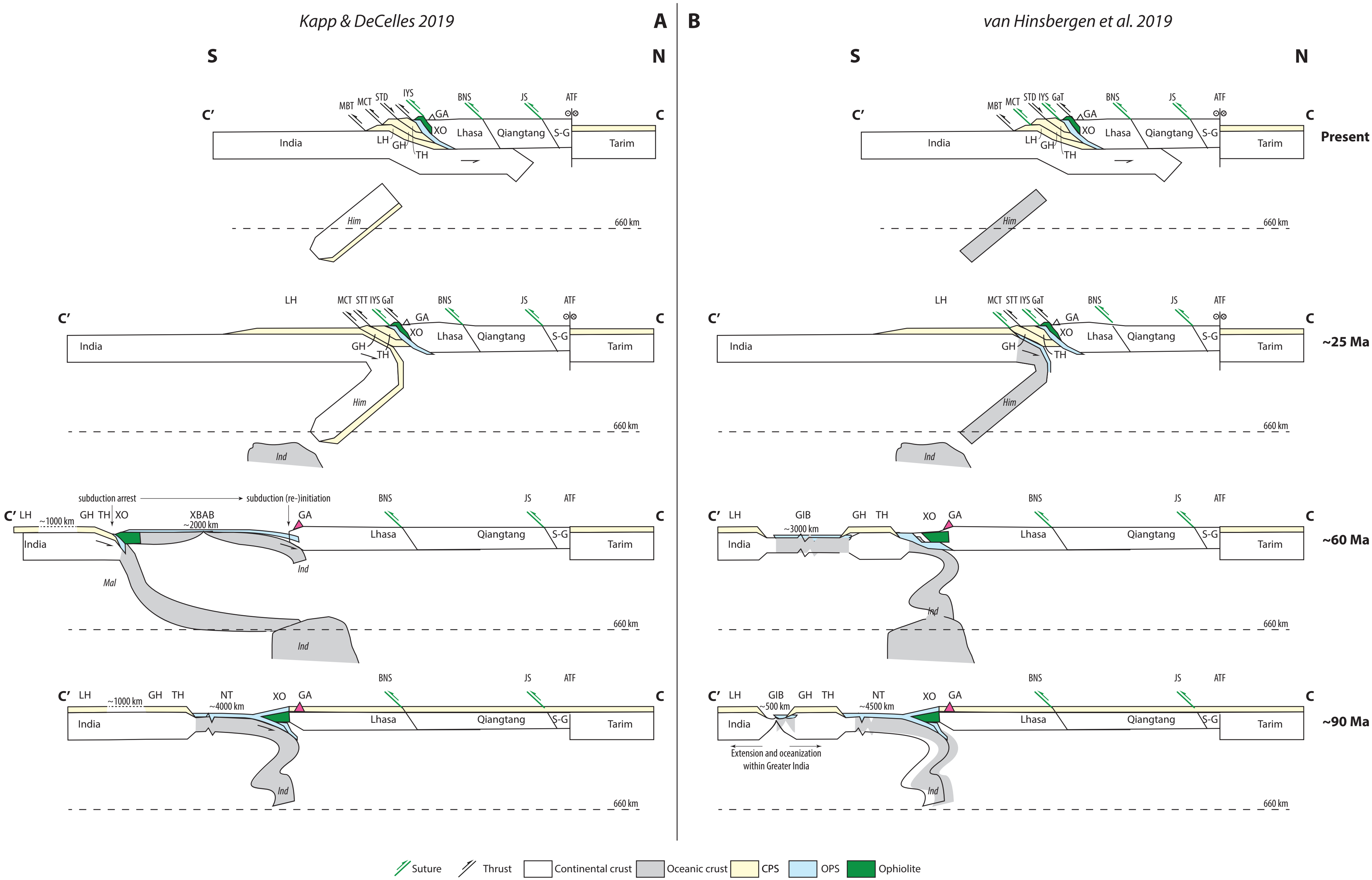

Figure 7

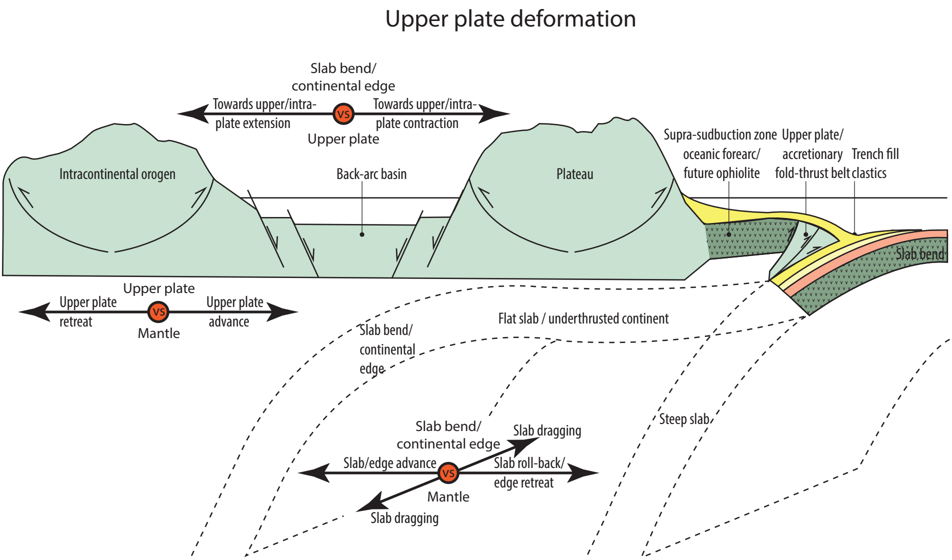

Upper plate deformation
Slab bend/
continental edge
Towards upper/intra-
plate extension
VS
Towards upper/intra-
plate contraction
Upper plate
Intracontinental orogen
Back-arc basin
Plateau
Supra-sudbuction zone
oceanic forearc/
future ophiolite
Upper plate/
accretionary
fold-thrust belt
Trench fill
clastics
Slab bend
Upper plate
Upper plate
retreat
VS
Upper plate
advance
Mantle
Flat slab / underthrusted continent
Slab bend/
continental
edge
Steep slab
Slab bend/
continental edge
Slab dragging
Slab/edge advance
VS
Slab roll-back/
edge retreat
Mantle
Slab dragging

Figure 8

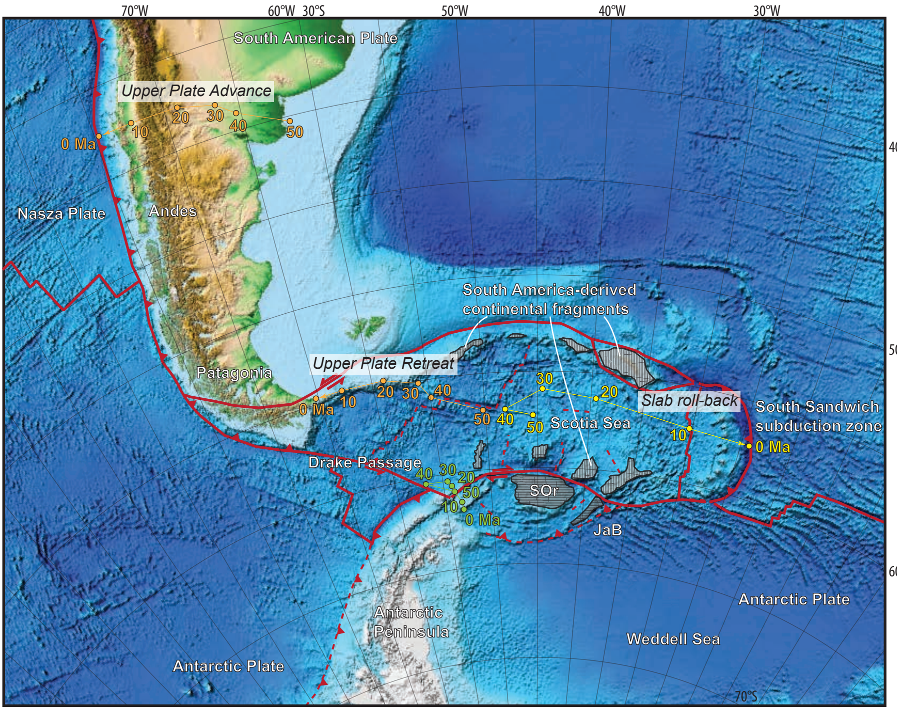
70°W
60°W
30°S
50°W
40°W
30°W
40°S
50°S
60°S
70°S
South American Plate
Upper Plate Advance
0 Ma
10
20
30
40
50
Nasza Plate
Andes
South America-derived
continental fragments
Patagonia
Upper Plate Retreat
0 Ma
10
20
30
40
50
30
20
40
50
Slab roll-back
10
0 Ma
Scotia Sea
South Sandwich
subduction zone
Drake Passage
40
30
20
50
10
0 Ma
SOr
JaB
Antarctic Plate
Antarctic
Peninsula
Weddell Sea
Antarctic Plate

Figure 9

Rock transfer from lower to upper plate

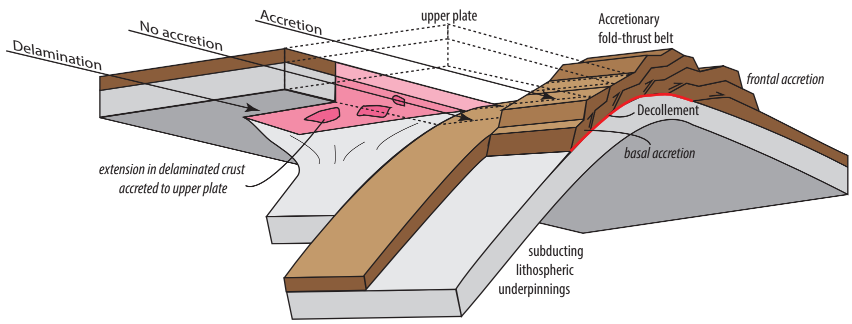

Figure 10

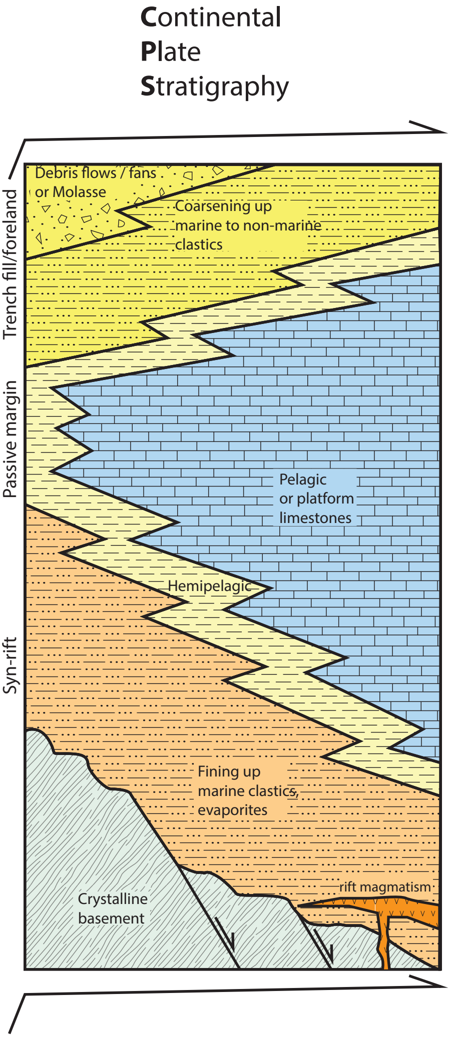

Continental
Plate
Stratigraphy
Trench fill/foreland
Passive margin
Syn-rift
Debris flows / fans
or Molasse
Coarsening up
marine to non-marine
clastics
Pelagic
or platform
limestones
Hemipelagic
Fining up
marine clastics,
evaporites
rift magmatism
Crystalline
basement

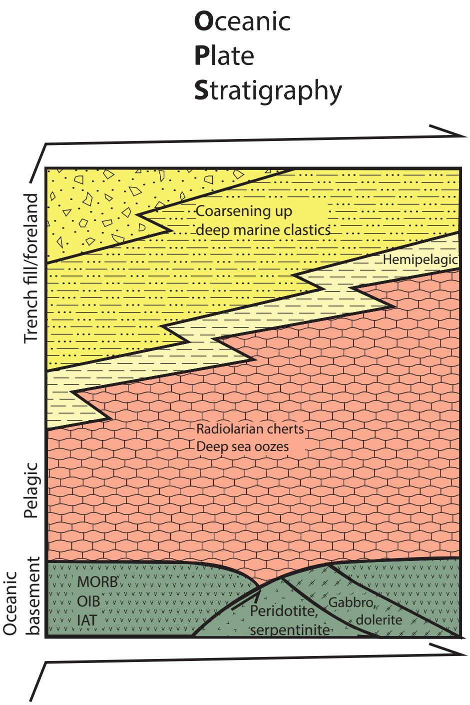

Oceanic
Plate
Stratigraphy
Trench fill/foreland
Pelagic
Oceanic
basement
Coarsening up
deep marine clastics
Hemipelagic
Radiolarian cherts
Deep sea oozes
MORB
OIB
IAT
Peridotite,
serpentinite
Gabbro,
dolerite

Figure 11

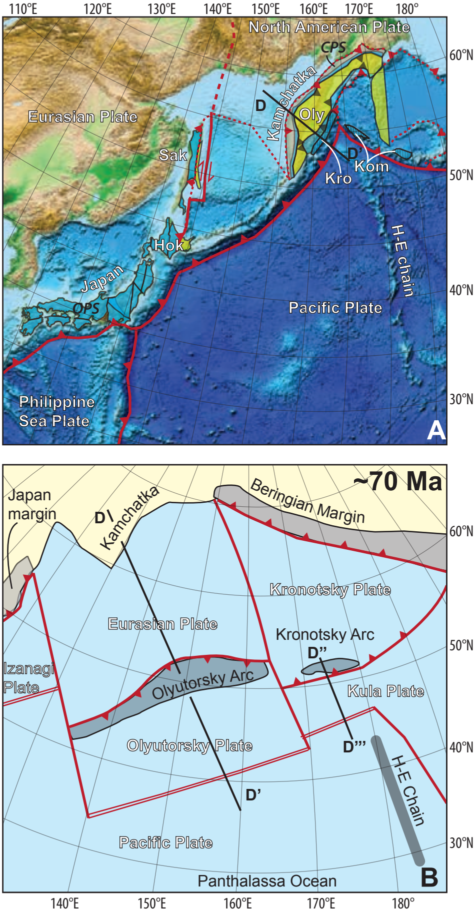

110°E
120°E
130°E
140°E
150°E
160°E
170°E
180°
North American Plate
CPS
60°N
Kamchatka
D
Oly
Eurasian Plate
Sak
D'
Kom
Kro
50°N
Hok
H-E chain
Japan
OPS
40°N
Pacific Plate
30°N
Philippine
Sea Plate
A
~70 Ma
Japan
margin
D
Kamchatka
Beringian Margin
60°N
Kronotsky Plate
Eurasian Plate
Kronotsky Arc
50°N
D''
Izanagi
Plate
Olyutorsky Arc
Kula Plate
Olyutorsky Plate
D'''
40°N
H-E Chain
D'
Pacific Plate
30°N
Panthalassa Ocean
B
140°E
150°E
160°E
170°E
180°

Figure 12

Interpreted evolution of orogenic architecture of the Kamchatka orogen

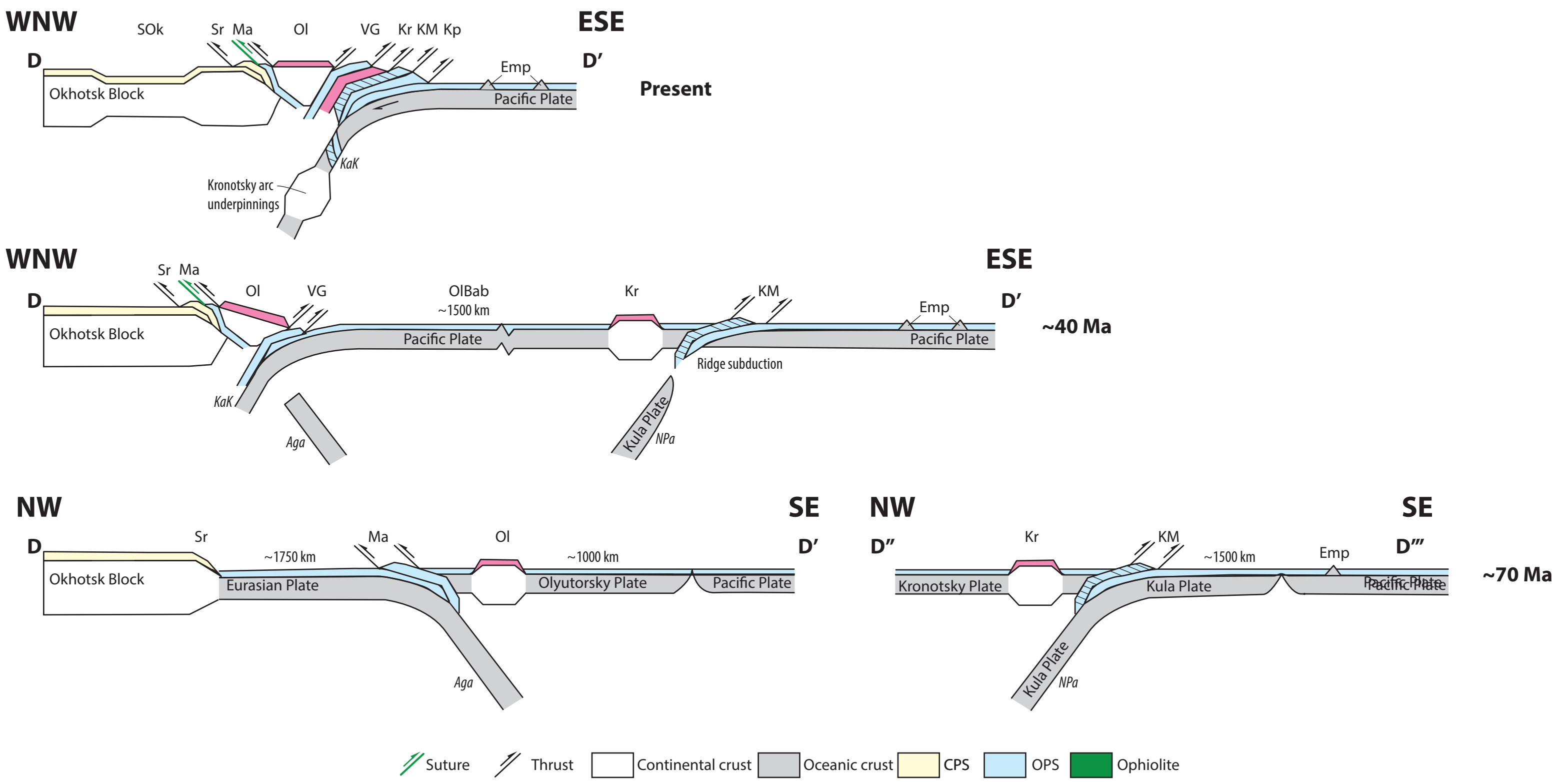

Figure 13

Timescale for the geological future

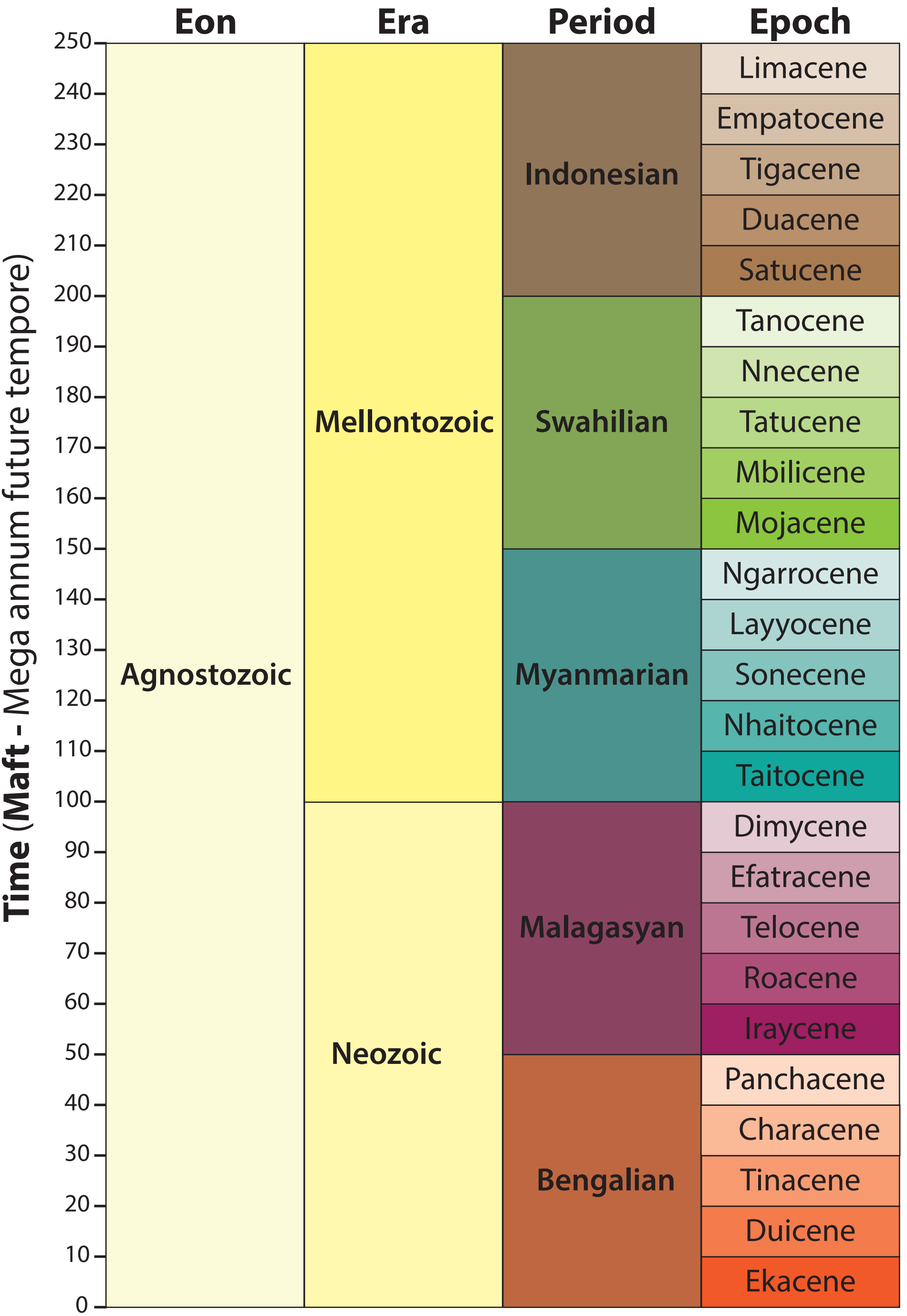

Figure 14

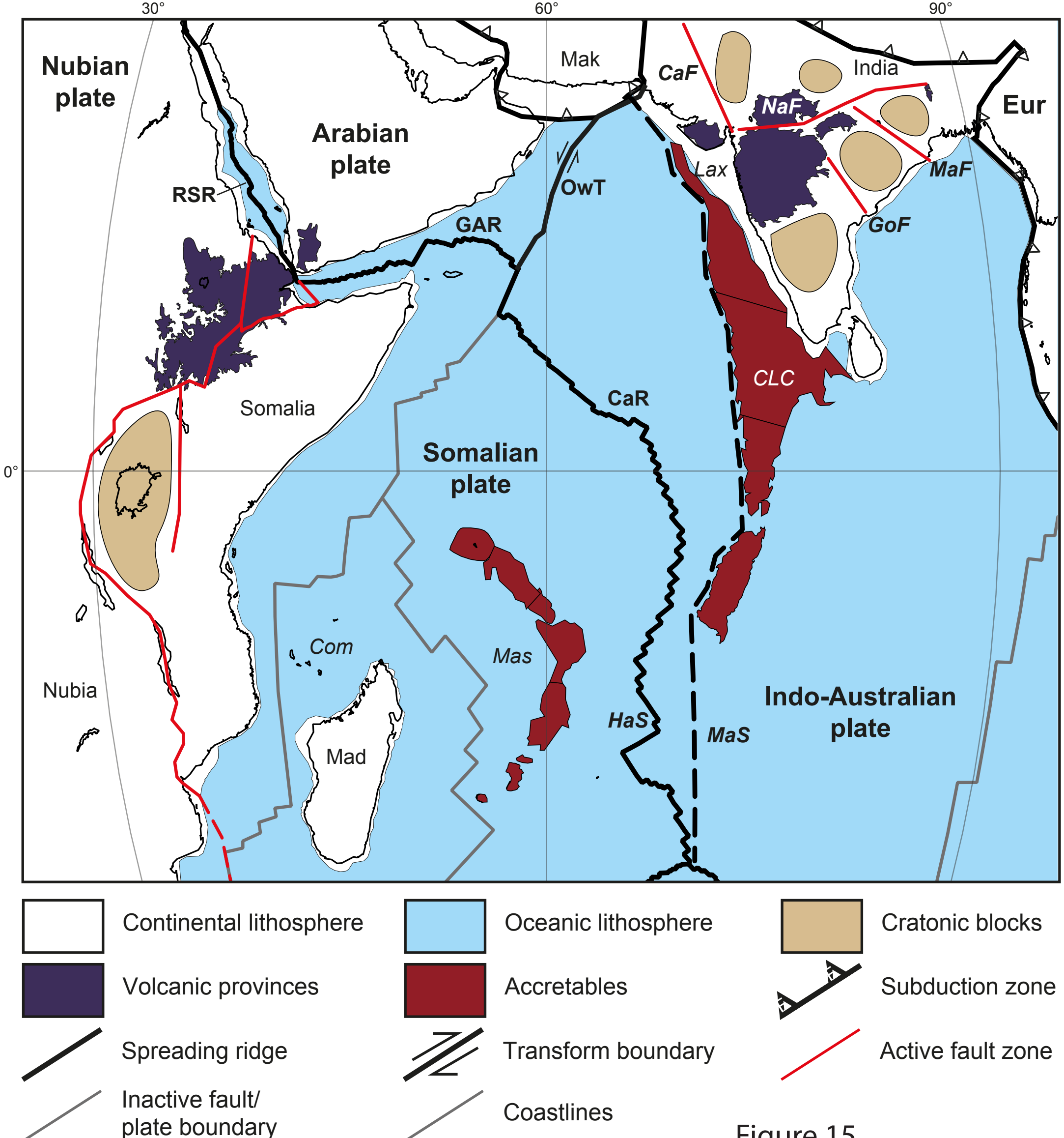
30°
60°
90°
0°
Nubian plate
Arabian plate
Mak
CaF
India
NaF
Eur
Lax
MaF
OwT
RSR
GAR
GoF
CLC
Somalia
CaR
Somalian plate
Com
Mas
Nubia
HaS
MaS
Indo-Australian plate
Mad
Continental lithosphere
Oceanic lithosphere
Cratonic blocks
Volcanic provinces
Accretables
Subduction zone
Spreading ridge
Transform boundary
Active fault zone
Inactive fault/ plate boundary
Coastlines

Figure 15

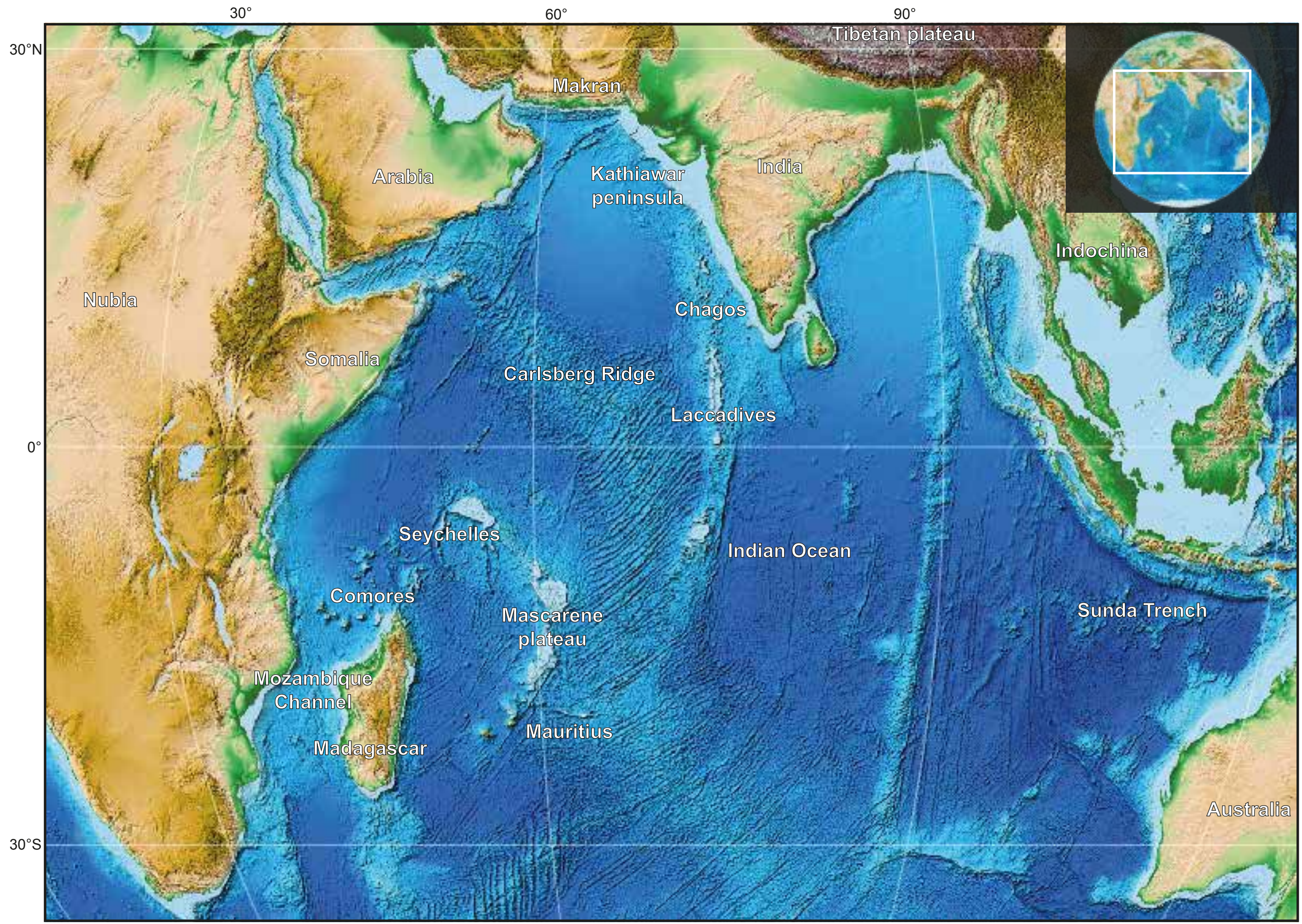
30°
60°
90°
30°N
0°
30°S
Tibetan plateau
Makran
Arabia
Kathiawar peninsula
India
Indochina
Nubia
Chagos
Somalia
Carlsberg Ridge
Laccadives
Seychelles
Indian Ocean
Comores
Mascarene plateau
Sunda Trench
Mozambique Channel
Mauritius
Madagascar
Australia

Figure 16

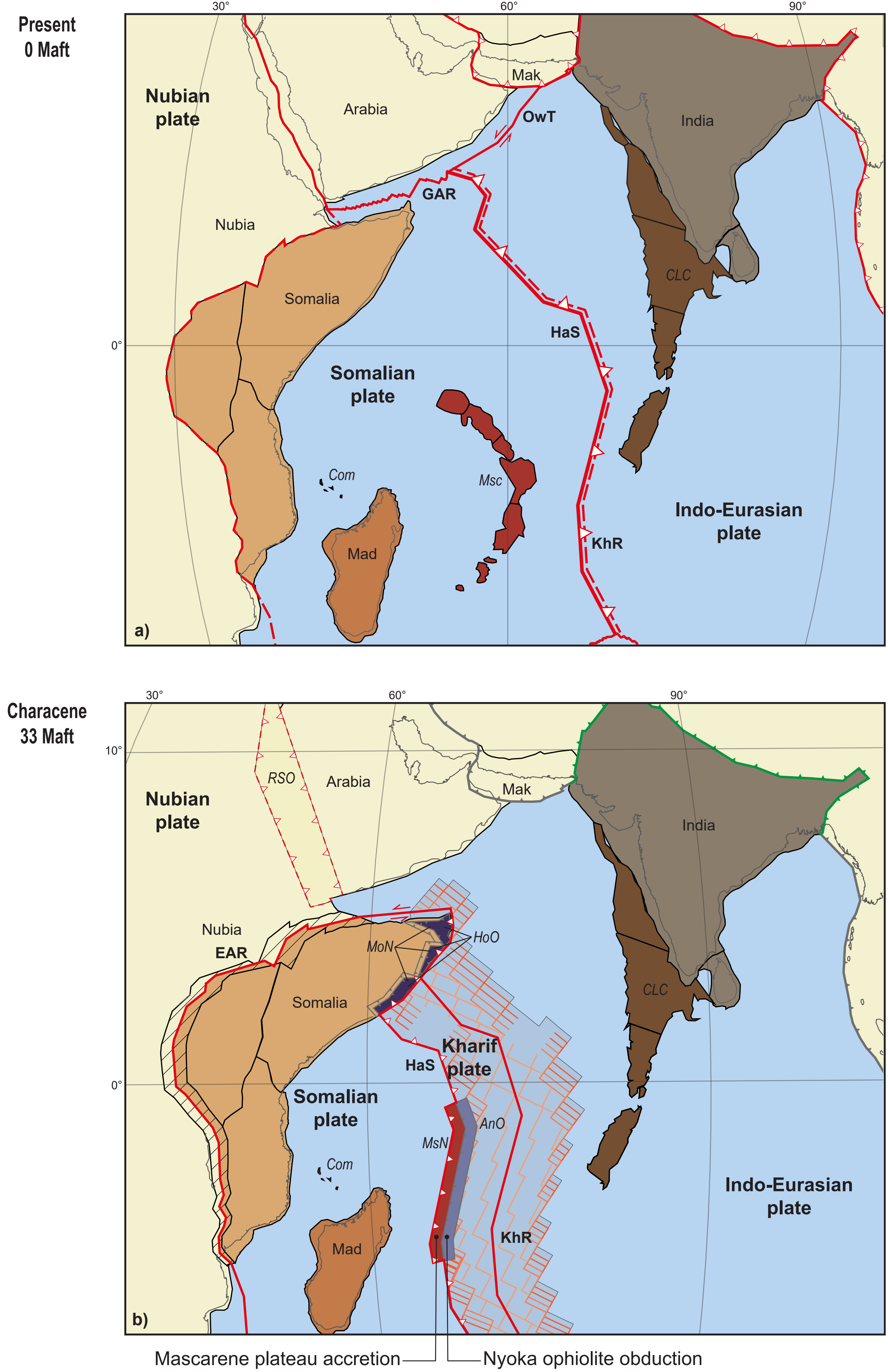
Present
0 Maft
30°
60°
90°
0°
Nubian plate
Arabia
Mak
OwT
India
GAR
Nubia
Somalia
CLC
HaS
Somalian plate
Com
Msc
Mad
Indo-Eurasian plate
KhR
a)
Characene
33 Maft
10°
RSO
Arabia
Mak
Nubian plate
India
Nubia
EAR
HoO
MoN
Somalia
CLC
Kharif plate
HaS
Somalian plate
AnO
MsN
Com
Indo-Eurasian plate
KhR
Mad
b)
Mascarene plateau accretion
Nyoka ophiolite obduction

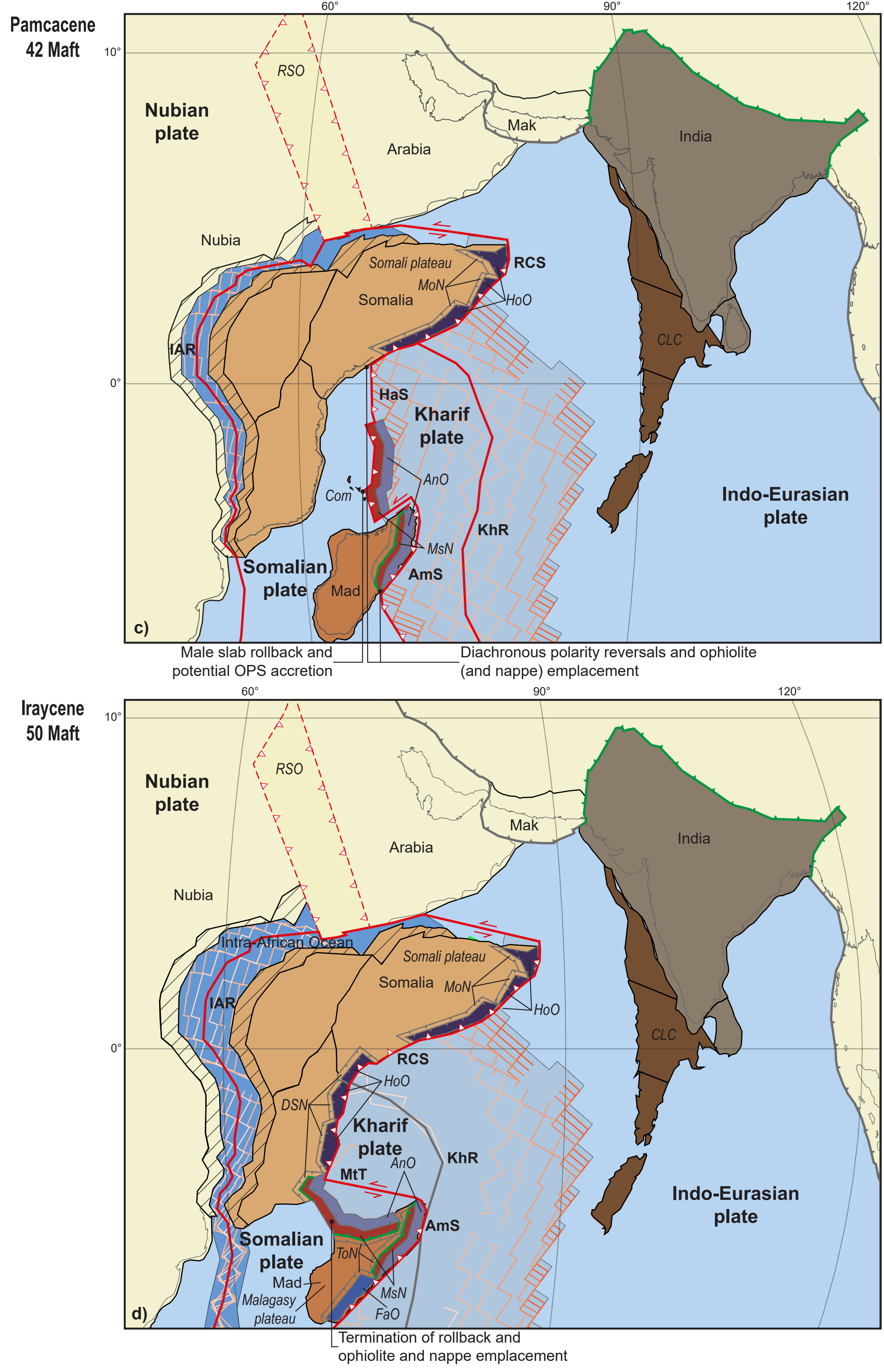

Pamcacene
42 Maft
60°
90°
120°
10°
0°
RSO
Nubian plate
Arabia
Mak
India
Nubia
Somali plateau
RCS
MoN
HoO
Somalia
IAR
CLC
HaS
Kharif plate
AnO
Com
MsN
KhR
Indo-Eurasian plate
Somalian plate
AmS
Mad
c)
Male slab rollback and
potential OPS accretion
Diachronous polarity reversals and ophiolite
(and nappe) emplacement
Iraycene
50 Maft
60°
90°
120°
10°
0°
RSO
Nubian plate
Arabia
Mak
India
Nubia
Intra-African Ocean
Somali plateau
Somalia
MoN
HoO
IAR
CLC
RCS
HoO
DSN
Kharif plate
AnO
KhR
MtT
AmS
Indo-Eurasian plate
Somalian plate
ToN
Mad
Malagasy plateau
MsN
FaO
d)
Termination of rollback and
ophiolite and nappe emplacement

Dimycene
100 Maft

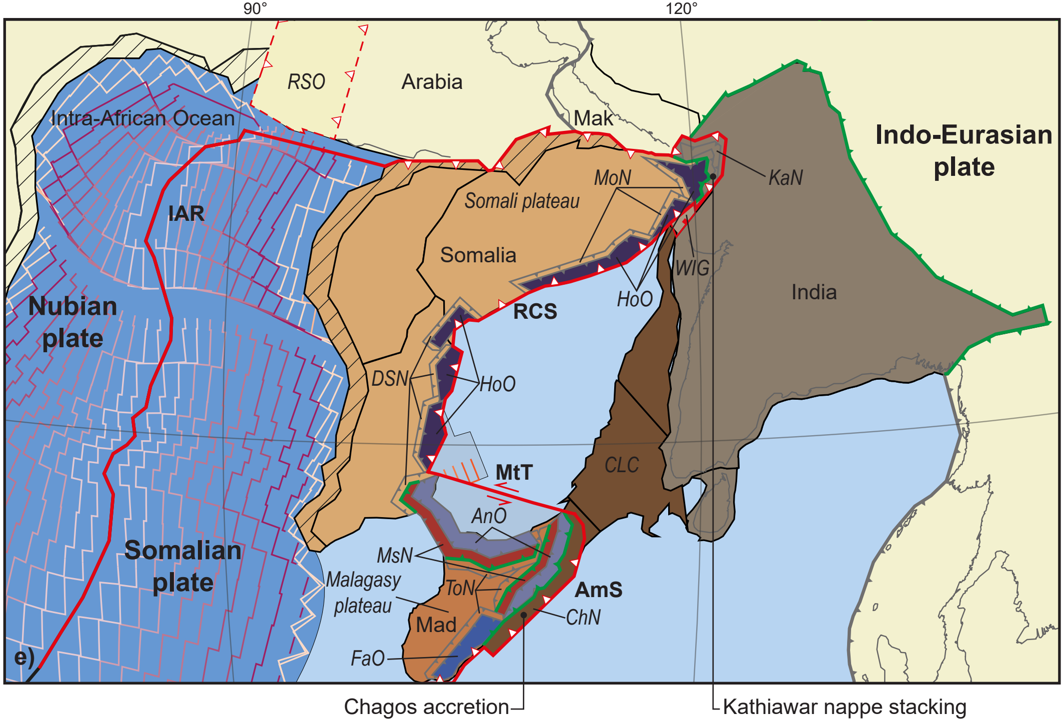

Tanocene
200 Maft

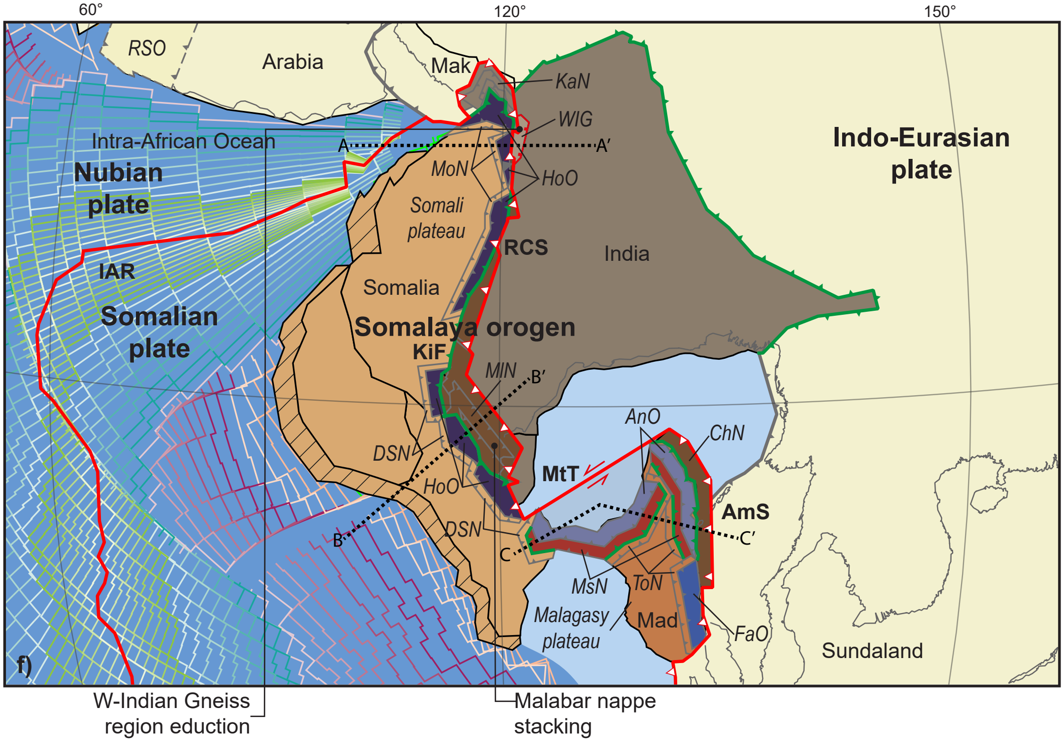

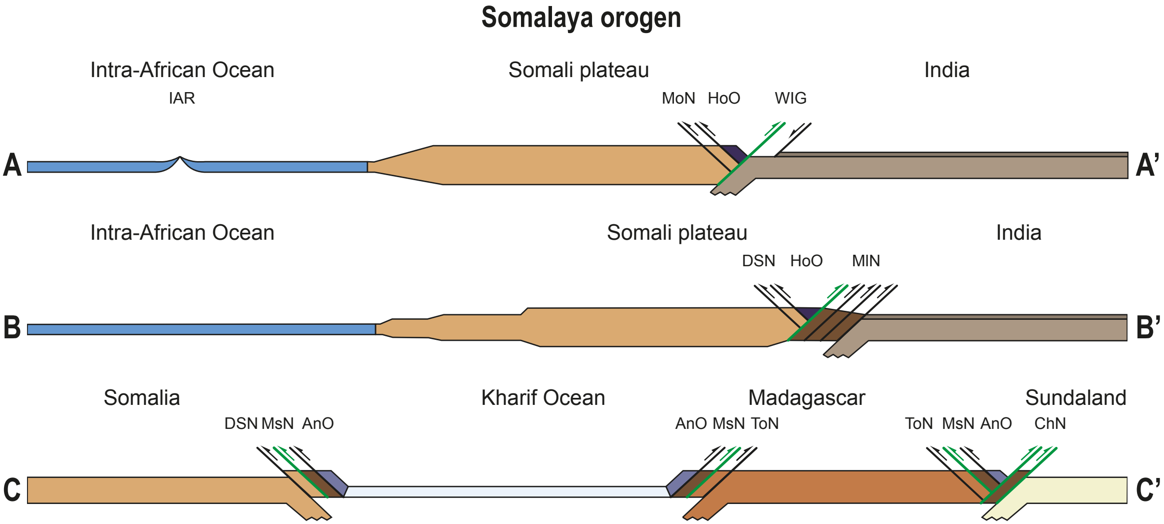

Somalaya orogen
Intra-African Ocean
Somali plateau
India
IAR
MoN
HoO
WIG
A
A'
Intra-African Ocean
Somali plateau
India
DSN
HoO
MIN
B
B'
Somalia
Kharif Ocean
Madagascar
Sundaland
DSN
MsN
AnO
AnO
MsN
ToN
ToN
MsN
AnO
ChN
C
C'

Figure 18

Present
0 Maft

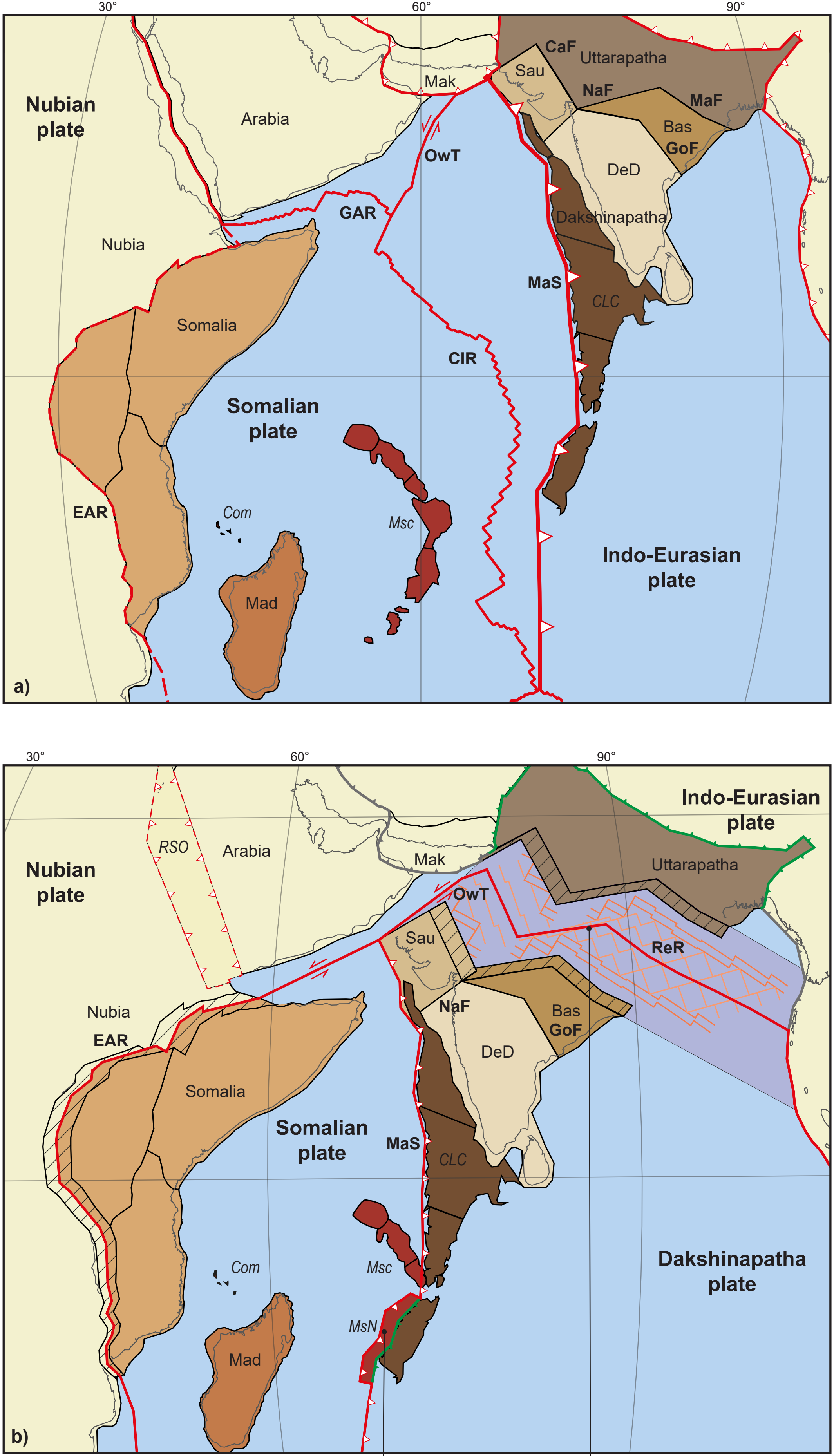

Characene
33 Maft

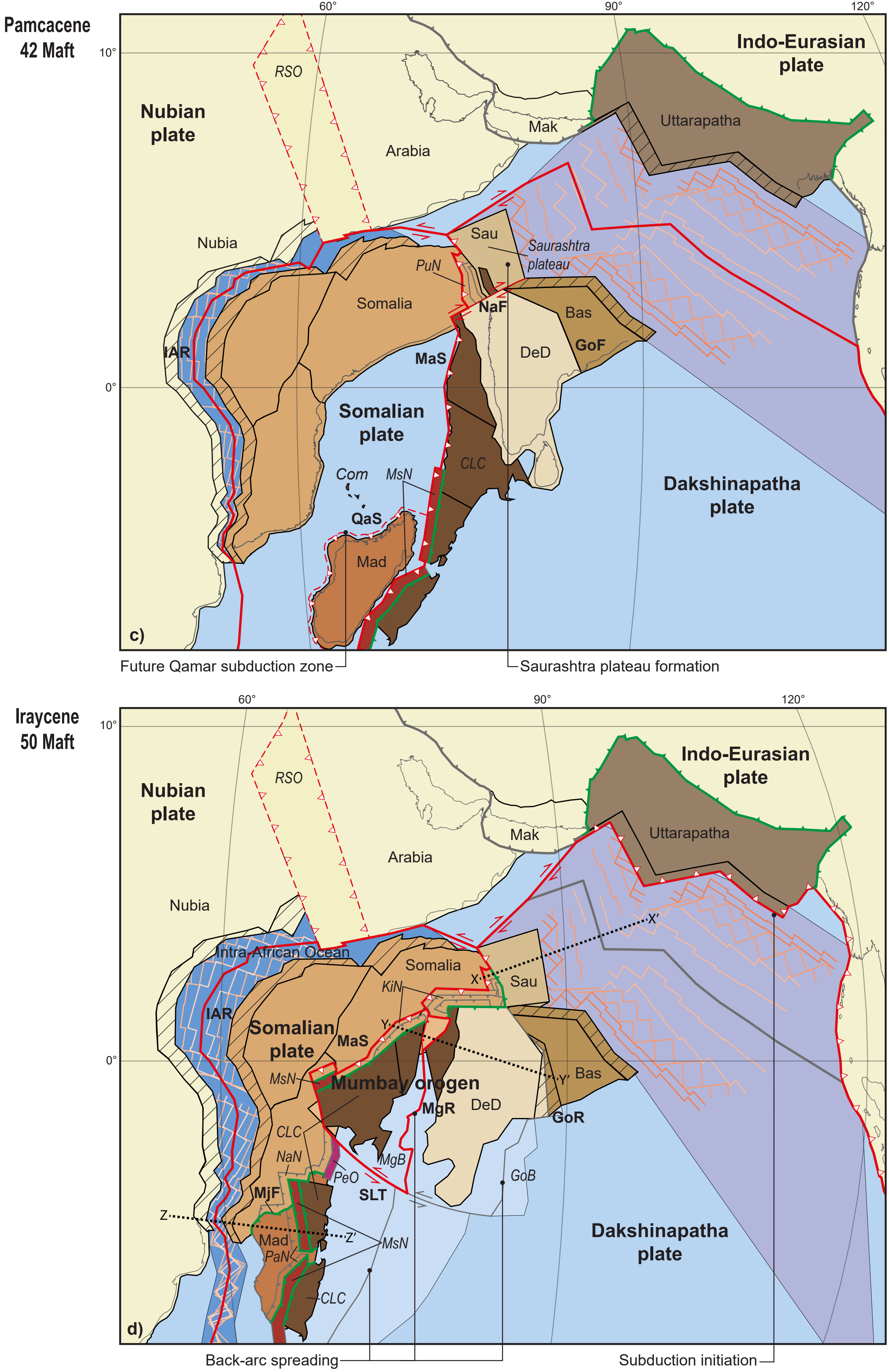
Pamcacene
42 Maft
60°
90°
120°
10°
0°
RSO
Nubian plate
Arabia
Mak
Indo-Eurasian plate
Uttarapatha
Nubia
Sau
Saurashtra plateau
PuN
Somalia
NaF
Bas
IAR
MaS
DeD
GoF
Somalian plate
CLC
Com
MsN
QaS
Mad
Dakshinapatha plate
c)
Future Qamar subduction zone
Saurashtra plateau formation
Iraycene
50 Maft
RSO
Nubian plate
Arabia
Mak
Indo-Eurasian plate
Uttarapatha
Nubia
Intra-African Ocean
Somalia
X
X'
Sau
KiN
IAR
Somalian plate
MaS
Y
Y'
Bas
MsN
Mumbay orogen
MgR
DeD
GoR
CLC
NaN
MgB
PeO
GoB
SLT
MjF
Z
Z'
MsN
Mad
PaN
CLC
Dakshinapatha plate
d)
Back-arc spreading
Subduction initiation

Dimycene
100 Maft

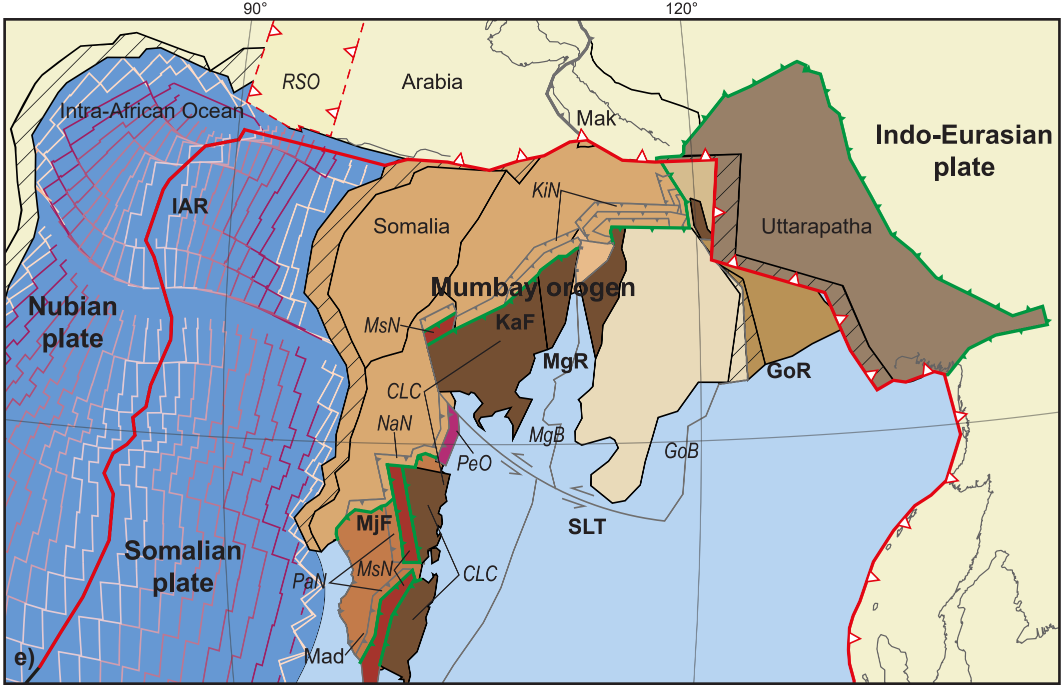

Tanocene
200 Maft

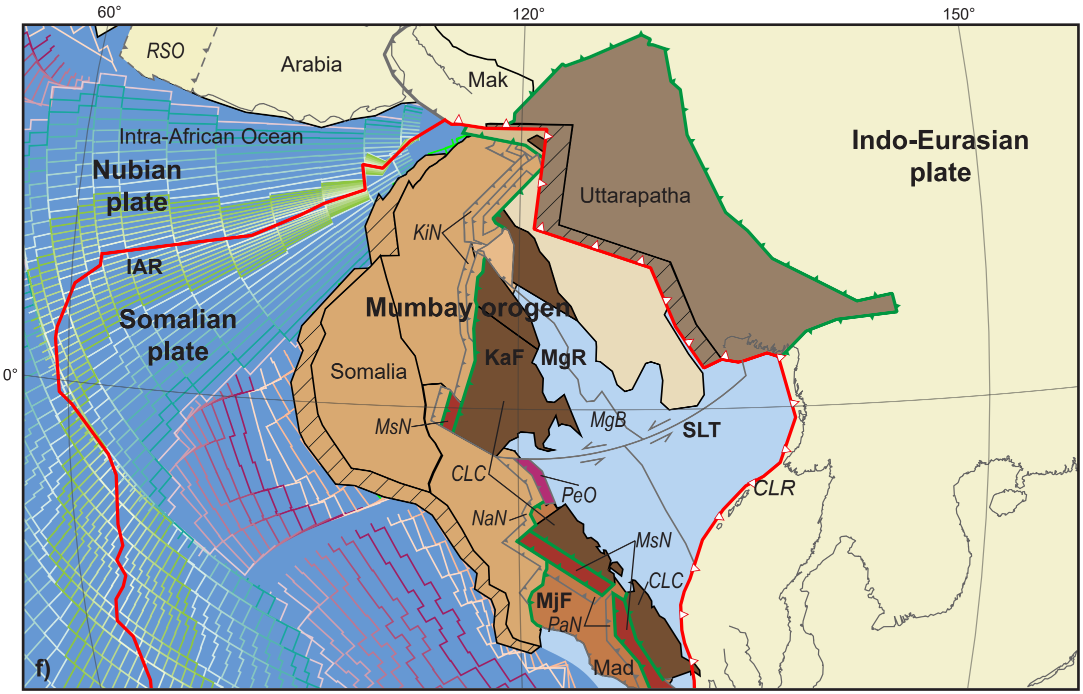

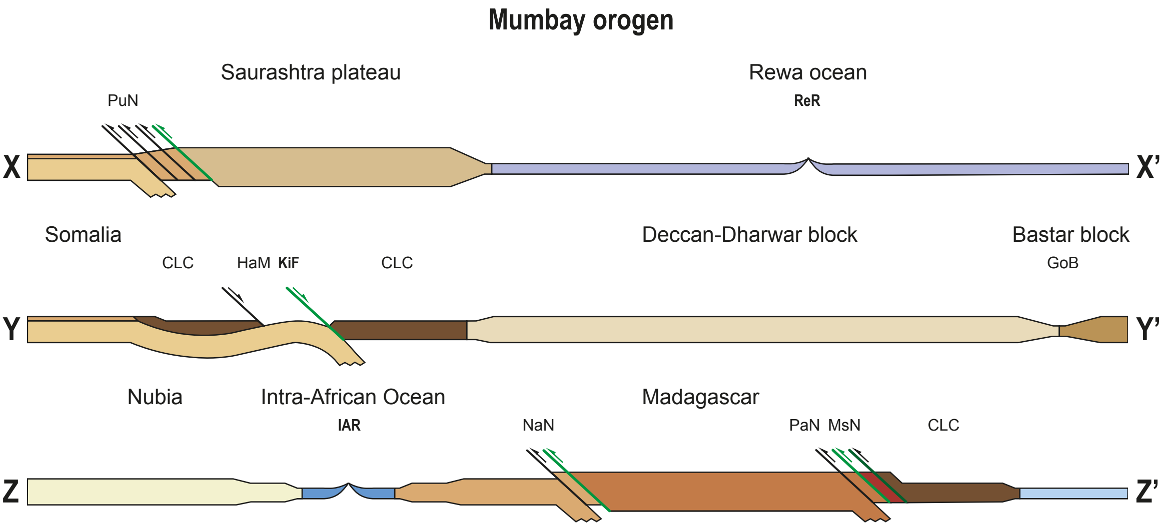
Mumbay orogen
Saurashtra plateau
Rewa ocean
PuN
ReR
X
X'
Somalia
Deccan-Dharwar block
Bastar block
CLC
HaM
KiF
CLC
GoB
Y
Y'
Nubia
Intra-African Ocean
Madagascar
IAR
NaN
PaN
MsN
CLC
Z
Z'

FIgure 20

1 Pre-drift extension is typically ~300 km, and perhaps up to 500 km for thickened crust

2 Ocean Plate Stratigraphy (OPS), derived from MORB, IAT, OIB, or LIP crust, *may or may not* accrete, as coherent nappes or as chaotic mélange

3 Oceanic Large Igneous Provinces may cause subduction cessation or polarity reversals, but eventually subduct, while leaving only minor accreted crustal relics

4 Subduction of continental crust will be associated with accretion of its Continental Plate Stratigraphy (CPS)

5 Extended continental crust (microcontinents, continental margins) will typically subduct

6 Non-extended continental crust does not subduct: if forced below an upper plate, it will likely horizontally underthrust untill the arrest of convergence

7 The forearc of oceanic upper plate lithosphere will be preserved as ophiolites if underthrusted by OPS/CPS nappes and, eventually, a continental margin, followed by slab break-off and subduction arrest.

8 Preservation of oceanic magmatic arcs lithosphere in the geological record requires a subduction polarity reversal oceanward of the arc following ophiolite obduction. Arcs on downgoing plates may leave OPS nappes in the geological record

9 Upper plate deformation is the result of the competition between absolute motion of the upper plate and the subducting slab

10 Upper plate lithospheric shortening is generally limited to 50-60%, after which shortening steps outboard